A QUASI-OPTICAL METHOD FOR CALCULATING PROPAGATION

OF LF RADIO WAVES IN THE PRESENCE OF AN IONOSPHERE

WITH HORIZONTAL GRADIENTS. PART I: RAY THEORY FOR

LOSSY MEDIA. PART II: DIFFRACTION BY THE EARTH

by

Richard Michael Jones

B. S. , California Institute of Technology, 1959

M. S. , University of Colorado, 1963

A thesis submitted to the Faculty of the Graduate

School of the University of Colorado in partial

fulfillment of the requirements for the degree of

Doctor of Philosophy

Department of Physics and Astrophysics

1968

6 October 1975

This copy of the thesis includes corrections of the following errors in the original copy:

1) sign errors in equations on pages 57, 63, 64, 66, 101, 102, 103, 109, 110, 111, 120, 121, 122, 123, 128, 129, 130, 131, 134, 135, and 136 -

all caused by the sign errors in evaluating the residues in contour integrals to go from equations (E-25) to (E-26) and from (E-36) to (E-37);

2) errors in equations on pages 9, 13, 25, 84, 87, 91, 96, 103, 104, 106, 107, and 108;

3) errors on pages 7, 14, 45, 51, 71, 76, 83, 93, 94, 95, 97, 111, 137, and 143.

This Thesis for the Doctor of Philosophy Degree by

Richard Michael Jones

has been approved for the

Department of Physics and Astro physics

by

_____

William A. Rense

_____

Richard C. Mockler

Jones, Richard Michael (Ph.D., Physics)

A Quasi-Optical Method for Calculating Propagation of LF Radio
Waves in the Presence of an Ionosphere with Horizontal Gra-
dients. Part I: Ray Theory for Lossy Media. Part II: Diffrac-
tion by the Earth.

Thesis directed by Professor William Rense

To predict communication conditions between a given transmit-
ter and receiver, or to use radio waves to measure ionospheric
characteristics, it is desirable to calculate the effect of the earth
and ionosphere on radio waves. The difficulty of obtaining a formal
solution of Maxwell's equations with the appropriate boundary and
initial conditions necessitates using approximate methods or restric-
ting the scope of the problem. Solutions have been found for a
sharply bounded concentric ionosphere and several non-concentric
extensions to that model, but no practical method is available for
treating an ionosphere which arbitrarily varies horizontally and
vertically.

Although geometrical optics (ray theory) can be applied to a
medium which varies arbitrarily, it has not previously been used
satisfactorily to calculate reflection coefficients below 100 kHz.
The diffractive corrections applied to ray theory to account for the
diffraction of radio waves by the earth have been unable to account
for the diffraction encountered in multihop propagation between the
earth and the ionosphere.

This thesis presents an extension of ray theory which satisfactorily calculates reflection of LF (30 to 300 kHz) radio waves from the ionosphere. This extension includes ionospheric losses in determining the ray path by using the complex refractive index (instead of just the real part) in Snell's law. The effect of losses in the D region is very important in determining the path of LF radio waves. Although the resulting ray paths, being in complex space, have less physical interpretation, they give accurate results. An accompanying approximation which compensates for the ray's missing the receiver is essential for ray tracing in complex space, and would also be very useful in ordinary ray tracing.

J. B. Keller's quasi-optical "geometrical theory of diffraction" represents diffraction by the earth by rays which travel along the ground. These diffracted rays, which are ordinary ground wave modes excited by a sky wave, can be represented more accurately by rays which travel at certain complex heights above the ground. By taking into account all the rays diffracted by the earth and reflected from the ionosphere, it is possible to calculate satisfactorily multi-hop propagation between the earth and ionosphere. Regarding caustics as equivalent to sources permits calculating the excitation of the ground wave by a caustic in the incident field (which nearly always occurs in waves reflected from the ionosphere).

Even for a concentric ionosphere, the calculations are simpli-

fied by using ray tracing in complex space and the geometrical

theory of diffraction.

This abstract is approved as to form and content. I recommend its
publication.

Signed _____
Faculty member in charge of dissertation

TABLE OF CONTENTS

LIST OF TABLES

LIST OF FIGURES

1. Introduction

Successful calculation of the terrestrial propagation of radio waves began 50 years ago when Watson (1918) calculated the propagation of radio waves around the earth by assuming the earth was surrounded by free space. He converted the rigorous zonal harmonic series to a contour integral using the now well-known Watson transformation and evaluated the integral by summing residues. Since his calculations gave much weaker signal strengths than observed at long distances, he concluded that this model could not account for terrestrial propagation of radio waves. The next year, Watson (1919) assumed a homogeneous conducting layer concentric with the earth in making calculations. This time, the calculations agreed qualitatively with measurements, supporting the hypothesis of Heavyside of an ionized layer above the earth which could reflect radio waves.

Around 1950, interest in calculating terrestrial radio wave propagation seemed to increase, perhaps because of the availability of computers making more complicated calculations practical. Bremmer (1949) gives a good background of the subject at that time. Johler and Berry (1962) presented a practical computer method for calculating the solution using the original zonal harmonics. However, the most popular method was still the residue series of Watson (1919), but interpreted as wave guide modes (Wait, 1960, 1962b, c; Johler and Berry, 1964).

Bremmer (1949, page 32) indicates a method of representing the field as a sum of terms separated according to the number of ionospheric reflections. Each term thus represents a wave which has reflected from the ionosphere a certain number of times, similar to geometrical optical rays, except that they are full-wave

solutions including diffraction by the earth. Wait (1961) developed this method in more detail, giving explicit expressions for the terms. Berry (1964c) indicated how this method could be used in making computer calculations. He identified a term as an ionospheric reflection coefficient, and pointed out that it could be replaced by a plane wave reflection coefficient calculated from a continuous ionospheric profile using a full-wave reflection coefficient program such as that of Johler and Harper (1962). Thus, it was possible to separate the calculation into two parts: the reflection coefficient, and the path integral. Berry and Chrisman (1965a, b) have calculated values of the path integral as a function of distance from the transmitter for various ionospheric heights, frequencies, and ground constants.

Several extensions have been made to this concentric, sharply-bounded model (Wait, 1967b). Wait (1964a) has allowed for the case of a non-homogeneous earth by considering a land/sea boundary. Wait (1962a, 1964b, c, d), Rugg (1967), and others have taken into account various types of nonconcentric ionospheric models at VLF by considering mode conversion in the earth-ionosphere wave guide.

However, there has been no satisfactory method that allows for the general case of an ionosphere which varies arbitrarily with height and horizontal position. The success of ray theory (geometrical optics) for arbitrarily varying ionospheric models at HF suggests using ray theory at the lower frequencies also. However, standard ray theory has not been able to calculate reflection of the lower frequencies from the ionosphere satisfactorily. The problem even shows up in a minor form at HF. Titheridge (1967) showed for vertical incidence, that the error in absorption and group path by neglecting the contribution of the phase integral into the complex plane is nearly canceled by using non-deviative

formulas rather than the supposedly more exact expressions. He did not indicate whether his result might apply to oblique incidence. Booker and Crain (1967) derived a theorem on absorption, using it to develop a method for calculating reflection of LF radio waves from a plane stratified medium, but the method is not as straightforward as standard ray theory.

A second problem is that geometrical optics does not take diffraction by the earth into account. Wait and Conda (1958, 1959) added diffraction corrections to geometrical optics to account for diffraction of plane waves into the shadow of the earth, but do not apply it to the case of sky waves reflected from the ionosphere. The full-wave solutions of Wait (1961) and Berry (1964c) show that the field of the mth hop attenuates slower with distance in the shadow than the groundwave. However, since they do not give a geometrical interpretation of the phenomenon, it is not clear how to make the geometric extension to the nonconcentric case.

Part I of the present work attacks the problem of calculating reflection from the ionosphere, and shows that including attenuation in addition to phase in calculating ray paths at LF substantially improves the accuracy of reflection coefficients. Considering both phase and attenuation leads to an extension of Fermat's principle that uses the complex phase refractive index (instead of just the real part) to determine ray paths having complex coordinates. Applying this method of ray tracing in complex space to a plane wave incident on a plane stratified medium gives results which agree with the phase integral method, but its greater generality allows it to apply to a more arbitrary representation of the ionosphere.

Part II adapts Keller's (1962) geometrical theory of diffraction to calculate the signal strength of rays diffracted by the earth into its shadow. A diffracted wave can be represented accurately by a ray which travels at a specific complex height

above the ground. Including all of the rays that contribute to the total field gives the correct attenuation with distance in the shadow. Comparison with the rigorous solution for a concentric iono-sphere shows that a caustic in the incident field behaves like a point source in exciting a ground wave mode.

PART I: RAY THEORY FOR LOSSY MEDIA

2. Introduction to Part I.

Ray theory has long been used as an approximate method for calculating reflection and refraction of HF radio waves by the ionosphere. With the abundance of large digital computers, ray tracing programs have been written to calculate ray paths in the ionosphere on a fairly routine basis. In most cases ray theory is a good approximation at HF, and the main area for advancement is in developing models to realistically represent the important features of the ionosphere.

So far, however, ray theory has not been successfully applied at LF and VLF, where two objections to the application exist. First, the wavelength is longer, so that the ionosphere may change considerably over a wavelength, and the "slowly varying" assumption usually considered necessary for ray theory to hold is thus invalid. Second, at HF the permittivity of the ionosphere varies with position and the conductivity is nearly zero, but at LF and VLF the situation is reversed: the permittivity is approximately that of free space, and the spatial variation of conductivity determines the reflection and refraction properties of the ionosphere. That is, the real part of the phase refractive index is nearly 1, and the imaginary part varies with position. In physical terms the wavelength is nearly independent of position, but the attenuation coefficient varies. Thus, standard ray theory, which is based entirely on the spatial variation of wavelength, ignores the main properties of the medium at LF and VLF.

Using the modified ray theory proposed in this paper solves the second problem by including the effects of attenuation in determining ray paths. The method's successful calculation of reflection coefficients for profiles which are not "slowly varying" indicates that such a criterion is really too restrictive.

List of Symbols For Part I

A	in section 3, a parameter which represents focusing in section 4, (see fig. 1)
B	See fig. 1
C	in sections 5 and 6, $\cos \varphi_0$ in section 4, (see fig. 1) in appendices A and B, $\sqrt{1 - V_y^2}$
E	electric field
G_1	transmitting antenna gain factor
G_2	receiving antenna gain factor
N	electron density
N_0, N_1, N_2, N_3	electron density at heights h_0, h_1, h_2, h_3 for an exponential profile (see table 1)
P	complex or generalized phase path
P_A, P_B, P_C	phase path at points A, B, C of figure 1
R	plane-wave reflection coefficient from a plane strati- fied ionosphere referred to the height h_0
$\hat{R}$	reflection coefficient from a plane stratified ionosphere referred to the height 0 for a transmitter-receiver separation y
S	$\sin \varphi_0$
V	same as V_h
V_h	vertical component of the wave normal direction in appendices A and B, normalized so that $V_h^2 + V_y^2 = n^2$
V_y	horizontal component of the wave normal direction in appendices A and B, normalized so that $V_h^2 + V_y^2 = n^2$
V_0	in appendix A, see (A-18)
X	normalized electron density, the X in the Appleton- Hartree formula, equal to $\dfrac{\omega_N^2}{\omega^2} = \dfrac{Ne^2}{m\epsilon_0 \omega^2}$

Z	normalized collision frequency, the Z in the Appleton-Hartree formula, equal to $\frac{\nu}{\omega}$
a, a_1, a_2	exponential increase of a collision frequency with height (see table 2)
b, b_1, b_2, b_3	exponential decrease of electron density with height (see table 3)
e	charge of the electron
f_N	plasma frequency, $f_N^2 = 80.6 \times 10^{-6} N$ MHz^2, for N in electron/cm^3
h	height (may be complex)
h_0	in (23), height defining an exponential refractive index profile
h_0, h_1, h_2, h_3	height defining exponential electron density and collision frequency profiles (see tables 1 and 2)
i	$\sqrt{-1}$
k	wave number (propagation constant) of free space, equal to $\frac{2\pi}{\lambda}$
log	natural logarithm
m	mass of the electron
n	complex refractive index, equal to $\mu - i\chi$
n_0	complex refractive index at the transmitter
n_1, n_2	complex refractive index in media 1 and 2
s	in appendix A, the real part of V_y, defined in (A-27) otherwise, path length
s_1, s_2	path length at the endpoints of the ray path
t	in the term $e^{i\omega t}$, time; in (A-27) through (A-41), the imaginary part of V_y; otherwise, the independent variable in Hamilton's or Haselgrove's equations
u_0	a normalizing factor giving the strength of the transmitting antenna

$\vec{v}$ a vector pointing in the wave normal direction (may be complex)

v $\sqrt{v_j v_j}$

v_j the jth component of $\vec{v}$, normalized so that $v_j v_j = n^2$ or μ^2

$\vec{x}$ vector location of a point on the ray path (may be complex)

$\vec{x}_0$ vector location of the receiver

x_j jth component of $\vec{x}$ (may be complex)

x_{0j} jth component of $\vec{x}_0$

y the horizontal component of a point on the ray path (equal to x_2), also the same for the total ray path (that is, the ground range, which may be complex)

α the angle between the ray direction and the wave-normal direction

β exponential decrease of n^2 with height in an exponential ionospheric model (see (23))

γ angle between the wave normal direction and a straight line connecting a ray path point and the receiver (see fig. 1)

δ in $e^{i\delta}$, an initial condition determining the initial direction of the ray path in complex space; otherwise, used to indicate the variation of an integral (calculus of variations)

ϵ_0 permittivity of free space

λ wavelength in free space

μ real part of the phase refractive index

μ_1, μ_2 real part of the phase refractive index in media 1 and 2

ν	electron collision frequency
ν_0, ν_1, ν_2	collision frequency at a height h_0, h_1, h_2 for an exponential profile (see table 2)
π	3.141592654 . . .
φ	phase of the reflection coefficient (see (32))
φ_0	angle of incidence of the ray on the ionosphere
φ_1, φ_2	angle of the wave normal with the vertical in media 1 and 2
χ	imaginary part of the phase refractive index
ω	angular wave frequency
ω_N	angular plasma frequency, equal to $\sqrt{\dfrac{Ne^2}{m\varepsilon_0}} = 2\pi f_N$

3. Ray Tracing in Complex Space[1]

Ray theory calculates the field of a radio wave at some distance from a source by integrating along some path (the "ray path") connecting the source with the observation point. Ray theory gives the radiation field strength at point 2 due to a time harmonic source at point 1 as

$$E = u_0 e^{i\omega t} G_1 A e^{-ik \int_{s_1}^{s_2} \mu \cos\alpha \, ds} e^{-k \int_{s_1}^{s_2} \chi \cos\alpha \, ds} G_2, \qquad (1)$$

where α is the angle between the ray direction and the wave normal direction; u_0 is the strength of the source; G_1 is the transmitting antenna pattern factor, which depends on the direction in which the ray leaves the transmitter; and G_2 is the receiving antenna pattern factor and depends on the ray's angle of arrival at the receiver. The factor A accounts for focusing and de-focusing due to convergence and divergence of the rays. It is calculated by assuming conservation of energy in a narrow tube of rays (Keller, 1962). The term

$$\int \mu \cos\alpha \, ds - i \int \chi \cos\alpha \, ds = \int n \cos\alpha \, ds = P \qquad (2)$$

is called the phase integral (Budden, 1961). The quantity P is called the generalized or complex phase path. The real part of P gives the phase of the wave, while the imaginary part gives the attenuation of the wave due to absorption by the medium.

---

[1]
Epstein (1930) and Bremmer (1949, p. 174) mention the possibility of ray paths having complex coordinates that are determined by the complex form of Snell's law, but do not propose calculating ray paths in complex space. In fact, Epstein showed that if the absorption is small the ray path does not differ much from that existing in the absence of any absorption. However, Kelso (1964, p. 192) points out that this does not apply at reflection.

From the many paths that carry the wave, we must find those which make the greatest contribution to the field. The usual criterion for choosing these ray paths is Fermat's principle (Budden, 1961),

$$\delta \int \mu \cos \alpha \, ds = \delta \int v_i \, dx_i = 0, \tag{3}$$

where (3) uses the summation convention over repeated indices

$$v_i \, dx_i \equiv \sum_{i=1}^{3} v_i \, dx_i, \tag{4}$$

and $\vec{v}$ points in the wave normal direction and is normalized so that

$$|v| = \sqrt{v_i \, v_i} = \sqrt{v^2} = \mu, \tag{5}$$

where μ is the real part of the phase refractive index.

The physical basis for this criterion is wave interference. Waves within a wavelength of such a path will tend to interfere constructively, whereas waves far from this path will tend to cancel each other. Application of Fermat's principle to stratified media leads to Snell's law to give the bending going from medium 1 to medium 2.

$$\mu_1 \sin \varphi_1 = \mu_2 \sin \varphi_2 \tag{6}$$

For continuously varying media, Fermat's principle leads to the system of differential equations given by Haselgrove (1954) or to Hamilton's equations for calculating the ray path. With the Hamiltonian

$$H = \frac{v^2 - \mu^2}{2}$$

Hamilton's equations become

$$\frac{dx_j}{dt} = v_j - \mu \frac{\partial \mu}{\partial v_j}$$

$$j = 1, 2, 3, \tag{7}$$

$$\frac{dv_j}{dt} = \mu \frac{\partial \mu}{\partial x_j}$$

where x_j is a generalized coordinate, and v_j is a generalized momentum.

For the choice of independent variable in (7) the generalized phase path is given by

$$\frac{dP}{dt} = \mu^2 - i\mu\chi. \tag{8}$$

The mathematical basis for Fermat's principle is the asymptotic evaluation of integrals. Consider all possible paths connecting the source with the observation point. According to Huygen's principle, each of these paths will contribute to the observed field, and each contribution will have the form of (1). The total field will be the sum of these contributions, and, since the paths vary continuously from one to the next, the sum will involve an integration over these paths. (Not along these paths; this integration should not be confused with the phase integral along a particular path). The integration over the paths can be performed by the saddle-point method (Budden, 1961). The main point in the technique is to separate out those terms in the integrand which vary rapidly with the independent variable (usually exponential terms). In our case, the integrand is of the form (1), and depends on the path of integration of the phase integral. If

$$\nabla\chi << \nabla\mu, \tag{9}$$

then the quickly varying term of (1) is

$$e^{-ik\int \mu \cos\alpha \, ds}. \tag{10}$$

The saddle-point method chooses the paths making the greatest contributions to the integral. The condition for choosing those paths is Fermat's principle, (3).

However, if (9) is not satisfied, then both exponentials in (1) must be considered quickly varying, and the saddle-point method gives

$$\delta \int n ds = \delta \int \mu\, ds - i\, \delta \int \chi\, ds = 0 \tag{11}$$

as the condition which determines the ray path. Notice that (11) is a complex equation and requires both the real and imaginary parts to be zero. Thus, (11) gives two conditions for determining the ray path whereas (3) gives only one. These two conditions can be satisfied only by allowing the points on the ray path to have complex coordinates. The physical interpretation of (11) is that the ray path must have both minimum wave interference and minimum attenuation.

Just as Fermat's principle led to Snell's law and Haselgrove's equations, (11) leads to an extension of Snell's law for stratified media,

$$n_1 \sin\varphi_1 = n_2 \sin\varphi_2, \tag{12}$$

and to an extension of Haselgrove's equations for continuously varying media,

$$\frac{dx_j}{dt} = e^{i\delta} \left(v_j - n\frac{\partial n}{\partial v_j} \right)$$

$$j = 1,\ 2,\ 3. \tag{13}$$

$$\frac{dv_j}{dt} = e^{i\delta}\, n\frac{\partial n}{\partial x_j}$$

The generalized phase path is now given by

$$\frac{dP}{dt} = e^{i\delta}\, n^2. \tag{14}$$

The constant $e^{i\delta}$ gives a needed parameter to determine the initial direction of the ray. The v_j's in (13) are now normalized so that

$$v_j\, v_j = n^2. \tag{15}$$

Although a ray path which is a solution of (13) satisfies (11), it does not necessarily connect the given source and observation point. This is the basic inconvenience of ray tracing. To find the ray path connecting the source and observation point one must use trial and error. The path may always be started at the source. This determines the initial values for the x_j. Requiring the path to end at the given observation point puts six conditions on the ray path (the real and imaginary parts of the three spatial coordinates at the observation point; the imaginary parts will always be zero). In making the trial ray paths, one has control of six things — when to stop the ray and the following five initial conditions:

1-4. The initial values of two of the v_j's (real and imaginary parts). Only two of the v_j's are independent because of (15).

5. The constant phase factor δ.

This is quite a bit more complicated than the corresponding case for ray tracing in real space. There are only three conditions on ray paths in real space (the three coordinates of the observer). In making trial ray paths in real space, one chooses the initial values of two of the v_j's and decides when to stop the ray. In practice, however, it is usually sufficient to calculate a few rays which surround the observation point and then interpolate to find an approximation for the generalized phase path for the ray path connecting the source with the observation point. Section 4 shows another approximation which often allows one to calculate the phase integral with only one ray.

4. A Useful Approximation for Ray Paths Which Miss the Observation Point

The phase integral in (1) should be calculated along a path that satisfies the generalized Fermat's principle (11) and connects

the source with the observation point. Solutions of (13) are ray paths that satisfy (11). The ray paths begin at the source if the coordinates of the source are chosen as the initial coordinates of the ray. The ray will end at the chosen observation point only with a proper choice of the rest of the initial conditions.

If the initial conditions are such that the ray barely misses the observation point, an approximate method can be used to calculate the phase and amplitude at the observation point. Consider the situation shown in figure 1. A ray has entered the figure in the upper left-hand corner and has stopped at A, a distance $|\vec{x}_o - \vec{x}|$ from the observation point at C. If the ray were to continue, it would not intersect the observation point, but would make its closest approach at B. If the wave fronts in the neighborhood of A, B, and C are nearly plane, then B lies on the same wave front as C, and the value of the generalized phase path at B is nearly the same as at C. If n is nearly constant in this neighborhood, then the value of the generalized phase path at B (or C) is approximately

$$P_C \approx P_B \approx P_A + n \, |\vec{x}_o - \vec{x}| \, \cos \gamma. \qquad (16)$$

However, since from (15)

$$|v| = n \qquad (17)$$

and $\vec{v}$ gives the wave normal direction,

$$P_C \approx P_A + \vec{v} \cdot (\vec{x}_o - \vec{x}) = P_A + v_j \, (x_{oj} - x_j). \qquad (18)$$

The approximation (18) is valid for both ordinary ray tracing and ray tracing in complex space, where all the quantities except $\vec{x}_o$ in (18) may be complex. The size of the neighborhood for which (18) gives accurate results depends on the situation and the desired accuracy. Again, the approximation depends on ∇n and
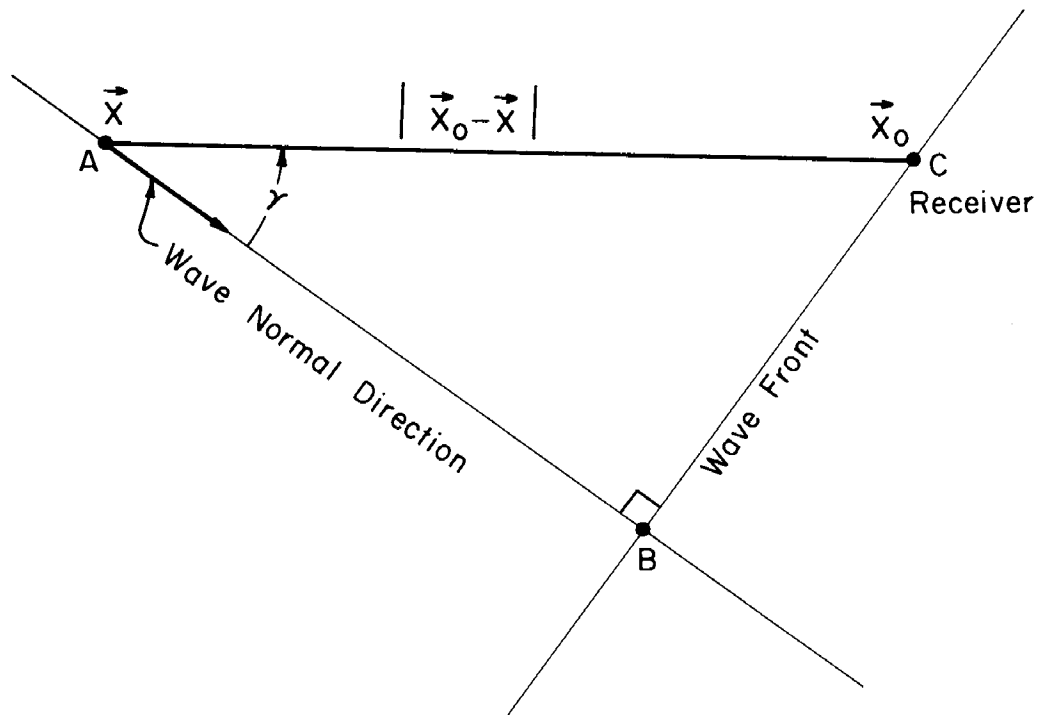
Figure 1.   Geometry of a ray missing the receiver.

the curvature of the wave fronts being small in the neighborhood
of A, B, and C. For isotropic media, the curvature of the wave
fronts is small when neighboring rays are nearly parallel.

5. Application to Calculating Reflection of Radio Waves from a Plane-Stratified Medium

The following example uses ray tracing in complex space to
calculate analytically the reflection coefficient of radio waves
incident on a plane-stratified medium. For plane waves this
method gives the same reflection coefficient in this case as
the phase integral method (Budden, 1961). This is reasonable
since the only difference between the two methods is the
path of integration, which will make no difference if the
integrated function is analytic or if the paths of inte-
gration are topologically equivalent with respect to any
nonanalytic points.

Neglecting the earth's magnetic field, the complex refractive
index of the ionosphere given by the Appleton-Hartree formula is

$$n^2 = 1 - \frac{X}{1 - iZ},$$ (19)

where X and Z are the normalized electron density and collision
frequency respectively. At LF and VLF, $Z \gg 1$ during the day,
so that (Wait and Walters, 1963)

$$n^2 \approx 1 - i \frac{X}{Z}.$$ (20)

The overall behavior of the lower ionosphere can usually be
approximated by exponential variations of both electron density
and collision frequency with height (Wait and Walters , 1963):

$$Z = e^{-a(h-h_1)} \tag{21}$$

$$X = e^{b(h-h_2)}. \tag{22}$$

From (20), (21), and (22) then,

$$n^2 = 1 - ie^{(a+b)h-(ah_1 + bh_2)} = 1 - ie^{\beta (h-h_0)}. \tag{23}$$

The model (23) is advantageous because exact full-wave and ray solutions can be found for the reflection of radio waves from such an ionosphere.

Appendix A integrates (13) and (14) from $h = 0$ to the point where $h = 0$ again after reflection from the ionospheric model (23). The result from (A-21) and (A-23) is that the complex phase path is

$$P = \frac{2}{\beta \sqrt{1 - n_0^2 S^2}} \log \frac{\sqrt{1 - n_0^2 S^2} + n_0 C}{\sqrt{1 - n_0^2 S^2} - n_0 C} - \frac{4 n_0 C}{\beta}, \tag{24}$$

and the ground range is

$$y = \frac{2 n_0 S}{\beta \sqrt{1 - n_0^2 S^2}} \log \frac{\sqrt{1 - n_0^2 S^2} + n_0 C}{\sqrt{1 - n_0^2 S^2} - n_0 C}, \tag{25}$$

where

$$n_0^2 = 1 - ie^{-\beta h_0} \tag{26}$$

and S and C are the sine and cosine respectively of the (complex) angle of incidence φ_0 of the ray on the ionosphere.

However, the phase path (24) corresponds to a measurable quantity only when the ground range (25) is real. If the real part of φ_0 is specified, then requiring y to be real determines the imaginary part of φ_0. Appendix A calculates the imaginary part of φ_0 necessary to make y real in the limit of large h_0

(plane waves) and the corresponding P and y, which from (A-41) and (A-36) are

$$P = \frac{2}{\beta C} \left(2 \log 2C + \beta h_o - 2C^2 \right) - \frac{\pi i C}{\beta} \tag{27}$$

$$y = \frac{2S}{\beta C} \left(2 \log 2C + \beta h_o \right). \tag{28}$$

Appendix B arrives at the same result by using the approximation of section 4.

The reflection coefficient (the ratio of the downcoming wave at $h = 0$ a distance y from the transmitter to the upgoing wave at the transmitter) is (Budden, 1961, p. 437):

$$\hat{R} = i \exp \left(-\frac{2\pi i}{\lambda} P \right). \tag{29}$$

The factor i outside the exponential in (29) is a Stokes constant (Budden, 1961) connecting the upgoing and downgoing waves at reflection. It can also be interpreted as the phase shift given to the wave after it has passed through the surface caustic at reflection (Kouyoumjian, 1965; Lewis, Bleistein, and Ludwig, 1967).

For comparison with other calculations, it is convenient to calculate the reflection coefficient as the ratio of the downcoming to the upgoing wave at the same point referred to some level. The appropriate expression to convert to a reflection coefficient at the same point referred to the level h_o is (Budden, 1961, p. 85)

$$R = \hat{R} \exp \left(-\frac{2\pi i}{\lambda} \left(- y \sin \varphi_o - 2 h_o \cos \varphi_o \right) \right). \tag{30}$$

Combining (27), (28), (29), and (30) gives

$$R = i \exp \left(-\frac{2\pi i}{\lambda} \left(\frac{4C}{\beta} (\log 2C - 1) - \frac{\pi i C}{\beta} \right) \right), \tag{31}$$

or

$$R = |R| e^{i\varphi}, \tag{32}$$

where

$$|R| = \exp\left(-\frac{2\pi^2 C}{\beta\lambda}\right) \tag{33}$$

$$\varphi = \frac{\pi}{2} - \frac{2\pi}{\lambda}\frac{4C}{\beta}\left(\log 2C - 1\right). \tag{34}$$

We can compare this with the reflection coefficient calculated by standard ray theory. Appendix C shows that when one applies standard ray theory to this same ionospheric profile (23), the ray is not reflected, but in fact turns up because the real part of the refractive index increases with height. Thus, in this case, standard ray theory gives a completely inaccurate reflection coefficient of zero.

6. Analytical Comparison with a Full-Wave Solution

The full-wave solution for the amplitude and phase of the reflection coefficient for horizontally polarized waves incident at an angle φ_0 on the ionospheric model (23) (referred to the level h_0) is (Wait and Walters, 1963; Budden, 1961, p. 357)

$$|R| = \exp\left(\frac{-2\pi^2 C}{\lambda\beta}\right) \tag{35}$$

$$\varphi = \pi + \frac{8\pi C}{\lambda\beta}\log\left(\frac{2\pi}{\lambda\beta}\right) + 2\arg\left[\left(-i\frac{4\pi C}{\lambda\beta}\right)!\right]. \tag{36}$$

The complex ray theory solution given by section 5, which agrees with that given by Budden's phase integral method, is

$$|R| = \exp \left(- \frac{2\pi^2 C}{\lambda \beta} \right) \tag{37}$$

$$\varphi = \frac{\pi}{2} - \frac{8\pi C}{\lambda \beta} \left(\log 2C - 1 \right). \tag{38}$$

As Budden (1961) points out, the magnitude agrees exactly with the full wave solution, and calculation shows that the phase is in error by at most $\pi/2$, and that this error approaches 0 as $C/(\lambda\beta)$ increases.

7. Numerical Comparison with Full-Wave Solutions

To show that complex ray theory gives accurate results, we compare reflection coefficients calculated by complex ray theory with those calculated by a full-wave method for plane waves incident on a plane stratified medium whose index of refraction is given by (19) for the electron density and collision frequency profiles shown in figures 2 and 3.

The complex ray solutions are found by numerically integrating (13) and (14) from h = 0 back again to h = 0 after reflection and applying the approximation of section 4 to correct for the endpoint's being in complex space. The transmitter is far enough below the reflection height for these point-source solutions to approximate plane-wave solutions.

The full-wave solutions are found using the method of Johler and Harper (1962), i.e., by approximating the medium by many thin homogeneous slabs (ten per free space wavelength) and finding a solution to Maxwell's equations which satisfies all the boundary conditions.

The three electron density profiles used in the comparisons are described in table 1 and shown in figure 2. The two collision frequency profiles are described in table 2 and shown in figure 3.
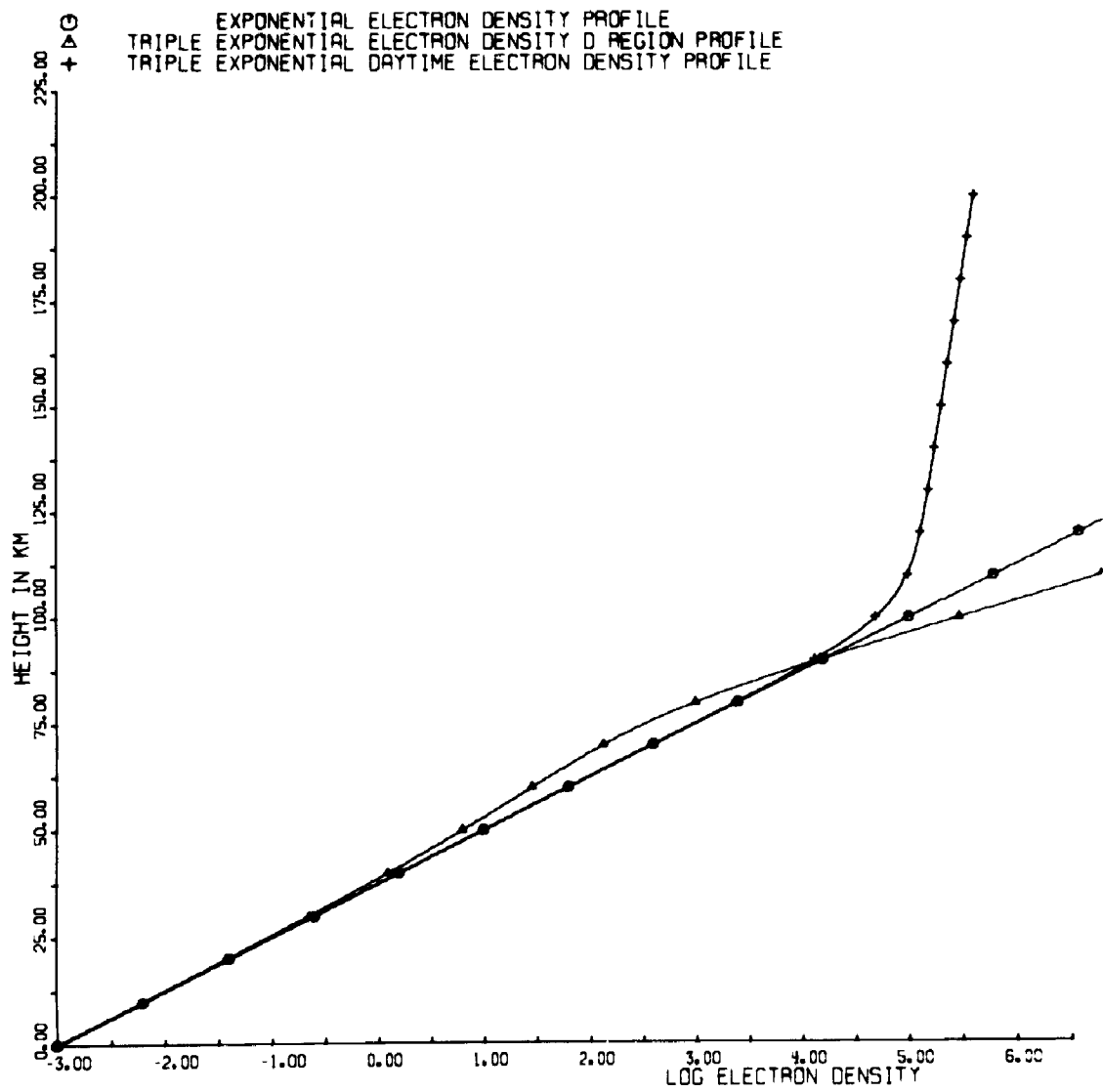
Figure 2. Electron density profiles used in the comparisons.
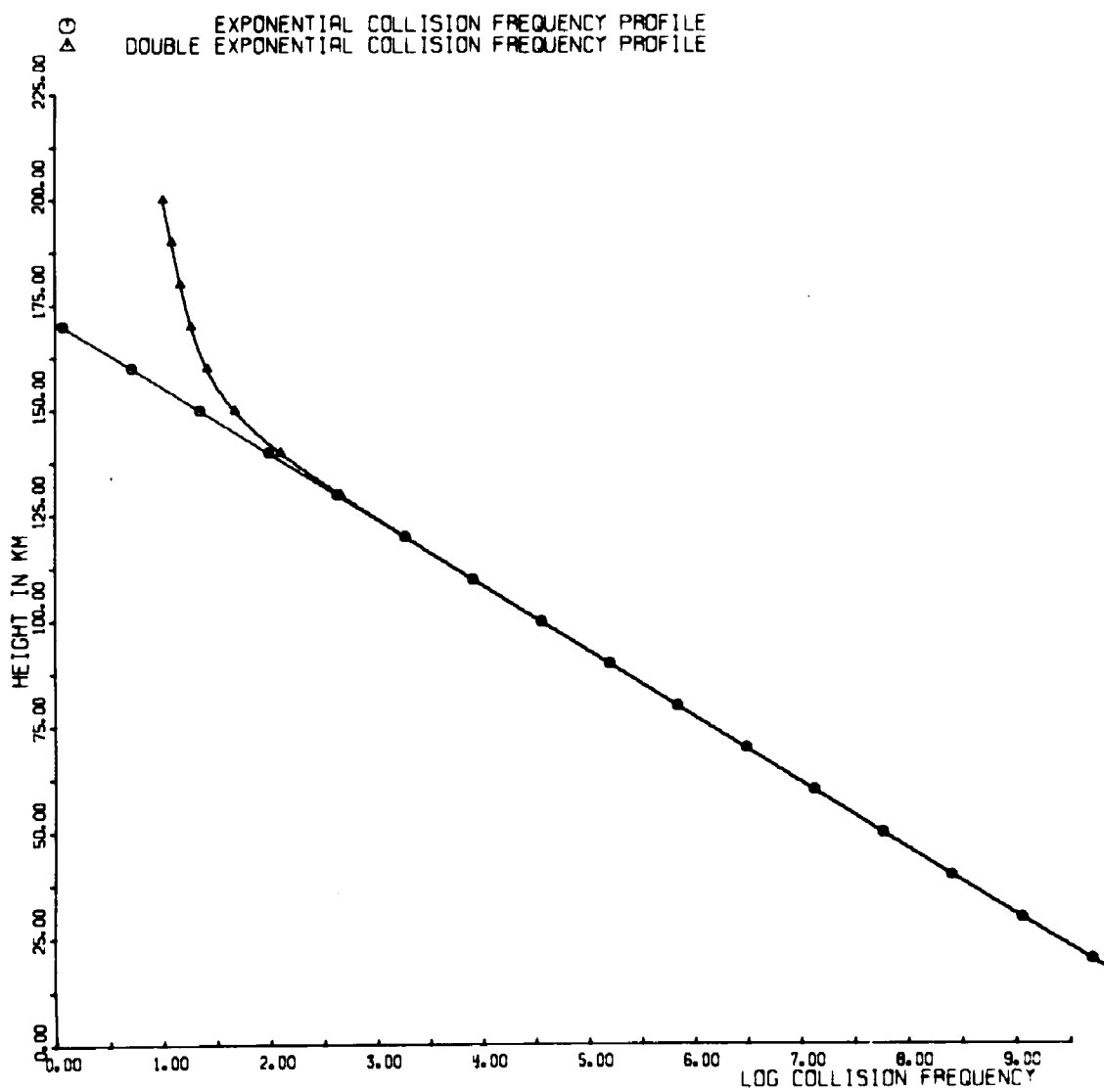
Figure 3.   Collision frequency profiles used in the comparisons.

Table 1. Electron density profiles used in the comparisons

Exponential Profile

$$N = N_0 e^{b(h-h_0)}$$

$N_0 = 10^5$ electrons/cm^3, $h_0 = 100$ km, $b = .184$ km^{-1}

This is an exponential approximation to some daytime D-region profiles published by Belrose and Burke (1964).

Triple-Exponential D-Region Profile

$$N = \cfrac{1}{\cfrac{1}{N_1 e^{b_1(h-h_1)}} + \cfrac{1}{N_2 e^{b_2(h-h_2)}}} + N_3 e^{b_3(h-h_3)}$$

$N_1 = 10^5$ electrons/cm^3, $h_1 = 100$ km, $b_1 = .184$ km^{-1}

$N_2 = 10^3$ electrons/cm^3, $h_2 = 87.5$ km, $b_2 = .109$ km^{-1}

$N_3 = 10^3$ electrons/cm^3, $h_3 = 81.5$ km, $b_3 = .307$ km^{-1}

The lower part of this profile is the same as the single exponential profile above. The upper part is an approximation by two exponential segments of the mean midday profile published by Knecht (1965).

Triple-Exponential Daytime Profile

$$N = \cfrac{1}{\cfrac{1}{N_1 10^{b_1(h-h_1)}} + \cfrac{1}{N_2 10^{b_2(h-h_2)}} + \cfrac{1}{N_3 e^{b_3(h-h_3)}}}$$

$N_1 = 10^5$ electrons/cm^3, $h_1 = 100$ km, $b_1 = .08$ km^{-1}
(notice that $10^{.08} \approx e^{.184}$)

$N_2 = 10^5$ electrons/cm^3, $h_2 = 100$ km, $b_2 = \frac{1}{150}$ km^{-1}

$N_3 = 1.3 \times 10^6$ electrons/cm^3, $h_3 = 350$ km, $b_3 = -.01$ km^{-1}

The lower part of this profile is nearly the same as the single exponential profile above. The middle part of the profile is an exponential approximation to the bottom side of a typical f_2 layer. The upper part of the profile is an exponential approximation to the topside of a typical f_2 layer.

Table 2. Collision frequency profiles used in the comparison

---

exponential profile

$$\nu = \nu_o \, e^{-a \, (h-h_o)}$$

$\nu_o = 3.65 \times 10^4$ collisions/sec, $h_o = 100$ km, $a = .148$ km^{-1}

This profile is an exponential approximation to the measurements reported by Belrose and Burke (1964).

---

double exponential profile

$$\nu = \nu_1 \, e^{-a_1 \, (h-h_1)} + \nu_2 \, e^{-a_2 \, (h-h_2)}$$

$\nu_1 = 3.65 \times 10^4$ collisions/sec, $h_1 = 100$ km, $a_1 = .148$ km^{-1}

$\nu_2 = 30$ collisions/sec, $h_2 = 140$ km, $a_2 = .0183$ km^{-1}

The lower part of this profile is the same as the single exponential profile above. The upper part is an exponential approximation to the 140 km through 300 km section of a theoretical collision frequency profile based on a standard atmosphere (Handbook of Geophysics and Space Environments, 1965, p. 2-5).

Exponential Electron Density Profile, Exponential Collision Frequency Profile.

If both the electron density and collision frequency profiles are exponential, then the reflection coefficients should be those given by (35) and (36) for the horizontal polarization full-wave solution and (37) and (38) for the complex ray solution. The numerical calculations show that they are (for the cases where $Z \gg 1$). Figure 4 shows the amplitude as a function of frequency for an angle of incidence of 60 degrees for both horizontal and vertical polarization full-wave solutions and for the complex ray solutions (marked geometrical optics). To the left of the absorption band $Z > 1$, and to the right $Z < 1$. Notice that the ray solutions agree with the horizontal polarization full-wave solutions for all frequencies and differ from the vertical polarization solutions only below 30 kHz, and then by at most 7 dB.

Figure 5 shows the phase difference between the reflection coefficient calculated with complex ray theory, and the full wave horizontal and vertical polarization solutions as a function of frequency from 1 kHz through 10 MHz. Notice that the phase error for vertical polarization is about 210 degrees at 1 kHz, decreases to 30 degrees at 30 kHz, and becomes negligible before entering the absorption band at 100 kHz. The error for horizontal polarization is much less.

Exponential Collision Frequency Profile, Triple Exponential D-region Profile

This comparison tests the sensitivity of the accuracy of the complex ray method to bends in the electron density profile. Figure 6 shows the amplitude of the reflection coefficient for an angle of incidence of 60° as a function of frequency from 1 kHz
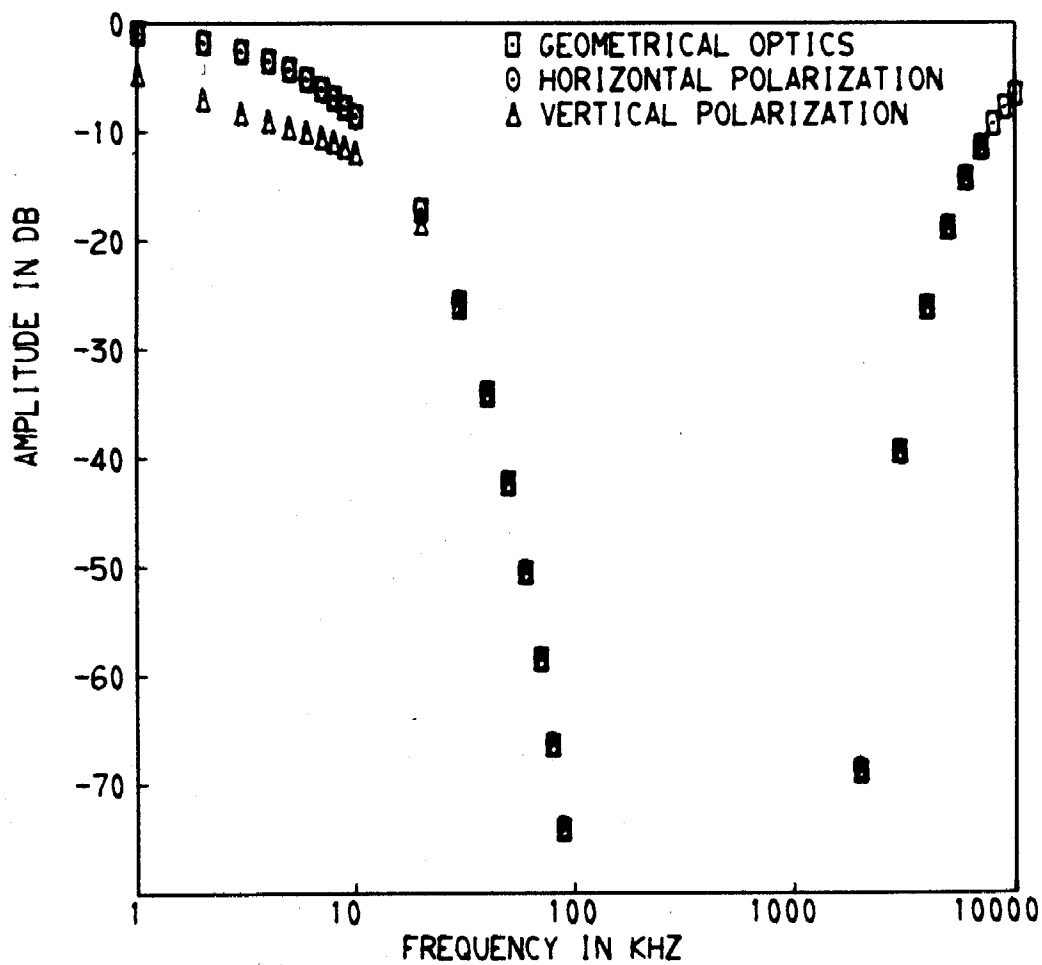
Figure 4.   Comparison of ray theory with full-wave theory—
amplitude of the reflection coefficient for an angle
of incidence of 60°, exponential electron density
and collision frequency profiles.
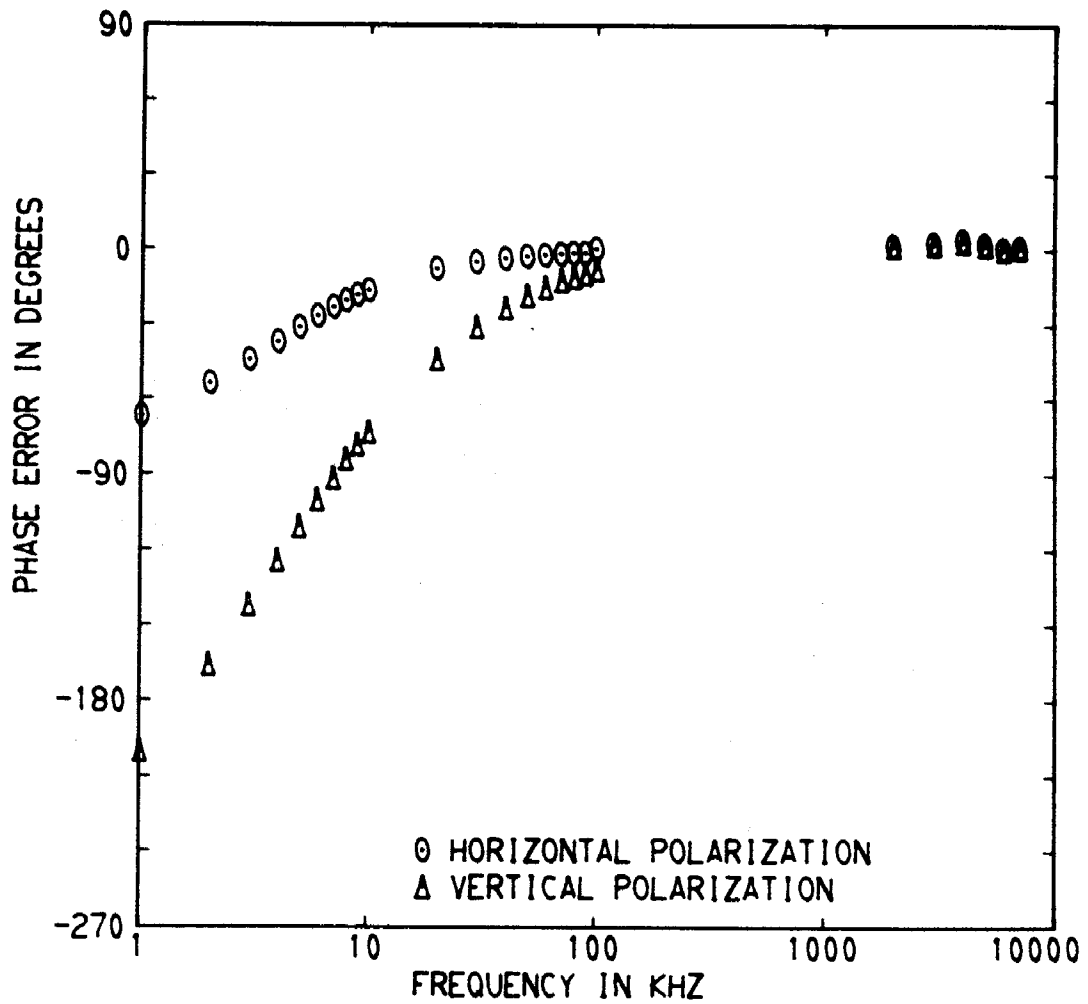
Figure 5. Comparison of ray theory with full-wave theory—phase error for an angle of incidence of 60°, exponential electron density and collision frequency profiles.
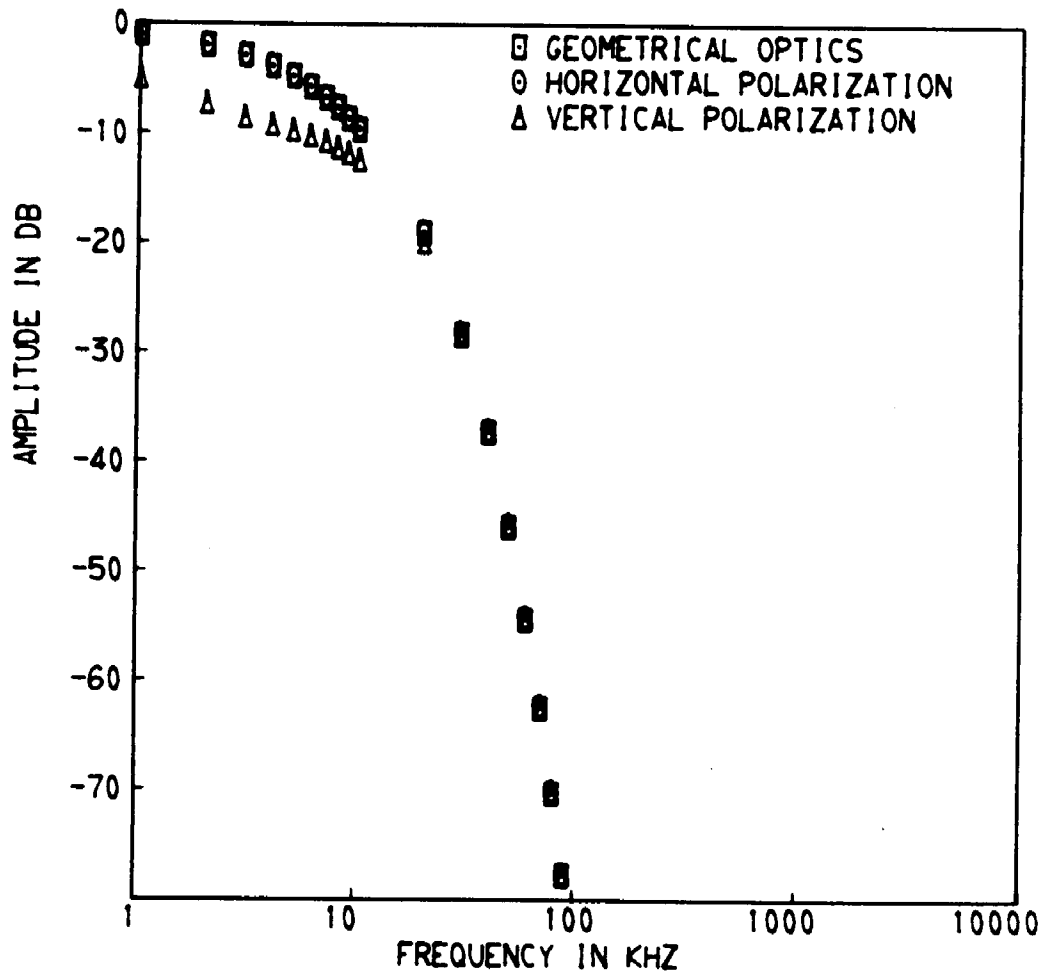
Figure 6. Comparison of ray theory with full-wave theory—
amplitude of the reflection coefficient for an angle
of incidence of 60°, triple-exponential electron
density D-layer profile, exponential collision fre-
quency profile.

through 100 kHz for both horizontal and vertical polarization full wave solutions and for the complex ray solutions. The behavior is essentially the same as for the exponential electron density profile.

Figure 7 shows the phase errors for the same case. Again, the behavior is similar to the previous case.

Triple Exponential Daytime Electron Density Profile, Double Exponential Collision Frequency Profile

This electron density profile represents a typical daytime ionosphere having definite E and E_2 layers, but no structure in the D region. This collision frequency profile, which is made up of two exponential segments, is meant to approximate a typical collision frequency profile with no fine structure. Figures 8 and 9 show the amplitude of the reflection coefficient as a function of frequency for angles of incidence of 0° (normal incidence) and 60°. The behavior is essentially like that of the other two cases, except that there is no difference between the amplitudes of the reflection coefficient for horizontal and vertical polarization at normal incidence. Figures 10 and 11 show the difference in phase of the complex ray solutions and the full wave solution for horizontal and vertical polarization. The behavior is essentially like that of the other two cases except that for normal incidence there is a constant phase difference of 180° between vertical and horizontal polarization due to a difference in definitions of the reflection coefficient for the two polarizations.

Significance of the Phase and Amplitude Errors

For most applications the amplitude errors for these cases are negligible except for vertical polarization below 30 kHz. The
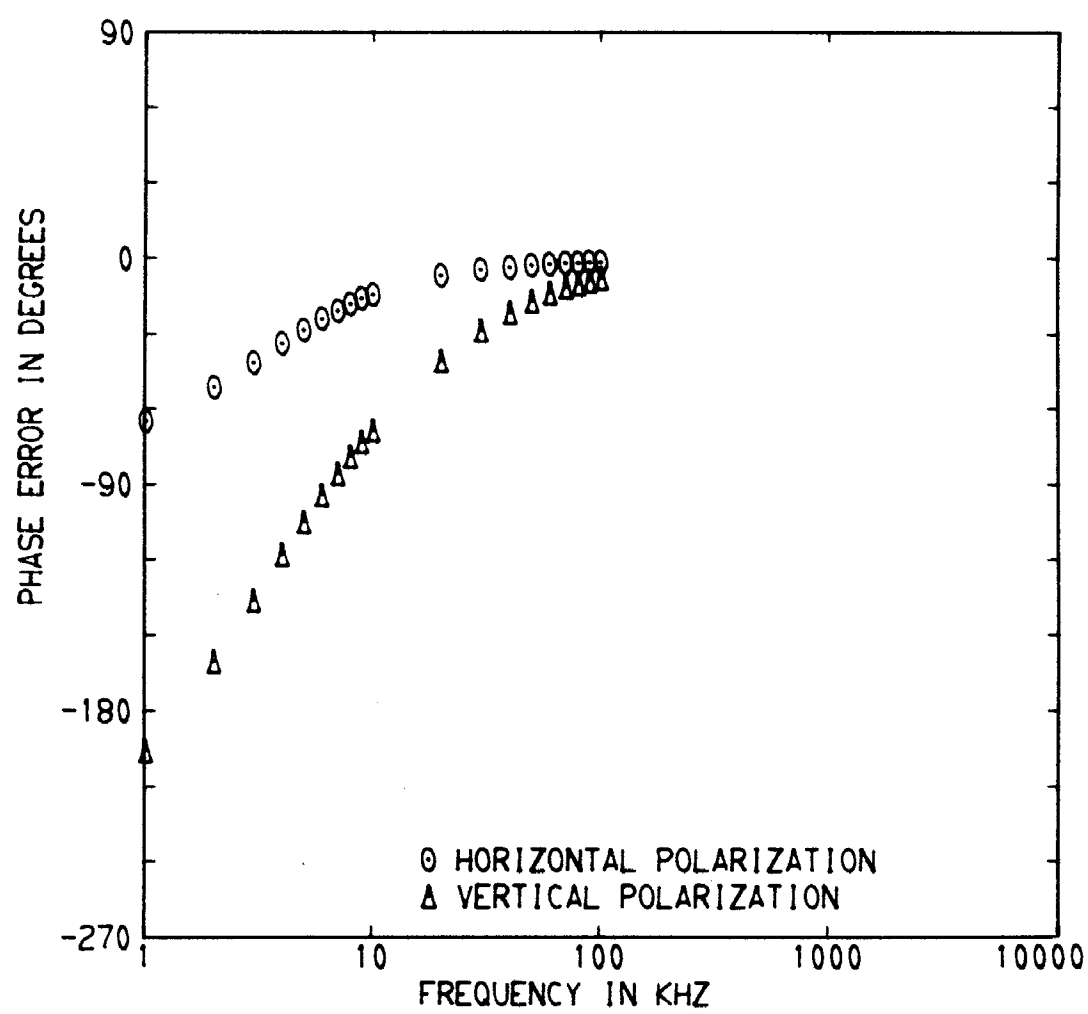
Figure 7. Comparison of ray theory with full-wave theory—
phase error for an angle of incidence of 60°, triple-
exponential electron density D-layer profile, exponential
collision frequency profile.
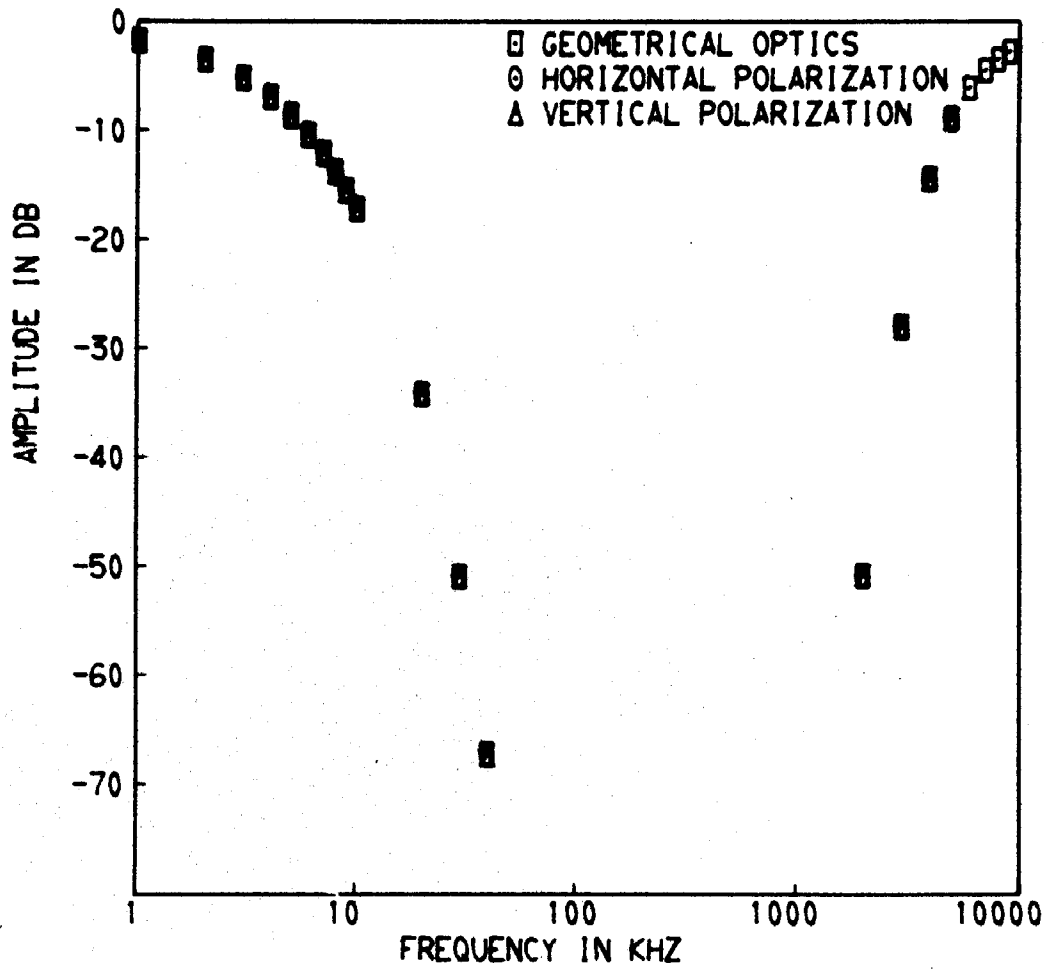
Figure 8.   Comparison of ray theory with full-wave theory—
amplitude of the reflection coefficient for an angle
of incidence of 0°, triple-exponential electron density
profile (daytime model), double-exponential collision
frequency profile.
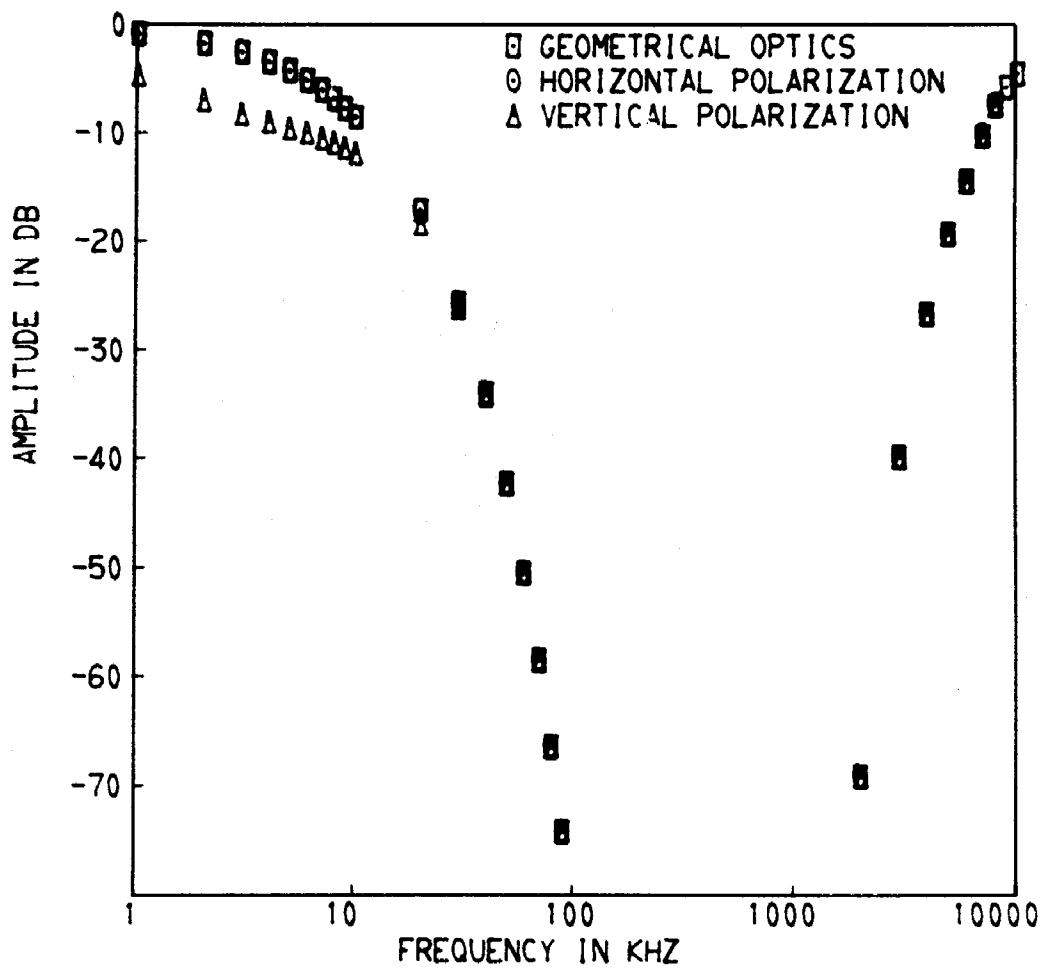
Figure 9.   Comparison of ray theory with full-wave theory—
amplitude of the reflection coefficient for an angle
of incidence of 60°, triple-exponential electron
density profile (daytime model), double-exponential
collision frequency profile.
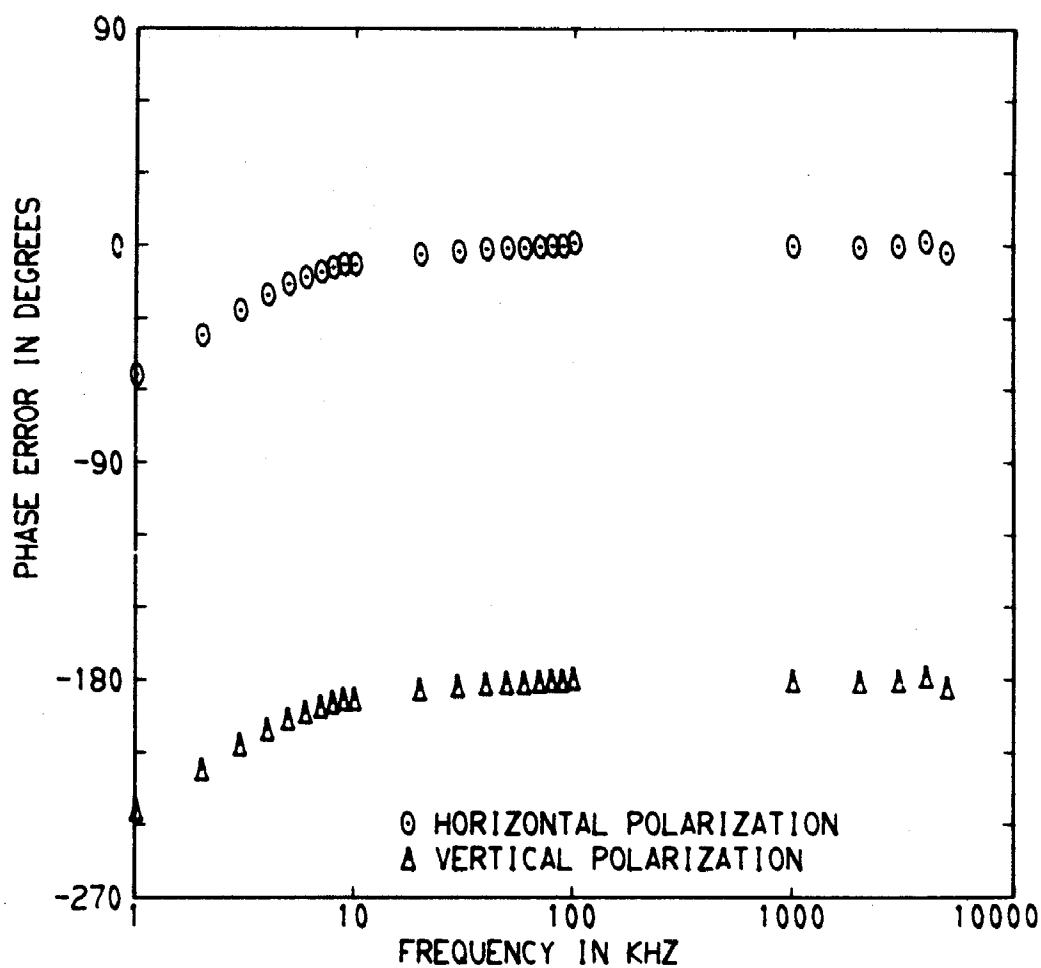
Figure 10. Comparsion of ray theory with full-wave theory—
phase error for an angle of incidence of 0°, triple-
exponential electron density profile (daytime model),
double-exponential collision frequency profile.
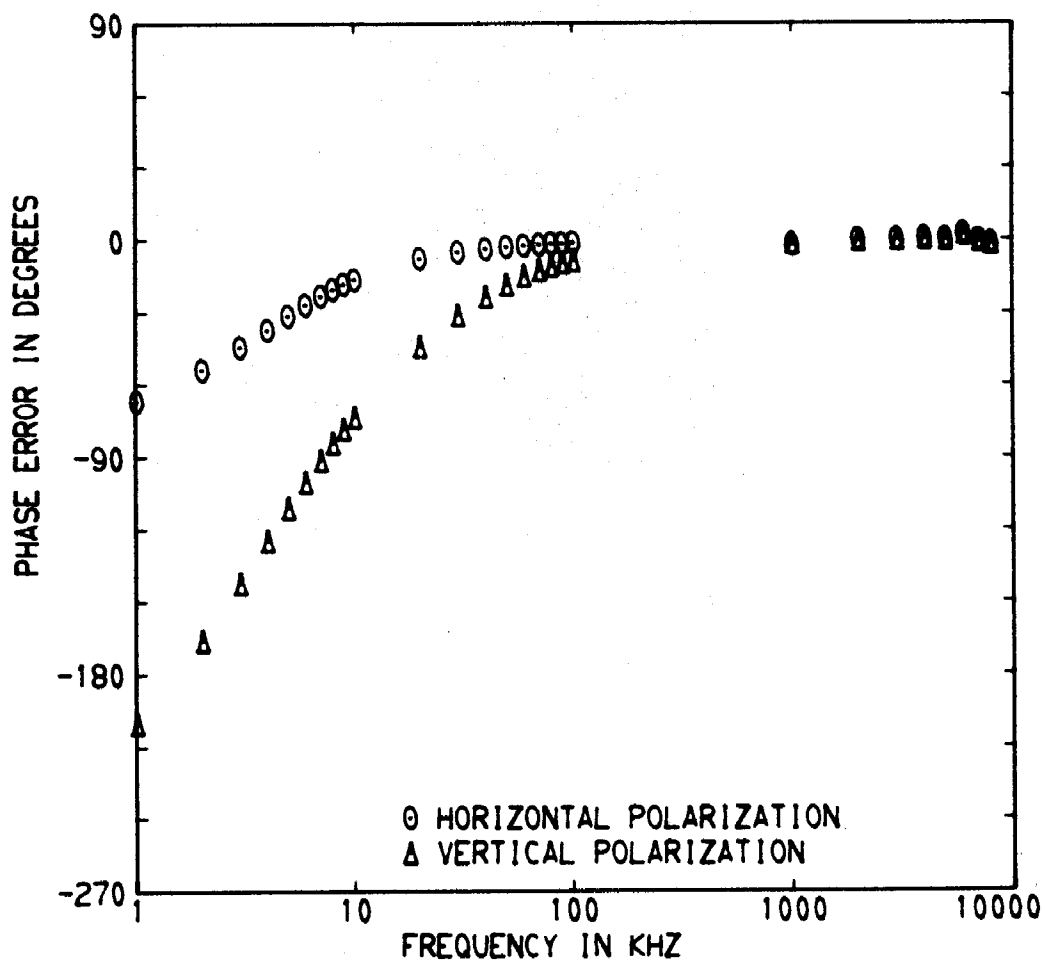
Figure 11. Comparison of ray theory with full-wave theory—
phase error for an angle of incidence of 60°, triple-
exponential electron density profile (daytime model),
double-exponential collision frequency profile.

phase errors increase with decreasing frequency and are greater for vertical than for horizontal polarization.

Also, the phase and amplitude errors decrease with increasing angle of incidence (for oblique incidence) so that the errors for angles of incidence of 70° or 80° should be less than those shown here for 60° for the same cases.

8. Discussion of Part I

The preceding sections demonstrate that ray tracing in complex space can accurately calculate reflection of plane waves from a plane-stratified isotropic medium. Since the method is not restricted to the above case, it is appropriate and useful to extend its application to more general cases. After extending the method, it is unfortunately no longer possible to test its accuracy for the more general cases because practical full-wave solutions are not available for comparison. Nevertheless, the method is useful because it gives solutions to previously insoluble problems.

The method applies to the following generalized cases:

1) An ionosphere that varies arbitrarily but smoothly and slowly.

2) An anisotropic ionosphere.

In making practical calculations it is necessary to include focusing by the ionosphere, defocusing due to reflection from a curved earth (Keller and Keller, 1950), and the reflection coefficient of the ground. This requires a ray tracing program for complex space able to handle arbitrary ionospheric models and to include reflection from a spherical earth for multihop paths. No such program now exists. (The program used for the calculations in section 7 handled only plane-stratified media.) A ray tracing program suitable for modification to trace rays in complex space is one by Jones (1966). It would need two modifications:

1) Change from ray tracing in real space to ray tracing in complex space.

2) Add calculation of focusing in complex space.

The ray tracing program would calculate multihop ray paths for various directions of transmission and punch the results (including phase, amplitude, ground range, and focusing) on cards. A second program would read these cards, include ground-reflection coefficients and antenna patterns, and combine all the contributions from the different rays (usually for different numbers of hops) arriving at the receiver.

As in ordinary ray tracing, the above solution is not valid in two cases:

1) Near a caustic, where a continuum of rays all converge on a point, line, or surface, calculation of focusing by "conservation of energy in a narrow tube of rays" gives an infinite field strength. Although geometrical optics fails to give accurate results near a caustic, the correct field can be calculated in terms of Airy functions (Ludwig, 1966).

2) When a ray grazes the surface of the earth, it excites a diffracted ray which travels along the surface of the earth into the geometrical optical shadow of the earth. Such diffracted rays are important in calculating the total field at LF and therefore must be considered. In fact, they are often more important than the geometrical optical rays. Part II applies the geome-

trical theory of diffraction to solve the problem of diffraction by the

earth.

PART II: DIFFRACTION BY THE EARTH

9. Introduction to Part II

The method of part I, ray tracing in complex space, would be adequate for calculating LF terrestrial radio propagation if diffraction could be ignored. But diffraction must be considered because at LF considerable energy is diffracted around the surface of the earth into the geometrical optical shadow. It is important whenever a discontinuity exists in the medium. In terrestrial radio propagation, the earth's surface diffracts radio waves.

Keller (1962) in his geometrical theory of diffraction (GTD) postulates that diffraction effects can be taken into account in a way analogous to the way geometrical optics deals with propagation of electromagnetic waves in media not involving diffraction, that is, by assuming that the main signal observed is due to energy traveling from the transmitter to the receiver along a number of ray paths which satisfy Fermat's principle. In the case of surface diffraction, the diffracted rays travel along the surface of discontinuity, which in terrestrial radio propagation is along the surface of the earth.

The GTD is not self-contained; that is, it depends on the full-wave solution to a canonical problem to calculate the energy coupled into the diffracted rays. It first calculates the GTD solution for diffraction by a sphere using an unknown diffraction coefficient and then, to evaluate it, compares this solution with the asymptotic high frequency approximation to the rigorous solution to scattering by a sphere. The various necessary coefficients can be

evaluated by comparison with special cases of the rigorous solution.

One important case not covered in the above comparison is that of a surface caustic in the field incident on the sphere. Because of focusing, waves reflected from the ionosphere form a surface caustic in the wave incident on the earth. Its effect can be found by examining the asymptotic high frequency approximation to the rigorous solution of radio propagation between a homogeneous spherical earth and a homogeneous spherically concentric ionosphere (fig. 12). This reveals that the surface caustic behaves like a smeared-out point source in exciting diffracted rays. Separating those terms which depend on the particular ionospheric model (fig. 12) from those which do not, allows application of the method to more general cases, including nonconcentric ionospheres.
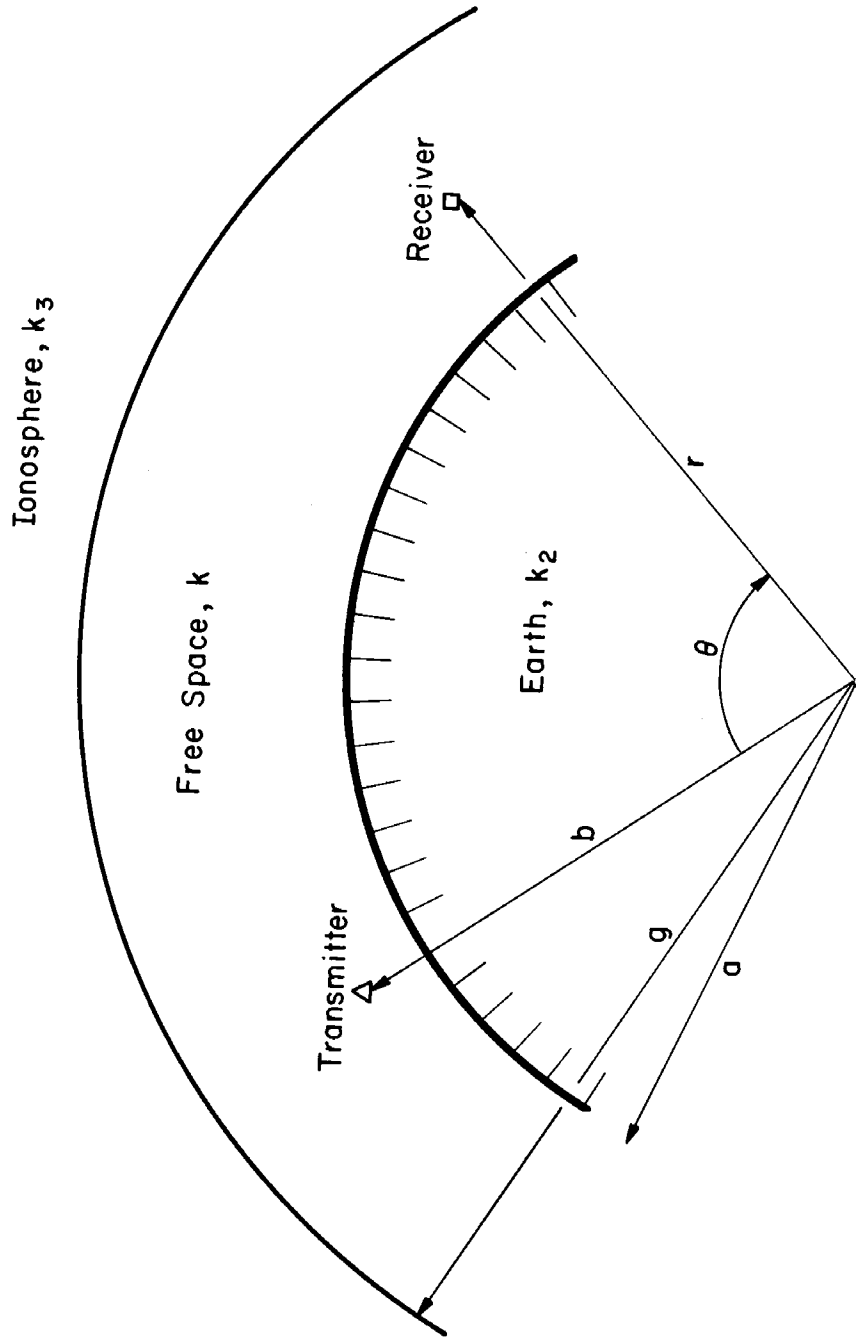
Figure 12. Geometry of the sharply-bounded, concentric ionospheric model.

List of Symbols For Part II

A	defined in (E-36)
Ai(t)	an Airy function
Bi(t)	an Airy function
C	see table 3
D	same as D_ν, a diffraction coefficient (groundwave excitation factor)
D_ν	a diffraction coefficient (groundwave excitation factor (see table 3)
E_r	vertical component of the electric field of a radio wave
E_D	direct field
E_0	ground-reflected field
E_m	mth hop sky wave field (after m reflections from the ionosphere)
$G_\nu(b)$	height gain function (see table 3)
$G_\nu(r)$	height gain function (see table 3 and (I-2) and (I-6))
GTD	geometrical theory of diffraction
$H_\nu^{(1)}(x)$	a Hankel function of kind 1 and order ν with argument x
$H_\nu^{(2)}(x)$	a Hankel function of kind 2 and order ν with argument x
L	a transmitting antenna normalization factor (see (E-1))
LF	low frequency
O	see figure 13
P	see figure 13
P_i	see figure 19
$P_n(\cos\theta)$	a Legendre polynomial of degree n

$P_{\nu-\frac{1}{2}}(\cos\theta)$ a Legendre function of degree $\nu-\frac{1}{2}$

Q see figure 13

Q_i see figure 19

R ground reflection coefficient (see (E-5))

R_ℓ an effective groundwave excitation factor of a point source (see table 3)

S_ℓ shedding coefficient (see table 3)

T ionospheric reflection coefficient (see (E-6))

$\hat{T}$ ionospheric reflection coefficient including the phase integral from the ground up to the ionosphere

Z_g surface impedance of the ground

a radius of the earth

b distance from the transmitter to the center of the earth

e see (K-17)

$f(\nu)$ see (E-7)

$f_m(t)$ see (E-35)

g distance from the earth to the concentric ionosphere of figure 12

h height

i $\sqrt{-1}$

k propagation constant of free space, equal to $\dfrac{2\pi}{\lambda}$

k_2 propagation constant of the earth

k_3 propagation constant of the ionosphere

ℓ in (F-1), an arbitrary distance from a dipole transmitting antenna
in (G-1), a distance defined in (G-10) and figure 16
in (H-1), a small distance from the transmitter
in (J-6), a distance defined in figure 17
in (K-6), a small distance from the point of shedding

ℓ'	in (K-6), a small distance from a caustic in the incident field
ℓ_0	a distance defined in figure 19
$\ell_1,\ \ell_2$	distances defined in figure 18
ℓ_i	a distance defined in figure 19
ℓ_{m+1}	a distance defined in figure 19
ℓ_R	distance from the receiver to the sphere $\dfrac{\nu}{k}$ along a tangent
ℓ_T	distance from the transmitter to the sphere $\dfrac{\nu}{k}$ along a tangent
m	number of hops (reflections from the ionosphere)
n	in appendix E, an integer in section 12, complex phase refractive index
p	same as $p_a{}^g$
$p_a{}^b, p_a{}^r, p_a{}^g,$ $p_b{}^a, p_b{}^g, p_r{}^a$	see general definition of $p_x{}^y$ in (E-3)
q	normalized surface impedance of the ground (see (E-18))
r	distance from the receiver to the center of the earth
s	as used in $\int n\,ds$, path length as a subscript, it labels ground wave modes
t	as used in $e^{i\omega t}$, time otherwise, argument of an Airy function (in (E-29) → (E-32), in (E-58) → (E-68), and outside of appendix E, the same as t_s)
t_s	a root of (E-19)
$w_1(t), w_2(t)$	Airy functions defined in (D-4)
y_b, y_g, y_r	see (E-54)

α	great circle angle traveled by the ground wave along the ground ((K-18) for example)
α_i	see figure 19
$\alpha_1, \alpha_2, \alpha_3, \alpha_m, \alpha_{m-1}$	special cases of α_i
$\hat{\alpha}$	nearly the same as α (see (E-39))
β	see (F-4)
β_1, β_2	see (F-7) and figures 14 and 15
β_3	see (F-11) and figure 15
η_0	impedance of free space
θ	in (E-1), the angle between the polar axis of the dipole transmitting antenna and a straight line from the transmitter and the observer; otherwise, the central angle between the transmitter and receiver (see figure 12)
θ_0	in appendix G, the angle defined in (G-11) in appendix H, the angle defined in (H-5) and figure 16 in appendix K, the angle defined in figure 19
θ_1, θ_2	the angles defined in figure 18
θ_{m+1}	the angle defined in figure 19
λ	wavelength in free space
ν	order of a Hankel function (in (E-29) $\rightarrow$ (E-32), in (E-58) $\rightarrow$ (E-68), and outside of appendix E, same as ν_s)
ν_s	see (E-27)
π	3.141592654 . . .
φ	the angle of the ray with the local vertical
ω	the angular wave frequency

10. Keller's Geometrical Theory of Diffraction
Applied to Scattering by a Sphere

The geometrical theory of diffraction (GTD) is an extension of geometrical optics in that the GTD also includes diffracted rays, which are associated with discontinuities in the medium. In many ways they are analogous to the reflected and refracted rays of geometrical optics. Just as there are reflection and transmission coefficients in geometrical optics, there are diffraction coefficients in the geometrical theory of diffraction.

Diffracted rays have many of the properties of the ordinary rays of geometrical optics. Like reflected and refracted rays, diffracted rays obey Fermat's principle. Applied to the sphere, this principle gives the paths shown in figure 13 for various locations of the source and observation point (transmitter and receiver). In figure 13a the ray following the curvature of the sphere is the diffracted ray, and the ray shed tangentially from the sphere is also an ordinary geometrical optics ray. Several properties of the diffracted ray can be inferred from this application of Fermat's principle:

a) Surface diffracted rays are produced when geometrical optics rays graze the surface.

b) Surface diffracted rays are produced when a source is on or near the surface.

c) Surface diffracted rays follow a great circle on a sphere.

d) Surface diffracted rays shed geometrical optical rays tangen-

(a)

(b)

(c)
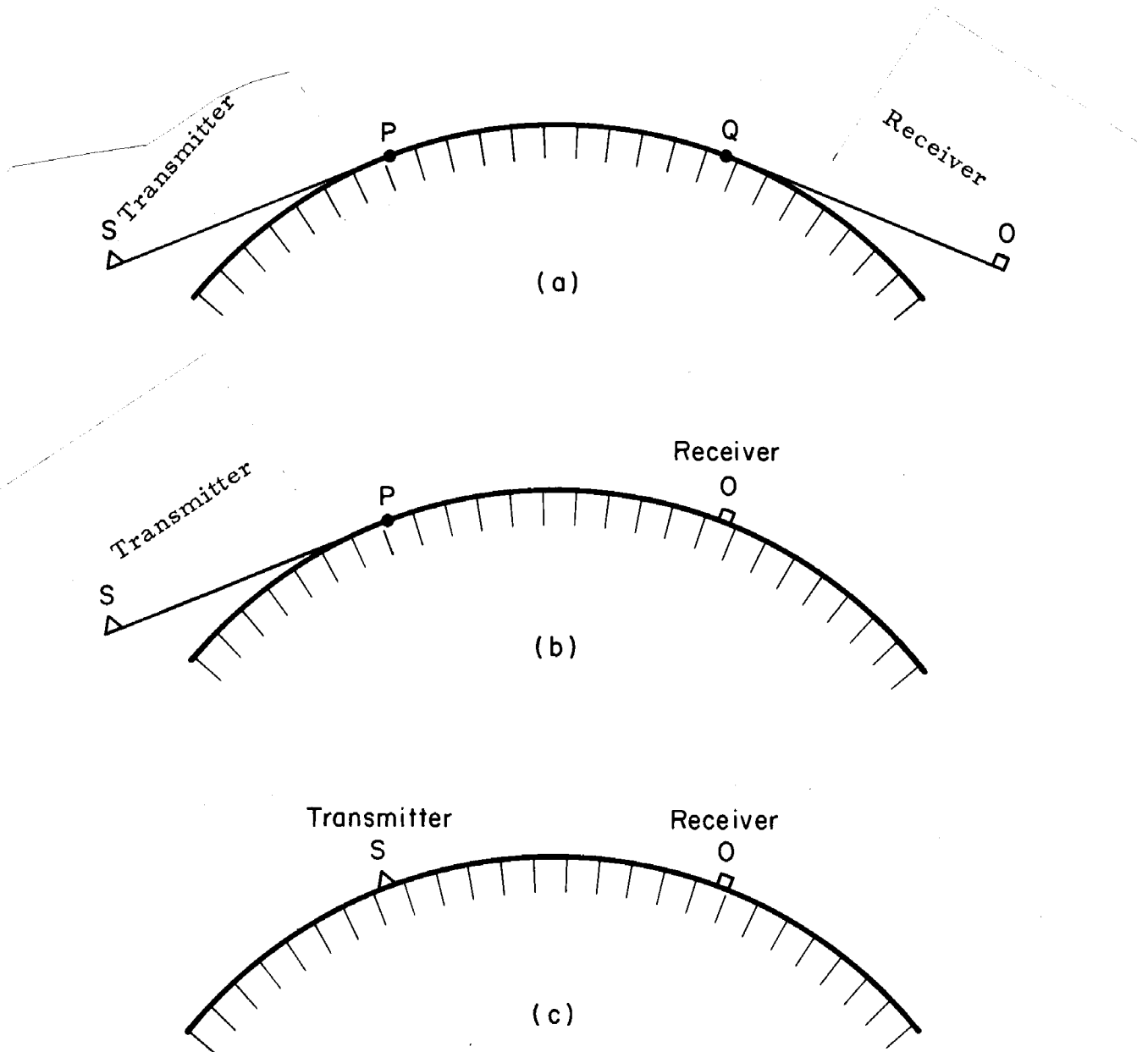
Figure 13. Diffracted rays of the geometrical theory of diffraction.

tially from the sphere.

Once generated, diffracted rays behave like the ordinary rays of geometrical optics with respect to reflection, refraction, focusing, and attenuation. For instance, the surface-diffracted ray will undergo azimuthal focusing on the sphere.

The GTD cannot evaluate diffraction coefficients. This must be done by comparing the GTD solution with an asymptotic high frequency approximation to the rigorous solution for scattering by a sphere. When the comparison is made, the rigorous solution can be interpreted in terms of surface rays traveling around the sphere and shedding rays tangentially. In fact, an infinite number of these rays exists, each with its own characteristic wavelength and attenuation coefficient. These are the familiar groundwave modes of terrestrial radio propagation. For LF radio propagation, the propagation constants of these modes, though differing slightly, are nearly equal to the propagation constant of free space for that frequency.

Application of the GTD assumes that diffraction is a local phenomenon. If the diffracting body is not spherical, the theory still applies if the body behaves locally like a sphere with a radius equal to the local radius of curvature of the body at the point of incidence of the ray. We also assume that the theory applies to diffraction of waves with phase fronts of a more general shape than those of the known rigorous solution.

11. Interpretation of LF Terrestrial Radio
Propagation in Terms of the
Geometrical Theory of Diffraction

In applying the GTD to LF terrestrial radio propagation, I use the basic method of Levy and Keller (1959), but depart slightly in detail. Specifically, I use a slightly different path for the diffracted ray and define diffraction coefficients differently in constructing the GTD solution. Appendices G, H, I, and J compare the GTD solution with the rigorous solution to evaluate the diffraction coefficients.

11.1 Characteristics of the Groundwave

Before applying the GTD, it is necessary to know the characteristics of the groundwave. These are found from the rigorous solution for scattering of radio waves by a sphere in appendix E. The groundwave varies along the ground as

$$e^{-i\nu\theta} , \tag{11.1}$$

where θ is the great circle angle from the point of excitation of the groundwave, and ν is the characteristic (angular) propagation constant of the groundwave mode ν. The height variation of the vertical component of the electric field is

$$\frac{H_\nu^{(2)}(kr)}{r^{\frac{3}{2}}} , \tag{11.2}$$

where $H_\nu(kr)$ is a Hankel function, and r is the distance from the center of the earth.

11.2 Interpretation of the Asymptotic High Frequency
Approximation to Scattering by a Sphere

The GTD solution constructed with a path slightly different

from that used by Levy and Keller (1959) for the diffracted

rays agrees more closely with the asymptotic approxi-

imation to the rigorous solution. By examining this approximation

to the rigorous solution, appendix F proposes two paths for the dif-

fracted ray. The first, which seems more appropriate for $\left|\frac{\nu}{k}\right| > a$,

is shown in figure 14. This ray is composed of three parts: a

straight line from the transmitter tangent to a sphere of radius $\frac{\nu}{k}$,

an arc along the sphere $\frac{\nu}{k}$, and a ray shed tangentially from the

sphere $\frac{\nu}{k}$ and traveling in a straight line to the receiver. The sec-

ond, shown in figure 15, seems to be more appropriate for $\left|\frac{\nu}{k}\right| < a$

and is also composed of three parts: a straight line from the trans-

mitter to the earth incident at an angle $\sin^{-1}\frac{\nu}{ka}$, an arc along the

ground, and a straight line to the receiver leaving the earth at the

same angle $\sin^{-1}\frac{\nu}{ka}$. Both satisfy Fermat's principle according

to Keller's (1962) specification for diffracted rays.

Since $\left|\frac{\nu}{k}\right| > a$ for all groundwave modes, the path of figure 14

is more useful for interpreting LF terrestrial radio propagation

and is therefore used in constructing the GTD solution. In this

interpretation, the groundwave is represented by a ray which

travels horizontally at a height $\frac{\nu}{k} - a$. Since ν is complex, the

radius $\frac{\nu}{k}$ is complex, so there is no real height $\frac{\nu}{k} - a$ where the ray

A diffracted ray representation of the ground wave for $|\nu/k| > a$.

Figure 14.

Receiver

$\frac{\nu}{k} \tan \beta_2 = \sqrt{r^2 - \left(\frac{\nu}{k}\right)^2}$

$r = \frac{\nu}{k} \sec \beta_2$

β_2

$\frac{\nu}{k}$

$\theta - \beta_1 - \beta_2$

θ

$\frac{\nu}{k}$

β_1

a

Center of Earth

Surface of Earth

$b = \frac{\nu}{k} \sec \beta_1$

$\frac{\nu}{k} \tan \beta_1 = \sqrt{b^2 - \left(\frac{\nu}{k}\right)^2}$

Transmitter

Figure 14

Figure 15. A diffracted ray representation of the ground wave
for $|\nu/k| < a$.
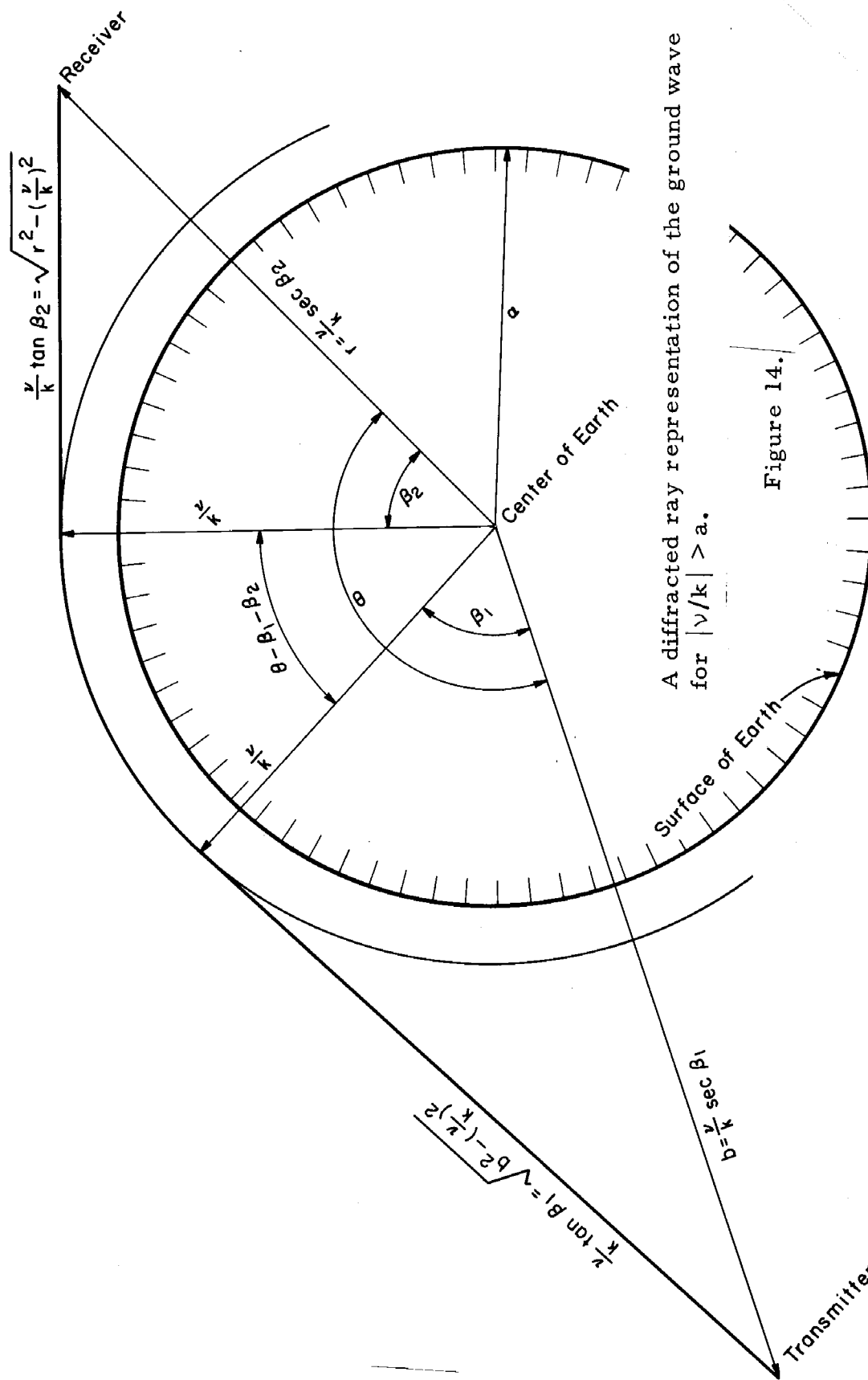
appears to travel. Since part I shows that rays in complex space are useful, I will continue to talk of rays grazing and shedding from the sphere $\frac{\nu}{k}$.

11.3 Definition of Diffraction Coefficients

Although the definition of diffraction coefficients is somewhat arbitrary, a given application makes one definition more useful than another. In applying the GTD to LF radio propagation, I could have used the diffraction coefficients defined by Levy and Keller (1959), but I found that definitions based on the following guidelines simplify the results:

1) Define all coefficients as dimensionless. (Since the coefficients of Levy and Keller have the dimensions of length$^{\frac{1}{4}}$, they are not strictly analogous to reflection and transmission coefficients.)

2) Relate the incident field to the ground wave field with a diffraction coefficient (excitation factor).

3) Treat a source near the ground as a special case.

4) Relate the ground wave to the field radiated from the ground wave with a shedding coefficient.

11.4 Excitation of the Groundwave

A groundwave is excited when a ray from a distant source grazes the sphere of radius $\frac{\nu}{k}$. It is useful to define the diffraction coefficient as an excitation factor equal to the ratio of the ground wave field at the height $\frac{\nu}{k}$ - a to the incident field at the same point. Appendix G compares the GTD solution with the rigorous solution of appendix E for the case of figure 16 to evaluate this diffraction coefficient as

$$D_\nu = \frac{-2i \sqrt{\pi}}{t - q^2} \frac{w_1(0)}{w_1(t)^2} \quad , \tag{11.3}$$

where the various terms are explained in table 3.

A point source (short vertical dipole) at a height $\frac{\nu}{k}$ -a can also excite a groundwave. For this case it is useful to define a factor R_ℓ as the ratio of the effective excitation field (as though from a distant source) to the radiation field of the point source a small distance ℓ from the source. Appendix H compares the GTD with the rigorous solution of appendix E for the case of figure 17 to evaluate this coefficient as

$$R_\ell = e^{i\,\pi/4}\, w_1(0) \left(\frac{ka}{2}\right)^{\frac{1}{6}} \left(\frac{\ell}{a}\right)^{\frac{1}{2}}. \tag{11.4}$$

11.5 The Height Gain Function

A point source near the ground, at a height other than $\frac{\nu}{k}$ -a, still excites a groundwave, but its effectiveness depends on its height. Although a height gain function $G_\nu(b)$ is usually defined relative to the ground, it is more useful here to define it as the
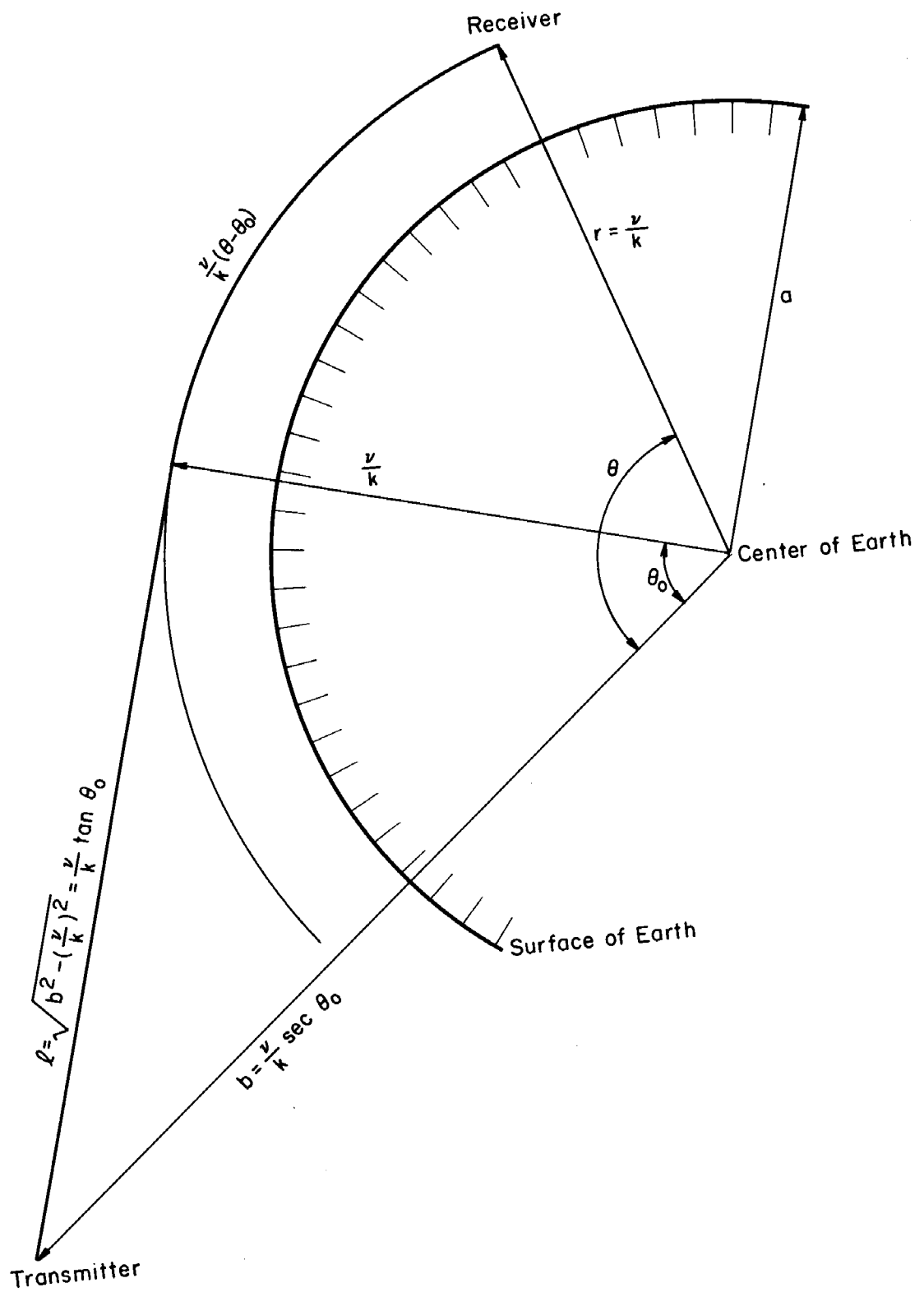
Figure 16. Diffracted rays for the case used to evaluate the diffraction coefficient.
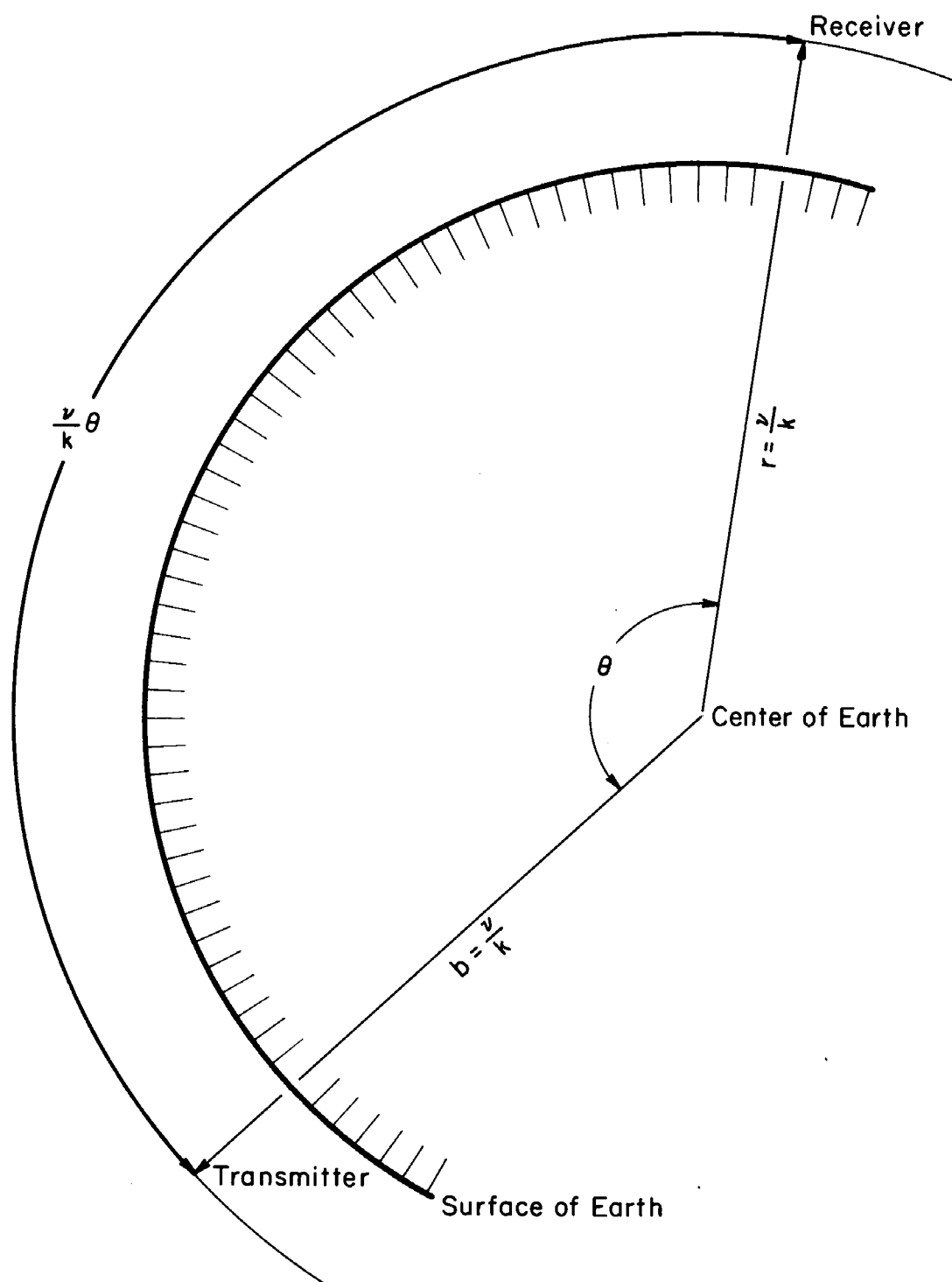
Figure 17. Diffracted rays for the case used to evaluate the point-source excitation factor.

ratio of the effect of a point source at a height b - a in exciting a

groundwave mode to that at a height $\frac{\nu}{k}$ -a. Appendix I, using the

dependence on the transmitter height of the field scattered by a

sphere, evaluates the height gain function

$$. \ G_\nu(b) = \left(\frac{\nu}{kb}\right)^{\frac{3}{2}} \sqrt{\frac{2}{k}} \left(\frac{-y_b}{b^2 - (\frac{\nu}{k})^2}\right)^{\frac{1}{4}} \left(\frac{\nu}{2}\right)^{\frac{1}{3}} \frac{w_1(y_b)}{w_1(0)} \ , \qquad (11.5)$$

where

$$\frac{2}{3}(-y_b)^{\frac{3}{2}} = \sqrt{(kb)^2 - \nu^2} - \nu \cos^{-1}\frac{\nu}{kb} \ , \qquad (11.6)$$

or, for $b \approx \frac{\nu}{k}$,

$$G_\nu(b) = \left(\frac{\nu}{kb}\right)^{\frac{3}{2}} \frac{w_1\left((\frac{2}{\nu})^{\frac{1}{3}}(\nu - kb)\right)}{w_1(0)} \ . \qquad (11.7)$$

11.6 Radiation from the Groundwave

Equation (11.2) gives the height variation of the vertical com-

ponent of the electric field in the groundwave. Appendix I uses

(11.2) to calculate the ratio of the vertical component of the electric

field of the groundwave at a height r - a to that at a height $\frac{\nu}{k}$ - a.

The result is the same height gain function as (11.5)

$$G_\nu(r) = \left(\frac{\nu}{kr}\right)^{\frac{3}{2}} \sqrt{\frac{2}{k}} \left(\frac{-y}{r^2 - (\frac{\nu}{k})^2}\right)^{\frac{1}{4}} \left(\frac{\nu}{2}\right)^{\frac{1}{3}} \frac{w_1(y)}{w_1(0)} \ , \qquad (11.8)$$

where

$$\frac{2}{3}(-y)^{\frac{3}{2}} = \sqrt{(kr)^2 - \nu^2} - \nu \cos^{-1}\frac{\nu}{kr} \ . \qquad (11.9)$$

Although the height gain function (11.8) could be used for all heights, appendix F shows that the field at large heights can be interpreted as being radiated tangentially from the sphere $\frac{\nu}{k}$. It is then convenient to define a shedding coefficient S_ℓ equal to the ratio of the radiation field at a small distance ℓ from the point of shedding to the field of the ground wave at the same point. Appendix J compares the GTD solution with the rigorous solution given by appendix E for the case of figure 18 to evaluate this shedding coefficient:

$$S_\ell = \frac{e^{-i\,\pi/4}}{w_1(0)} \left(\frac{2}{ka}\right)^{\frac{1}{6}} \left(\frac{a}{\ell}\right)^{\frac{1}{2}}. \qquad (11.10)$$

Notice that S_ℓ is the reciprocal of R_ℓ.

Table 3 summarizes the definitions and values of these coefficients.
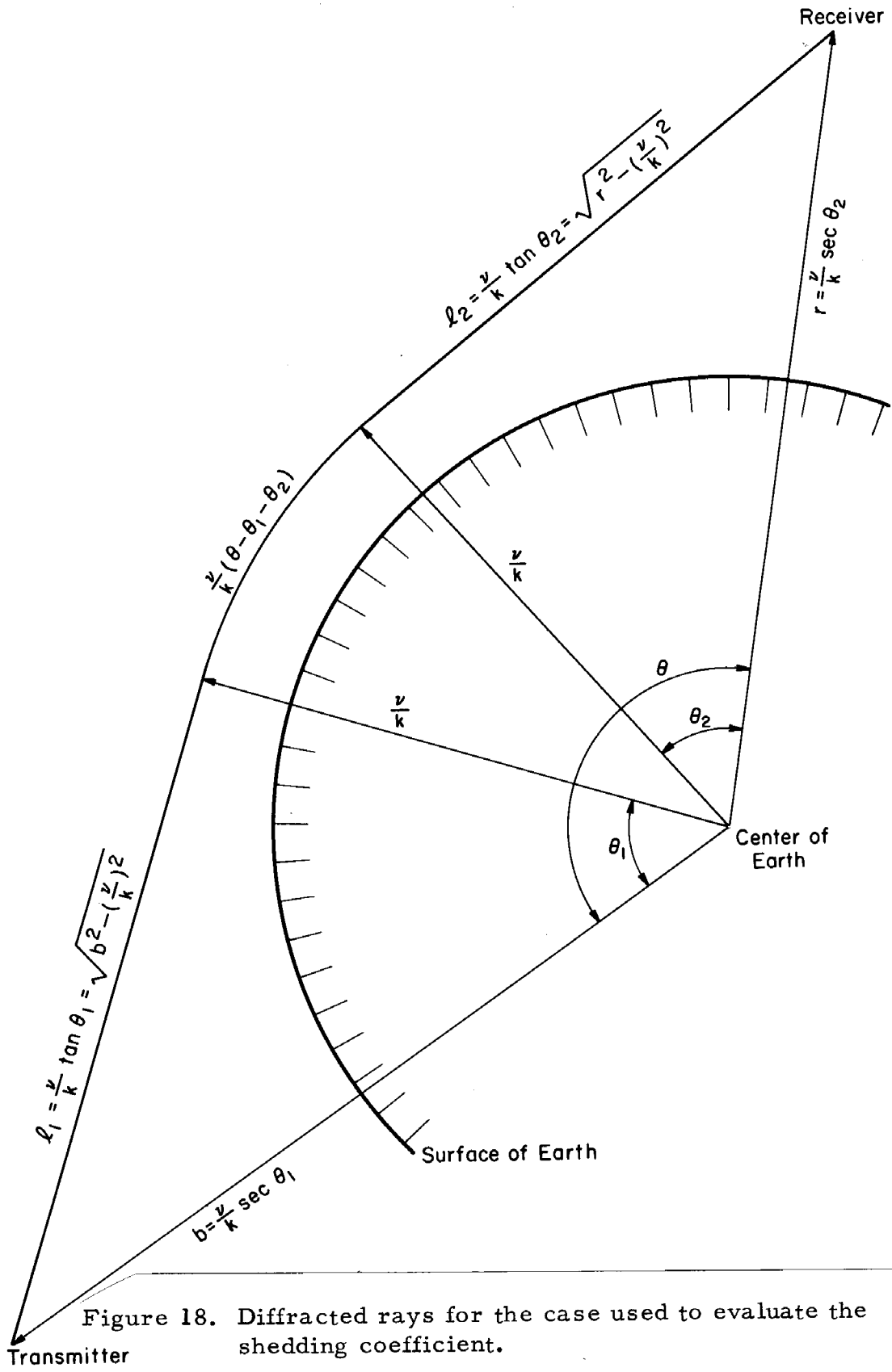
Figure 18. Diffracted rays for the case used to evaluate the shedding coefficient.

Table 3. Propagation, excitation, and radiation properties of the ground wave

Angular propagation constant. Propagation along the ground, $e^{-i\nu\alpha}$	$\nu = ka + \left(\frac{ka}{2}\right)^{\frac{1}{3}} t$ (see note)
Diffraction coefficient. An excitation factor equal to the ratio of the excited ground wave field at the height $\nu/k - a$ to the incident field of a horizontal ray at the same point.	$D_\nu = \frac{-2 i \sqrt{\pi}}{t - q^2} \frac{w_1(0)}{w_1(t)^2}$
Effective excitation factor of a point source. Ratio of the field effective in exciting a ground wave to that of a point source a small distance l from the source. It also applies to a focus or caustic in the incident field.	$R_l = e^{i\pi/4}\, w_1(0) \left(\frac{ka}{2}\right)^{\frac{1}{6}} \left(\frac{l}{a}\right)^{\frac{1}{2}}$
Height gain function. Ratio of the vertical component of the electric field of the ground wave at a height $h = r - a$ to that at a height $\nu/k - a$. Also equal to the ratio of the effect of a small vertical dipole source in exciting the ground wave at a height $h = r - a$ to that at a height $\nu/k - a$.	$G_\nu(r) = \left(\frac{\nu}{kr}\right)^{\frac{3}{2}} \sqrt{\frac{2}{k}} \left(\frac{-\gamma}{r^2 - \frac{\nu^2}{k}}\right)^{\frac{1}{4}} \left(\frac{\nu}{2}\right)^{\frac{1}{3}} \frac{w_1(y)}{w_1(0)}$ $\frac{2}{3}(-y)^{\frac{3}{2}} = \sqrt{(kr)^2 - \nu^2} - \nu \cos^{-1}\frac{\nu}{kr}$
Shedding coefficient. Ratio of the radiation field at a small distance l from the point of shedding along a tangent to the sphere ν/k to the field of the ground wave at the same point.	$S_l = \frac{e^{-i\pi/4}}{w_1(0)} \left(\frac{2}{ka}\right)^{\frac{1}{6}} \left(\frac{a}{l}\right)^{\frac{1}{2}} = \frac{1}{R_l}$
Coefficient of integration over important ray paths. Contribution of paths per central earth angle when a continuum of important paths connect the transmitter with the receiver.	$C = \frac{\left(\frac{ka}{2}\right)^{\frac{1}{3}}}{w_1(0)\sqrt{\pi}}$

Note:
α is the central earth angle measured from the excitation point.
k is the propagation constant of free space.
a is the radius of the earth.
t is a root of $w_1'(t) = q\, w_1(t)$
$w_1(t) = \sqrt{\pi}\,(Bi(t) - i\, Ai(t))$
Ai and Bi are Airy functions
$$q = -i\left(\frac{ka}{2}\right)^{\frac{1}{3}} \frac{Z_g}{\eta_0} = -i\left(\frac{ka}{2}\right)^{\frac{1}{3}} \sqrt{\left(\frac{k_2}{k}\right)^2 - \left(\frac{\nu}{ka}\right)^2} \bigg/ \left(\frac{k_2}{k}\right)^2 \approx -i\left(\frac{ka}{2}\right)^{\frac{1}{3}} \sqrt{\left(\frac{k_2}{k}\right)^2 - 1} \bigg/ \left(\frac{k_2}{k}\right)^2$$

Z_g is the surface impedance of the ground.
η_0 is the impedance of free space.

12. Multihop Propagation for Reflection From a Concentric Ionosphere

For the ionospheric model of figure 12 a short, vertical-dipole transmitting antenna at a distance b from the center of the earth is excited with a sinusoidal source $e^{i\omega t}$. Its radiation pattern is given by (E-1). A short, vertical-dipole receiving antenna at a great circle angle θ from the transmitting antenna is a distance r from the center of the earth.

If the earth cuts off the direct line-of-sight ray from the transmitter to the receiver, the vertical electric field at the receiver is

$$E_r = \sum_{m=0}^{\infty} E_m \, , \qquad (12.1)$$

where E_m is the field of the wave which has reflected from the ionosphere m times. From (E-32) and (E-58), using the interpretations of appendix K,

$$E_m = \frac{-L \, \pi\sqrt{2\pi} \, e^{i\pi/4}}{k \, b^{\frac{3}{2}} \, r^{\frac{3}{2}} \, m! \, \sqrt{\sin\theta}} \left(\frac{ka}{2}\right)^{\frac{1}{3}} \sum_{\nu} \nu^{\frac{5}{3}}$$

$$\frac{H_\nu^{(2)}(kb) \, H_\nu^{(2)}(kr)}{w_1(t)^2 \, (t - q^2)} \, e^{-i\nu(\theta \, - \, 2m \, \cos^{-1}\frac{\nu}{kg})} (D_\nu \, C \, \hat{\alpha} \, \hat{T})^m . \quad (12.2)$$

Equation (12.2) is valid for all m such that the receiver is in the shadow of the mth hop and that

$$\hat{\alpha} = \theta - 2m \cos^{-1}\frac{\nu}{kg} + i \, \frac{\cos^{-1}\frac{\nu}{kb}}{\sqrt{-y_b}} \frac{w_1'(y_b)}{w_1(y_b)} + i \, \frac{\cos^{-1}\frac{\nu}{kr}}{\sqrt{-y_r}} \frac{w_1'(y_r)}{w_1(y_r)}$$

$$- \left(\frac{2}{ka}\right)^{\frac{1}{3}} \left(\left(\frac{m + 1 - p_r^a - p_r^a}{2}\right)w_1(t) w_2(t)(t - q^2) + (m+1)iq + \frac{i(m+1)}{2(t-q^2)}\right) \quad (12.3)$$

is not too near zero. The coefficients D_ν and C are explained in table 3. The parameter

$$\hat{T} = T\, e^{-2i\sqrt{(kg)^2 - \nu^2}} \tag{12.4}$$

is interpreted as the complete ionospheric reflection coefficient including the phase integral from the height $\frac{\nu}{k} - a$ up to the iono-sphere and back. The generalization of (12.4) for an arbitrary concentric ionosphere is

$$\hat{T} = i\, e^{-ik\int_s nds}, \tag{12.5}$$

where the path of integration in (12.5) is determined by Hamilton's equations (or Haselgrove's equations) for ray tracing in complex space with the following conditions:

1) The ray must begin and end at the complex height $\frac{\nu}{k} - a$.

2) The ray must leave and arrive horizontally.

These conditions are not independent. Since the ionosphere is concentric, Bouguer's rule (Kelso, 1964),

$$n\, r\, \sin\varphi = \text{constant}, \tag{12.6}$$

must be satisfied. Thus, if the ray leaves the height $\frac{\nu}{k} - a$ horizontally, it must be horizontal when it gets back to that height. Notice that for a particular ionosphere only one ray path need be calculated for each frequency and each ground wave mode. The same ray path will apply for any number of hops and any distance (beyond the shadow boundary).

Two special cases of (12.2) are of interest. First, for the trans-

mitter and receiver high above the ground (see fig. 19), from (E-63),

$$E_m = - \frac{i\ L\ 2\sqrt{2\pi}\ e^{i\pi/4}}{k^2\ r^{\frac{3}{2}}\ b^{\frac{3}{2}}\ m!\ \sqrt{\sin\theta}} \left(\frac{ka}{2}\right)^{\frac{1}{3}} \sum_\nu \nu^{\frac{5}{3}} \frac{e^{-i\nu\alpha}}{w_1(t)^2(t-q^2)}$$

$$\frac{e^{-ik\ell_T}}{\sqrt{\ell_T}}\ \frac{e^{-ik\ell_R}}{\sqrt{\ell_R}} \left(D_\nu\ C\ \hat{\alpha}\ \hat{T}\right)^m , \qquad (12.7)$$

where, from (E-64)

$$\alpha = \theta - \cos^{-1}\frac{\nu}{kb} - \cos^{-1}\frac{\nu}{kr} - 2m\cos^{-1}\frac{\nu}{kg} \qquad (12.8)$$

is the great circle angle traveled by the ground wave mode, and

from (E-65)

$$\hat{\alpha} = \alpha - \left(\frac{2}{ka}\right)^{\frac{1}{3}} \left(\frac{m+1-p_b\frac{a}{}-p_r\frac{a}{}}{2}\ w_1(t)\ w_2(t)\ (t-q^2) + (m+1)\ iq \right.$$

$$\left. + \frac{i\ (m+1)}{2\ (t-q^2)}\right) . \qquad (12.9)$$

Second, for the transmitter and receiver on the ground, b = r = a,

so that, from (E-67),

$$E_m = \frac{L\sqrt{2\pi}\ e^{i\pi/4}}{k\ a^3\ m!\ \sqrt{\sin\theta}} \left(\frac{2}{ka}\right)^{\frac{1}{3}} \sum_\nu \nu^{\frac{5}{3}} \frac{e^{-i\nu\alpha}}{t-q^2} \left(D_\nu\ C\ \hat{\alpha}\ \hat{T}\right)^m , \qquad (12.10)$$

where

$$\alpha = \theta - 2m\cos^{-1}\frac{\nu}{kg} , \qquad (12.11)$$

and, from (E-68),

$$\hat{\alpha} = \alpha - \left(\frac{2}{ka}\right)^{\frac{1}{3}} \left(\frac{m-1}{2}\ w_1(t)\ w_2(t)\ (t-q^2) + (m-1)iq + \frac{i(m+1)}{2(t-q^2)}\right) . \qquad (12.12)$$
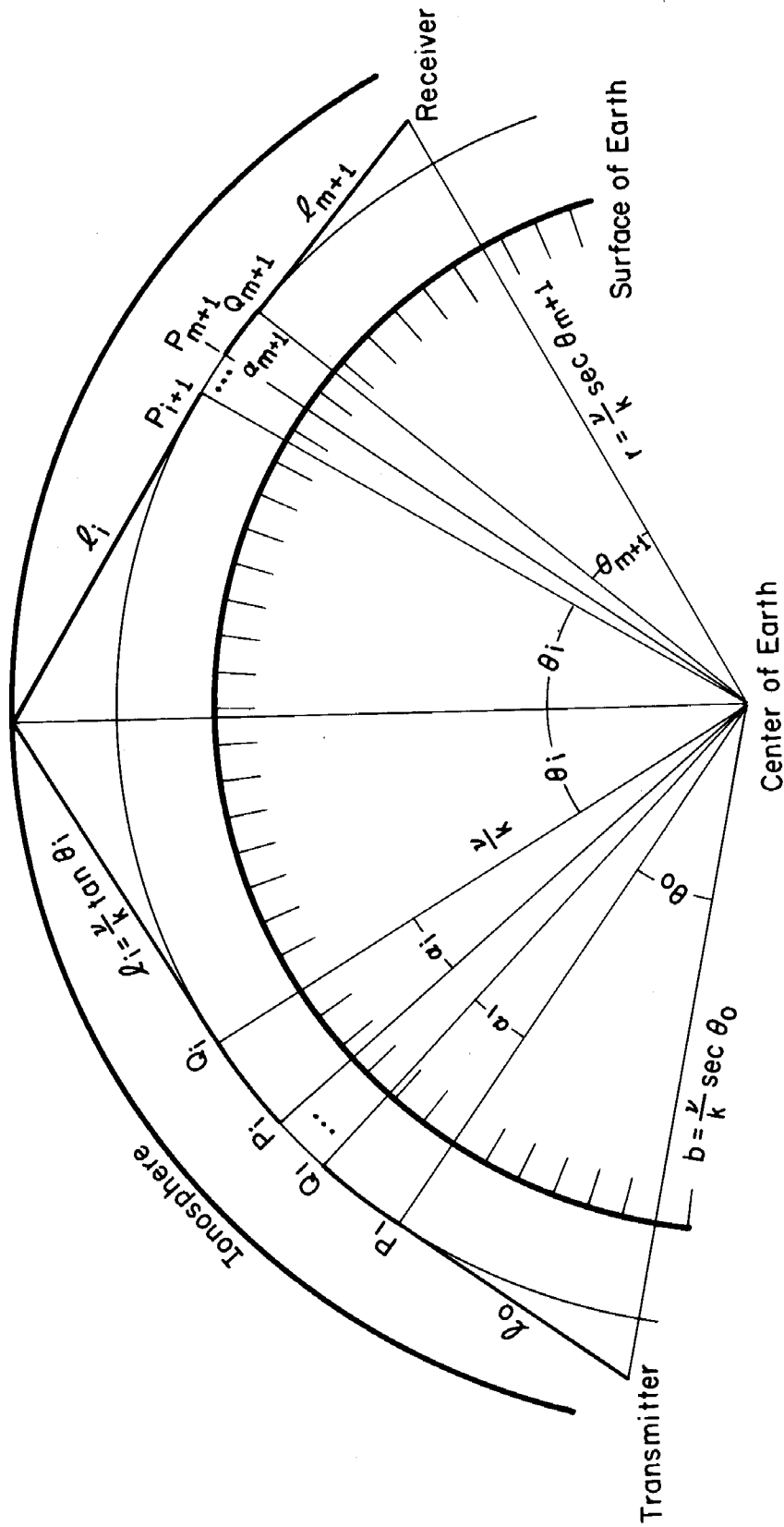
Figure 19. Diffracted rays for multihop propagation with reflection from a sharply-bounded, concentric ionosphere.

The difference between $\hat{\alpha}$ and α is due to excitation of and shedding

from the groundwave taking a nonzero amount of room. As can be

seen from (12. 12), this difference decreases with frequency. In fact,

it can often be neglected if the frequency is high enough or α is large

enough.

In generalizing (12. 10) to apply to an arbitrary concentric

ionosphere, the angle α is the total ground distance traveled by

the groundwave, and $\hat{T}$ is given by (12. 5). Often

$$\nu^{\frac{5}{2}} \approx (ka)^{\frac{5}{2}} \qquad (12.13)$$

is a good approximation. Notice that the factor $\hat{\alpha}^m$ in (12. 10) will

cause E_m to attenuate slower with distance than the ground wave.

Equation (12. 10) represents a rigorous solution of the problem

(with a few approximations). It is also derived in appendix K using

the geometrical theory of diffraction. Actually, the derivation in

appendix K really justifies the applicability of the GTD and interprets

the various factors in the solution in terms of the GTD. The agree-

ment with the rigorous solution backs these interpretations. In partic-

ular, it justifies treating a focus of rays reflected from the iono-

sphere as a source even when it is close to the ground.

Figure 20 shows a comparison of (12. 10) using only one ground-

wave mode with the more rigorous (E-12) (Berry and Chrisman,

1965a) for b=r=a, m=2, T=1, f=100 kHz, g-a=70 km, ground

conductivity $\sigma = .01$ mhos/m, and ground permittivity = 15. The
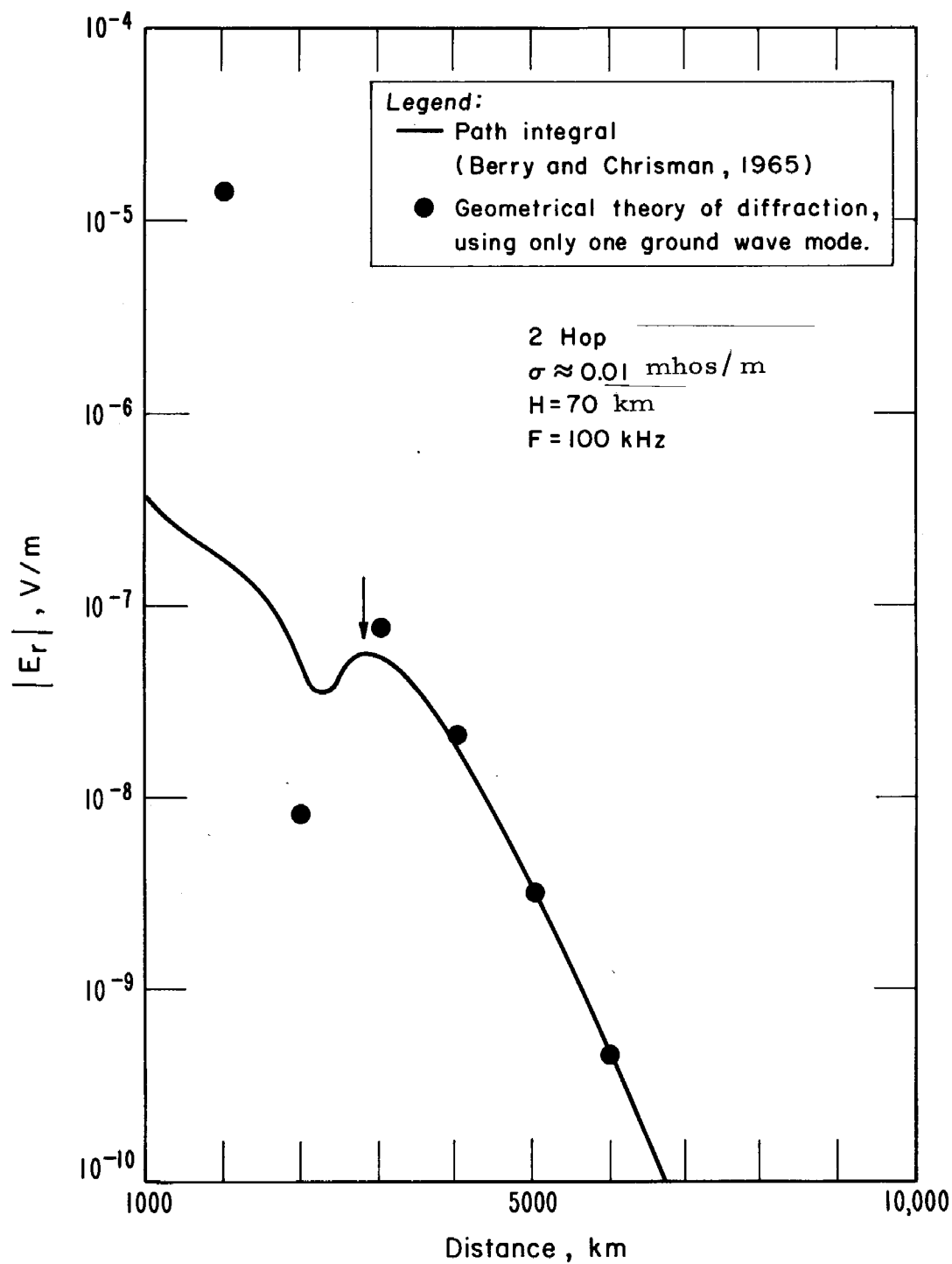
Figure 20. Comparison of the geometrical theory of diffraction
solution with the more rigorous path-integral repre-
sentation for multihop propagation with reflection
from a sharply-bounded, concentric ionosphere.

agreement in the shadow region tends to substantiate the approximation (E-42) used in deriving (12.10). At the shadow boundary (indicated by the arrow in fig. 20) and in the lit region (distance less than that indicated by the arrow), the agreement is not as good. The agreement would be improved by using more groundwave modes, but would still not be exact because of the approximation (E-42). This is not a serious limitation. Since diffraction is not an important effect in the lit region, geometrical optics is a better representation than groundwave modes in the lit region.

The dip in the curve of figure 20 can be interpreted as a pseudo-Brewster angle in the ground reflection coefficient when using a geometrical optics representation. When representing the field by groundwave modes, the dip is due to a minimum in $|\alpha^2|$ as a function of θ.

13. Reflection from an Ionosphere with Arbitrary Tilts or Horizontal Gradients

Application of the GTD to a tilted ionosphere is similar to that for a concentric ionosphere as far as excitation of and radiation from groundwave modes. The main difference between the two cases is in the rays which contribute to the total field. In the concentric case, a continuum of rays satisfy Fermat's principle and contribute equally to the total field for the mth hop. Going to the non-concentric case removes this degeneracy, so that only a finite number of rays will contribute to the mth hop field.

The ray paths are calculated by using ray tracing in complex space including focusing. For a representative 1-hop wave, there will be 2 rays for each groundwave mode: One which leaves the transmitter at just the right angle to graze the sphere ν/k after reflecting from the ionosphere, and one which sheds from the sphere ν/k at just the right place to arrive at the receiver after reflecting from the ionosphere. Very likely, the first ray will go through a caustic just before or after grazing the sphere ν/k. In that case, the factor R_ℓ must be used to account for excitation of the groundwave mode by a point source, and a height-gain function must be used to account for the height of that point on the caustic above the sphere ν/k. Also just as likely, the second ray will go through a caustic just before or after arriving at the receiver. In that case, one must divide by S_ℓ to calculate the field at the caustic and use a height gain function to calculate the field at the receiver.

Another possible ray is one which sheds from one ground
wave mode, reflects from the ionosphere, and arrives tangential
to the same or another groundwave mode. This ray thus gives
a means of coupling groundwave modes.

14. Discussion of Part II

Once the basic method for dealing with diffraction by the earth is known, it is necessary to develop a technique for practical calculations. It is sufficient to consider only a finite number of groundwave modes and hops. In using a computer to make the calculations, it is practical to organize the calculations into two parts:

a) Ionospheric ray tracing.

b) Combining the ray tracing results with ground reflection and diffraction.

The ray tracing program is used as described in section 8, but since diffraction is now included we must trace not only multihop rays leaving the transmitter in various directions, but also the multihop rays that shed from the groundwave. Of course, we do not trace all possible rays, but only a finite number. For instance, we may step the elevation angle of transmission in 1° steps and trace rays shedding from the ground wave at 100-km intervals.

A second program then takes the results of the ray tracing, interpolating when necessary, to calculate the ray paths contributing to the total field at the receiver. Where diffraction is not important, the method of section 8 is sufficient.

SUMMARY

The purpose of the research for this thesis was to include the effects of both arbitrary horizontal gradients in the ionosphere and diffraction by the earth in calculating the propagation of LF radio waves. On the whole, it is successful. First, using the complex phase refractive index to calculate ray paths allows calculation of the reflection of LF (and higher frequency) radio waves from an ionosphere in which the refractive index varies arbitrarily (but smoothly) in any direction. Second, an adaption of the geometrical theory of diffraction to LF terrestrial radio propagation takes into account diffraction by the earth of waves reflected from an ionosphere of arbitrary specification.

In the course of this study, I have discovered several interesting things:

a) Fermat's principle should apply to the complex refractive index, not just the real part, because attenuation and wave interference are both important in determining ray paths.

b) A diffracted ray which travels at a complex height ν/k - a is a more accurate representation of a ground wave mode than one which travels along the ground.

c) A wave containing a surface caustic incident on the ground behaves like a smeared-out point source in exciting a ground wave mode.

d) A multihop wave attenuates slower with distance than the groundwave because the number of rays contributing to the multihop wave increases with distance.

APPENDIX A

CALCULATION OF THE REFLECTION OF RADIO WAVES FROM

A PLANE-STRATIFIED EXPONENTIAL IONOSPHERE USING

COMPLEX RAY THEORY

The refractive index for this ionospheric model is given by (23).

$$n^2 = 1 - ie^{\beta (h-h_o)} . \tag{A-1}$$

Since this ionospheric model varies continuously, it is more convenient to use Haselgrove's equations rather than Snell's law to calculate the reflection of radio waves from the ionosphere. Since we are neglecting the earth's magnetic field, the ionosphere is isotropic, and Haselgrove's equations (13) and (14) for $\delta = 0$ simplify:

$$\frac{dh}{dt} = V_h \quad (a)$$

$$\frac{dy}{dt} = V_y \quad (b)$$

$$\frac{dV_h}{dt} = n\frac{\partial n}{\partial h} \quad (c) \tag{A-2}$$

$$\frac{dV_y}{dt} = n\frac{\partial n}{\partial y} \quad (d)$$

$$\frac{dP}{dt} = n^2 \quad (e) .$$

Equations (A-2) include only the two dimensions in the plane of incidence because the ray will remain in that plane if the medium is isotropic and horizontally stratified. Also, since (A-1) shows that n is only a function of h,

$$\frac{\partial n}{\partial h} = \frac{dn}{dh} \tag{A-3}$$

and

$$\frac{\partial n}{\partial y} = 0 , \qquad (A-4)$$

which implies

$$\frac{dV_y}{dt} = 0 \qquad (A-5)$$

and

$$V_y = \text{constant.} \qquad (A-6)$$

Using the initial conditions

$$V_h^2 + V_y^2 = n_o^2 , \qquad (A-7)$$

and (A-2a), we can integrate (A-2c) to give

$$V_h^2 = n^2 - V_y^2 . \qquad (A-8)$$

Because V_h varies monotonically over the path (positive for the up-going (incident) ray and negative for the downgoing (reflected) ray) and because (A-8) expresses n as a simple function of V_h, V_h is a convenient independent variable. Thus, (A-2) becomes (letting $V_h \rightarrow V$)

$$\frac{dh}{dV} = \frac{V}{n \frac{dn}{dh}} \qquad (a)$$

$$\qquad (A-9)$$

$$\frac{dy}{dV} = \frac{V_y}{n \frac{dn}{dh}} \qquad (b)$$

$$\frac{dP}{dV} = \frac{n^2}{n \frac{dn}{dh}} . \qquad (A-10)$$

From (A-1)

$$2n \frac{dn}{dh} = -i \beta e^{\beta (h-h_o)} = -\beta (1-n^2) \qquad (A-11)$$

and using (A-8), we have

$$2n \frac{dn}{dh} = -\beta(1 - V_y^2 - V^2) \quad , \qquad \text{(A-12)}$$

or

$$n \frac{dn}{dh} = -\frac{\beta}{2} (C^2 - V^2) , \qquad \text{(A-13)}$$

where

$$C^2 = 1 - V_y^2 \quad . \qquad \text{(A-14)}$$

Using (A-13), (A-14), and (A-8) in (A-9) and (A-10) gives

$$\frac{dh}{dV} = -\frac{2}{\beta} \frac{V}{C^2 - V^2} \qquad \text{(a)}$$

$$\frac{dy}{dV} = -\frac{2}{\beta} \frac{V_y}{C^2 - V^2} \qquad \text{(b)} \quad \text{(A-15)}$$

$$\frac{dP}{dV} = -\frac{2}{\beta} \frac{1 - C^2 + V^2}{C^2 - V^2} . \qquad \text{(c)}$$

We can calculate h without integrating (A-15a). Combining (A-1) and (A-8) gives

$$i \, e^{\beta (h-h_0)} = 1 - V_y^2 - V^2 = C^2 - V^2 . \qquad \text{(A-16)}$$

To calculate a reflection coefficient, we can integrate (A-15) beginning at h=0 and continuing until h=0 again after the ray has reflected from the ionosphere. The corresponding values of V are found by letting h=0 in (A-16). They are

$$V = \pm V_0 \qquad \text{(A-17)}$$

where

$$V_0 = \sqrt{C^2 - ie^{-\beta h_0}} . \qquad \text{(A-18)}$$

Thus (A-15) can be written

$$y = -\frac{2}{\beta} V_y \int_{V_0}^{-V_0} \frac{dV}{C^2 - V^2} , \qquad (A-19)$$

and

$$P = -\frac{2}{\beta} \int_{V_0}^{-V_0} \frac{dV}{C^2 - V^2} + \frac{2}{\beta} \int_{V_0}^{-V_0} dV. \quad (A-20)$$

From standard tables,

$$y = \frac{2}{\beta} \frac{V_y}{C} \log \frac{C + V_0}{C - V_0} , \qquad (A-21)$$

and

$$P = \frac{y}{V_y} - \frac{4 V_0}{\beta} , \qquad (A-22)$$

or

$$P = \frac{2}{\beta C} \log \frac{C + V_0}{C - V_0} - \frac{4 V_0}{\beta} . \qquad (A-23)$$

The results in (A-21) and (A-23) correspond to measurable quantities only when y is real. Since V_0 is complex (from A-18), V_y and C must also be complex for y to be real. From (A-21) and (A-18),

$$y = \frac{2V_y}{\beta C} \log \frac{C + \sqrt{C^2 - ie^{-\beta h_0}}}{C - \sqrt{C^2 - ie^{-\beta h_0}}} . \qquad (A-24)$$

Given the real part of V_y, which determines the angle of incidence on the ionosphere, we need to find the imaginary part of V_y necessary to make y in (A-24) real. We use this value of V_y to calculate C to substitute in (A-23) to find P, which will give the amplitude and phase of the reflected wave. For finite h_0, (A-23) and (A-24) are the solutions (not including focusing and inverse

distance losses) for a point source at a height h_0 below the reflection height. We can use (A-23) and (A-24) to find numerical solutions to the point source problem by varying the imaginary part of V_y until y is real.

However, we can also use (A-23) and (A-24) to calculate analytic solutions for a plane wave source by letting $h_0 \to \infty$. This gives from (A-24)

$$y = \lim_{h_0 \to \infty} \frac{2 V_y}{\beta C} \log \frac{4 C^2}{i e^{-\beta h_0}}, \qquad (A-25)$$

or

$$y = \lim_{h_0 \to \infty} \frac{2 V_y}{\beta C} \left[\log (4 C^2) - i \frac{\pi}{2} + \beta h_0 \right]. \qquad (A-26)$$

Let

$$V_y = s + i t . \qquad (A-27)$$

Equation (A-26) shows that as $h_0 \to \infty$ the imaginary parts of V_y and C need only be very small for y to be real. Therefore we can assume

$$t \ll s . \qquad (A-28)$$

From (A-14), (A-27), and (A-28),

$$C^2 \approx (1 - s^2) (1 - \frac{2 i \, st}{1 - s^2}), \qquad (A-29)$$

$$C \approx \sqrt{1 - s^2} \, (1 - \frac{i \, st}{1 - s^2}), \qquad (A-30)$$

and

$$\frac{V_y}{C} \approx \frac{s\left(1 + i\,\frac{t}{s}\right)}{\sqrt{1-s^2}\left(1 - \frac{i\,st}{1-s^2}\right)} \approx \frac{s}{\sqrt{1-s^2}}\left(1 + \frac{i\,t}{s(1-s^2)}\right). \tag{A-31}$$

Using (A-27), (A-29), and (A-31) in (A-26) gives

$$y = \lim_{h_0 \to \infty} \frac{2\,s}{\beta\sqrt{1-s^2}}\left(1 + \frac{i\,t}{s(1-s^2)}\right)$$
$$\left(\log 4(1-s^2) - \frac{2\,i\,st}{1-s^2} + \beta h_0 - i\frac{\pi}{2}\right), \tag{A-32}$$

or

$$y = \lim_{h_0 \to \infty} \frac{2\,s}{\beta\sqrt{1-s^2}}\left[\left\{\log 4(1-s^2) + \beta h_0\right\} + i\left\{\frac{\pi}{2} + \frac{t}{s(1-s^2)}\right.\right.$$
$$\left.\left.\left(\beta h_0 + \log 4(1-s^2) - 2s^2\right)\right\}\right]. \tag{A-33}$$

Setting

$$\mathrm{Imag}\,(y) = \lim_{h_0 \to \infty} \frac{2\,s}{\beta\sqrt{1-s^2}}\left\{-\frac{\pi}{2} + \frac{t}{s(1-s^2)}\right.$$
$$\left.\left(\beta h_0 + \log 4(1-s^2) - 2s^2\right)\right\} = 0 \tag{A-34}$$

gives

$$\lim_{h_0 \to \infty} \left(\beta h_0 + \log 4(1 - s^2) - 2s^2\right) t = \frac{\pi}{2}\,s(1-s^2) \tag{A-35}$$

and

$$y = \text{real } (y) \neq \lim_{h_0 \to \infty} \frac{2\,s}{\beta\sqrt{1-s^2}} \left\{ \log 4(1-s^2) + \beta h_0 \right\}. \qquad \text{(A-36)}$$

Substituting (A-29) into (A-18) gives for large h_0 and small t

$$V_0 \approx \sqrt{1-s^2} \left(1 - \frac{i\,st}{1-s^2} \right). \qquad \text{(A-37)}$$

Putting (A-36), (A-27), and (A-37) into (A-22) gives

$$P \approx \frac{2\,s}{\beta\sqrt{1-s^2}\,(s+it)} \left(\log 4(1-s^2) + \beta h_0 \right) - \frac{4}{\beta}\sqrt{1-s^2} \left(1 - \frac{i\,st}{1-s^2} \right),$$
$$\text{(A-38)}$$

which can also be written

$$P \approx \frac{2(1-i\frac{t}{s})}{\beta\sqrt{1-s^2}} \left(\log 4(1-s^2) + \beta h_0 \right) - \frac{4}{\beta}\sqrt{1-s^2} + \frac{4}{\beta}\sqrt{1-s^2}\,\frac{i\,st}{1-s^2}$$
$$\text{(A-39)}$$

or

$$P \approx \frac{2}{\beta\sqrt{1-s^2}} \left(\log 4(1-s^2) + \beta h_0 - 2(1-s^2) \right)$$

$$+ \frac{2\,i\,t}{\beta s\sqrt{1-s^2}} \left(-\log 4(1-s^2) - \beta h_0 + 2s^2 \right). \qquad \text{(A-40)}$$

Using (A-35) in (A-40) gives

$$P \approx \frac{2}{\beta\sqrt{1-s^2}} \left(\log 4(1-s^2) + \beta h_0 - 2(1-s^2) \right) - \frac{\pi\,i\,\sqrt{1-s^2}}{\beta}. \qquad \text{(A-41)}$$

APPENDIX B

USING THE APPROXIMATION OF SECTION 4 TO CALCULATE THE REFLECTION COEFFICIENT.

Equation (A-41), which gives the complex phase path of a ray which has its end points in real space and thus corresponds to a measurable amplitude and phase, was derived from (A-22) by varying the imaginary part of V_y until the ray ended in real space. An easier way to derive (A-41) from (A-22) is to use the approximation developed in section 4 to allow for the ray's missing the receiver. For this, the desired receiver location is the same as the point where the ray actually landed, except that the imaginary part of y is zero. This will cause the ray to end in real space, since the height of the end point is already real. From (18) the correction to be added to the phase path in (24) is

$$V_y \times (0 - i \ \text{Imag} \ (y) \ ). \qquad (B-1)$$

For large h_o, y is given by (A-26). If V_y and C are real, then from (A-26)

$$\text{Imag} \ (y) = \frac{-V_y \pi}{\beta C} . \qquad (B-2)$$

From (A-22) and (A-26),

$$P = \frac{2}{\beta C} \left[\log (4C^2) - i \ \frac{\pi}{2} + \beta h_o \right] - \frac{4C}{\beta} . \qquad (B-3)$$

Adding the correction (B-1) to (B-3), we get from (B-2)

$$P = \frac{2}{\beta C} \left[\log (4C^2) - i \ \frac{\pi}{2} + \beta h_o \right] - \frac{4C}{\beta} + \frac{V_y^2 \pi i}{\beta C} . \qquad (B-4)$$

Or from (A-14)

$$P = \frac{2}{\beta C} \left(\log (4C^2) + \beta h_0 - 2C^2 - i\frac{\pi}{2} C^2 \right), \qquad (B-5)$$

which agrees with the result in (A-41) obtained by varying the imaginary part of V_y.

APPENDIX C

CALCULATION OF THE REFLECTION COEFFICIENT FROM AN EXPONENTIAL PROFILE USING STANDARD RAY THEORY.

As in appendix A, the complex phase refractive index in the ionosphere will be approximated by

$$n^2 = 1 - i\, e^{\beta(h - h_0)} \qquad \text{(C-1)}$$

for LF and VLF. Using

$$n = \mu - i\chi , \qquad \text{(C-2)}$$

it is easy to show that

$$\mu^2 = \frac{1 + \sqrt{1 + e^{2\beta(h - h_0)}}}{2} , \qquad \text{(C-3)}$$

and

$$\chi^2 = \frac{-1 + \sqrt{1 + e^{2\beta(h - h_0)}}}{2} . \qquad \text{(C-4)}$$

Notice that

$$\mu^2 \to 1 \quad \text{as} \quad (h - h_0) \to -\infty \qquad \text{(C-5)}$$

and

$$\chi^2 \to 0 \quad \text{as} \quad (h - h_0) \to -\infty \qquad \text{(C-6)}$$

as expected.

However, notice also that

$$\mu^2 \geq 1 \quad \text{for all real } h$$

and that μ^2 increases as h increases. Therefore, if the ray path is determined by applying Snell's law or Haselgrove's equations to the real part of the phase refractive index (C-3), the ray will never reflect, but will continue climbing forever. Thus, standard ray

can never be used to calculate accurately the reflection coefficient for a medium described by (C-1).

APPENDIX D

HANKEL AND DEBYE APPROXIMATIONS
FOR HANKEL FUNCTIONS*

The Hankel approximation is valid for large ν (Berry, 1964b; Wait, 1961):

$$\sqrt{\frac{\pi}{2}} H_\nu^{(1)}(x) \approx \frac{-i(-t)^{\frac{1}{4}}}{(x^2-\nu^2)^{\frac{1}{4}}} \; w_2(t) = \frac{-i(-t)^{\frac{1}{4}}}{(\nu\tan\beta)^{\frac{1}{2}}} \; w_2(t)$$

(D-1)

$$\sqrt{\frac{\pi}{2}} H_\nu^{(2)}(x) \approx \frac{+i(-t)^{\frac{1}{4}}}{(x^2-\nu^2)^{\frac{1}{4}}} \; w_1(t) = \frac{i(-t)^{\frac{1}{4}}}{(\nu\tan\beta)^{\frac{1}{2}}} \; w_1(t),$$

where

$$\frac{2}{3}(-t)^{3/2} = \sqrt{x^2-\nu^2} - \nu \cos^{-1}\frac{\nu}{x} = \nu(\tan\beta-\beta) \; ,$$

(D-2)

$$\beta = \cos^{-1}\frac{\nu}{x} \; ,$$

(D-3)

and (Wait, 1961)

$$w_1(t) = \sqrt{\pi}\,(Bi(t) - i\,Ai(t)\,)$$

$$w_2(t) = \sqrt{\pi}\,(Bi(t) + i\,Ai(t)\,) \; .$$

(D-4)

From (D-2) and (D-3),

$$\left(\frac{\partial t}{\partial \nu}\right)_x = \frac{\cos^{-1}\frac{\nu}{x}}{(-t)^{\frac{1}{2}}} = \frac{\beta}{\sqrt{-t}}$$

(D-5)

and

$$\left(\frac{\partial t}{\partial x}\right)_\nu = -\frac{\sqrt{1-\left(\frac{\nu}{x}\right)^2}}{(-t)^{\frac{1}{2}}} = -\frac{\sin\beta}{\sqrt{-t}} \; .$$

(D-6)

*also see the discussion in the appendix of Wait (1967a).

From the above, for large x,

$$\frac{H\nu^{(1)'}(x)}{H\nu^{(1)}(x)} \approx \frac{1}{6x}\left(\frac{\tan\beta}{\tan\beta-\beta} - \frac{3}{\sin^2\beta}\right) - \frac{\sin\beta}{\sqrt{-t}}\frac{w_2'(t)}{w_2(t)} \approx -\frac{\sin\beta}{\sqrt{-t}}\frac{w_2'(t)}{w_2(t)}$$

and
<div style="text-align:right">(D-7)</div>

$$\frac{H\nu^{(2)'}(x)}{H\nu^{(2)}(x)} \approx \frac{1}{6x}\left(\frac{\tan\beta}{\tan\beta-\beta} - \frac{3}{\sin^2\beta}\right) - \frac{\sin\beta}{\sqrt{-t}}\frac{w_1'(t)}{w_1(t)} \approx -\frac{\sin\beta}{\sqrt{-t}}\frac{w_1'(t)}{w_1(t)} \;;$$

$$\frac{\frac{\partial}{\partial\nu}H\nu^{(1)}(x)}{H\nu^{(1)}(x)} \approx -\frac{1}{6\nu}\left(\frac{\beta}{\tan\beta-\beta} - \frac{3}{\tan^3\beta}\right) + \frac{\beta}{\sqrt{-t}}\frac{w_2'(t)}{w_2(t)} \approx \frac{\beta}{\sqrt{-t}}\frac{w_2'(t)}{w_2(t)}$$

<div style="text-align:right">(D-8)</div>

$$\frac{\frac{\partial}{\partial\nu}H\nu^{(2)}(x)}{H\nu^{(2)}(x)} \approx -\frac{1}{6\nu}\left(\frac{\beta}{\tan\beta-\beta} - \frac{3}{\tan^3\beta}\right) + \frac{\beta}{\sqrt{-t}}\frac{w_1'(t)}{w_1(t)} \approx \frac{\beta}{\sqrt{-t}}\frac{w_1'(t)}{w_1(t)} \;.$$

A simpler Hankel approximation is valid for $x \approx \nu$ (Berry, 1964b; Wait, 1961):

<div style="text-align:center">If $x \approx \nu$, then from (D-3) $\beta \approx 0$.</div> <div style="text-align:right">(D-9)</div>

Thus, the following expansion is valid:

$$\tan\beta \approx \beta + \frac{\beta^3}{3} \;,$$
<div style="text-align:right">(D-10)</div>

or

$$\tan\beta - \beta \approx \frac{\beta^3}{3} \;.$$
<div style="text-align:right">(D-11)</div>

From (D-11) and (D-2),

$$-t \approx \left(\frac{\nu}{2}\right)^{2/3} \beta^2 \ . \tag{D-12}$$

From (D-3) and (D-9),

$$\beta^2 \approx \frac{1}{\nu^2} (x^2 - \nu^2) \approx \frac{2}{\nu} (x - \nu) \ . \tag{D-13}$$

From (D-12) and (D-13),

$$t \approx \left(\frac{2}{\nu}\right)^{1/3} (\nu - x), \tag{D-14}$$

and

$$(-t) \approx \left(\frac{\nu}{2}\right)^{2/3} \frac{1}{\nu^2} (x^2 - \nu^2) = \frac{1}{4}\left(\frac{2}{\nu}\right)^{4/3} (x^2 - \nu^2), \tag{D-15}$$

or

$$\left(\frac{-t}{x^2 - \nu^2}\right)^{1/4} \approx \frac{1}{\sqrt{2}} \left(\frac{2}{\nu}\right)^{1/3} \ . \tag{D-16}$$

Using (D-16) in (D-1) gives

$$\sqrt{\pi} \ H\nu^{(1)}(x) \approx -i\left(\frac{2}{\nu}\right)^{1/3} w_2(t)$$

$$\tag{D-17}$$

$$\sqrt{\pi} \ H\nu^{(2)}(x) \approx i\left(\frac{2}{\nu}\right)^{1/3} w_1(t) \ .$$

From (D-12), (D-13), (D-5), and (D-6),

$$\left(\frac{\partial t}{\partial \nu}\right)_x \approx \left(\frac{2}{\nu}\right)^{1/3} \tag{D-18}$$

$$\left(\frac{\partial t}{\partial x}\right)_\nu \approx -\left(\frac{2}{\nu}\right)^{\frac{1}{3}}. \tag{D-19}$$

From (D-19) and (D-7),

$$\frac{H\nu^{(1)''}(x)}{H\nu^{(1)}(x)} \approx -\left(\frac{2}{\nu}\right)^{\frac{1}{3}} \frac{w_2'(t)}{w_2(t)}$$

$$\tag{D-20}$$

$$\frac{H\nu^{(2)'}(x)}{H\nu^{(2)}(x)} \approx -\left(\frac{2}{\nu}\right)^{\frac{1}{3}} \frac{w_1'(t)}{w_1(t)}.$$

From (D-18) and (D-8),

$$\frac{\frac{\partial}{\partial\nu} H\nu^{(1)}(x)}{H\nu^{(1)}(x)} \approx \left(\frac{2}{\nu}\right)^{\frac{1}{3}} \frac{w_2'(t)}{w_2(t)}$$

$$\tag{D-21}$$

$$\frac{\frac{\partial}{\partial\nu} H\nu^{(2)}(x)}{H\nu^{(2)}(x)} \approx \left(\frac{2}{\nu}\right)^{\frac{1}{3}} \frac{w_1'(t)}{w_1(t)}.$$

The Debye approximation for the airy function is valid when $|t| \to \infty$ (Wait, 1961):

$$w_1(t) \approx \frac{e^{-i\pi/4} e^{-i2/3(-t)^{3/2}}}{(-t)^{\frac{1}{4}}} \quad \text{for } 0 < \arg t < \frac{4}{3}\pi$$

$$\tag{D-22}$$

$$w_2(t) \approx \frac{e^{i\pi/4} e^{i2/3(-t)^{3/2}}}{(-t)^{\frac{1}{4}}} \quad \text{for } \frac{2}{3}\pi < \arg t < 2\pi.$$

For a discussion of the Stokes phenomenon, see Budden (1961).

From (D-22),

$$\frac{w_1'(t)}{w_1(t)} \approx i \sqrt{-t}$$

$$\text{(D-23)}$$

$$\frac{w_2'(t)}{w_2(t)} \approx -i \sqrt{-t} \quad .$$

The Debye approximation for Hankel functions is valid for x not near ν (Handbook of Mathematical Functions, 1964; Berry, 1964b). From (D-22), (D-1), and (D-2),

$$\sqrt{\frac{\pi}{2}} H\nu^{(1)}(x) \approx \frac{e^{-i\pi/4} e^{+i\sqrt{x^2-\nu^2}} e^{-i\nu \cos^{-1}\frac{\nu}{x}}}{(x^2-\nu^2)^{\frac{1}{4}}} = \frac{e^{-i\pi/4} e^{i\nu(\tan\beta-\beta)}}{(\nu \tan\beta)^{\frac{1}{2}}}$$

$$\text{(D-24)}$$

$$\sqrt{\frac{\pi}{2}} H\nu^{(2)}(x) \approx \frac{e^{i\pi/4} e^{-i\sqrt{x^2-\nu^2}} e^{+i\nu \cos^{-1}\frac{\nu}{x}}}{(x^2-\nu^2)^{\frac{1}{4}}} = \frac{e^{i\pi/4} e^{-i\nu(\tan\beta-\beta)}}{(\nu \tan\beta)^{\frac{1}{2}}} \quad .$$

From (D-7) and (D-23),

$$\frac{H\nu^{(1)'}(x)}{H\nu^{(1)}(x)} \approx i \sin\beta$$

$$\text{(D-25)}$$

$$\frac{H\nu^{(2)'}(x)}{H\nu^{(2)}(x)} \approx -i \sin\beta \quad .$$

From (D-8) and (D-23),

$$\frac{\frac{\partial}{\partial \nu} H\nu^{(1)}(x)}{H\nu^{(1)}(x)} \approx - i \beta$$

<div align="right">(D-26)</div>

$$\frac{\frac{\partial}{\partial \nu} H\nu^{(2)}(x)}{H\nu^{(2)}(x)} \approx i \beta \ .$$

APPENDIX E

THE RIGOROUS SOLUTION TO THE BOUNDARY VALUE
PROBLEM OF A TRANSMITTER BETWEEN THE EARTH
AND IONOSPHERE WHEN THEY CAN BE REPRESENTED
AS TWO HOMOGENEOUS, ISOTROPIC MEDIA BOUNDED
BY CONCENTRIC SPHERICAL SURFACES

Assume that we can represent the earth and the ionosphere as two (smooth) homogeneous, isotropic, concentric spherical surfaces of radii a and g respectively. (See fig. 12). A vertical, short, dipole, transmitting antenna at a distance b from the center of the earth is excited with a sinusoidal source ($e^{i\omega t}$). The strength of the source is such that the transverse electric field (time dependence suppressed) of the radiation field at distance ℓ from the dipole at an angle θ with the dipole axis is

$$E = ikL \sin\theta \; \frac{e^{-ik\ell}}{\ell} \; . \qquad (E-1)$$

The solution for the vertical component of the electric field a distance r from the center of the earth and a great circle angle θ from the transmitter was first given by Watson (1919). Since then, Berry (1964a, c), Johler (1966), and Johler and Berry (1962, 1964) have expressed the result in various forms.

Berry (1964c) expresses the solution for the case of a transmitter and receiver on the ground in a very concise and easy to interpret form. Using some algebra and the results of the other papers above, it is possible to derive Berry's (1964c) form of the solution for the more general case. For $r < b \cos\theta$ this solution expressed as a sum of zonal harmonics is

$$E_r = \frac{L}{k^3 \, r^{3/2} \, b^{3/2}} \sum_{n=0}^{\infty} n(n+\tfrac{1}{2})(n+1) \, P_n(\cos\theta) \frac{k\pi}{2} H^{(2)}_{n+\frac{1}{2}}(kb) H^{(1)}_{n+\frac{1}{2}}(kr)$$

$$\text{(E-2)}$$

$$\frac{(1 + p_a{}^r R)(1 + p_b{}^g T)}{1 - pRT} \qquad .$$

Interchanging b and r in (E-2) gives the solution for $b < r \cos\theta$. $P_n(\cos\theta)$ is a Legendre polynomial. $H^{(1)}_{n+\frac{1}{2}}(x)$ and $H^{(2)}_{n+\frac{1}{2}}(x)$ are Hankel functions.

$$p_x{}^y \equiv \frac{H^{(2)}_{n+\frac{1}{2}}(ky)}{H^{(2)}_{n+\frac{1}{2}}(kx)} \frac{H^{(1)}_{n+\frac{1}{2}}(kx)}{H^{(1)}_{n+\frac{1}{2}}(ky)} \qquad \text{(E-3)}$$

$$p = p_a{}^g \qquad \text{(E-4)}$$

$$R = - \cfrac{\cfrac{1}{k}\cfrac{H^{(1)'}_{n+\frac{1}{2}}(ka)}{H^{(1)}_{n+\frac{1}{2}}(ka)} - \cfrac{1}{k_2}\cfrac{H^{(1)'}_{n+\frac{1}{2}}(k_2a)}{H^{(1)}_{n+\frac{1}{2}}(k_2a)}}{\cfrac{1}{k}\cfrac{H^{(2)'}_{n+\frac{1}{2}}(ka)}{H^{(2)}_{n+\frac{1}{2}}(ka)} - \cfrac{1}{k_2}\cfrac{H^{(1)'}_{n+\frac{1}{2}}(k_2a)}{H^{(1)}_{n+\frac{1}{2}}(k_2a)}} \qquad (E-5)$$

which is interpreted as a ground reflection coefficient since it reduces to the Fresnel reflection coefficient when the Debye approximations are used.

$$T = - \cfrac{\cfrac{1}{k}\cfrac{H^{(2)'}_{n+\frac{1}{2}}(kg)}{H^{(2)}_{n+\frac{1}{2}}(kg)} - \cfrac{1}{k_3}\cfrac{H^{(2)'}_{n+\frac{1}{2}}(k_3g)}{H^{(2)}_{n+\frac{1}{2}}(k_3g)}}{\cfrac{1}{k}\cfrac{H^{(1)'}_{n+\frac{1}{2}}(kg)}{H^{(1)}_{n+\frac{1}{2}}(kg)} - \cfrac{1}{k_3}\cfrac{H^{(2)'}_{n+\frac{1}{2}}(k_3g)}{H^{(2)}_{n+\frac{1}{2}}(k_3g)}} \qquad (E-6)$$

which is interpreted as an ionospheric reflection coefficient.

Equation (E-2) can be converted to a contour integral by the well-known Watson transformation (Johler and Berry, 1962):

$$E_r = \int_c f(\nu)\, H_\nu^{(2)}(kb)\, H_\nu^{(1)}(kr)\, \frac{(1+p_a{}^r R)(1+p_b{}^g T)}{1 - pRT}\, d\nu \,, \qquad (E-7)$$

where

$$f(\nu) = \frac{-iL\pi}{4kr^{3/2}b^{3/2}}\, \frac{-\nu(\nu-\frac{1}{2})(\nu+\frac{1}{2})}{\cos\nu\pi}\, P_{\nu-\frac{1}{2}}(-\cos\theta) \qquad (E-8)$$

and ν is substituted for $n+\frac{1}{2}$ in using (E-3), (E-4), (E-5) and (E-6) in (E-7). The contour of integration is counter-clockwise in the lower half of the complex ν plane (Berry, 1964c).

There are three standard methods for evaluating (E-7) (Wait, 1962b):

1) Numerical integration in the complex ν plane.

2) Summation of the residues of the poles where pRT = 1. (Johler and Berry, 1964). This corresponds to summing wave guide modes.

3) Expansion of $\frac{1}{1-pRT}$ in a power series of pRT and interchanging summation and integration. This corresponds to summing wave hops. To be valid, pRT < 1 on the contour. (Wait, 1961; Berry, 1964c).

Below is a development of the third method following the work of Wait (1961) and Berry (1964c):

$$E_r = E_D + E_o + \sum_{m=1}^{\infty} E_m \tag{E-9}$$

$$E_D = \begin{cases} \int_C f(\nu) \, H_\nu^{(2)}(kr) \, H_\nu^{(1)}(kb) \, d\nu & \text{for } b < r \cos\theta \\[2mm] \int_C f(\nu) \, H_\nu^{(2)}(kb) \, H_\nu^{(1)}(kr) \, d\nu & \text{for } r < b \cos\theta \\[2mm] \int_C f(\nu) \, H_\nu^{(2)}(kb) \, H_\nu^{(2)}(kr) \, d\nu & \text{otherwise,} \end{cases} \tag{E-10}$$

which is interpreted as the direct line-of-sight ray from the transmitter to the receiver.

$$E_o = \int_C f(\nu) \, H_\nu^{(2)}(kr) \, H_\nu^{(2)}(kb) \, \frac{H_\nu^{(1)}(ka)}{H_\nu^{(2)}(ka)} \, R \, d\nu \tag{E-11}$$

is interpreted as the ray connecting the transmitter and receiver which has made one reflection from the ground. Equation (E-11) is valid for both $r < b$ and $r > b$ as can be seen from the symmetry between r and b.

$$E_m = \int_c f(\nu) \; H_\nu^{(1)}(kb) H_\nu^{(1)}(kr) \frac{H_\nu^{(2)}(ka)}{H_\nu^{(1)}(ka)} (1 + p_a{}^b R)(1 + p_a{}^r R)$$

$$R^{m-1}(pT)^m \; d\nu$$

(E-12)

is interpreted as the four rays which reflect m times from the ionosphere. These four rays came from the product $(1 + p_a{}^b R)(1 + p_a{}^r R)$.

For LF terrestrial radio propagation, and at higher frequencies, the dominant contributions to the integrals (E-10), (E-11), and (E-12) are for $\nu >> 1$. This allows us to replace the Legendre and Hankel functions with the first terms in their asympototic expansions (Berry, 1964b). (For the Hankel functions this is known as the Debye approximation.) These approximations are valid except where $\sin\theta$ is near 0, or the arguments of the Hankel functions are near ν. When these approximations are valid, it is possible to evaluate these integrals by the saddle-point method, which gives results that can easily be interpreted as geometrical-optical rays. For cases where values of ν near ka give important contributions to the integral, the saddle-point method cannot be used.

For the direct wave, making the Debye approximation and evaluating the integral by the saddle-point method corresponds to neglecting everything but the radiation field.

For the ground reflected wave, $\nu \approx ka$ indicates that diffraction effects are important. (This corresponds to rays that graze the earth and are then diffracted into the shadow.) When the receiver

is in the shadow, it is practical to evaluate (E-11) by summing the residues of the poles where the denominator of R in (E-5) is zero. This corresponds to summing groundwave modes, that is, summing contributions of waves which creep around the earth. Keller (1962) refers to these as creeping waves. Since diffraction is important, $\nu \approx$ ka gives the important contributions to the integral , and the simpler Hankel approximation may be used (see app. D):

$$\frac{H_\nu^{(1)\,'}(ka)}{H_\nu^{(1)}(ka)} \approx -\left(\frac{2}{ka}\right)^{\frac{1}{3}} \frac{w_2'(t)}{w_2(t)}$$

(E-13)

$$\frac{H_\nu^{(2)\,'}(ka)}{H_\nu^{(2)}(ka)} \approx -\left(\frac{2}{ka}\right)^{\frac{1}{3}} \frac{w_1'(t)}{w_1(t)} \ ,$$

where

$$t = \left(\frac{2}{ka}\right)^{\frac{1}{3}} (\nu - ka) \ .$$

(E-14)

Since the ground is a good conductor at LF, $k_2 a$ is not near ν, so the Debye approximations may be used:

$$\frac{H_\nu^{(1)\,'}(k_2 a)}{H_\nu^{(1)}(k_2 a)} \approx i\sqrt{1 - \left(\frac{\nu}{k_2 a}\right)^2} \ .$$

(E-15)

Substituting (E-13) and (E-15) into (E-5) gives

$$R \approx - \frac{-\frac{1}{k}\left(\frac{2}{ka}\right)^{\frac{1}{3}}\frac{w_2'(t)}{w_2(t)} - \frac{1}{k_2} i \sqrt{1-\left(\frac{\nu}{k_2 a}\right)^2}}{-\frac{1}{k}\left(\frac{2}{ka}\right)^{\frac{1}{3}}\frac{w_1'(t)}{w_1(t)} - \frac{1}{k_2} i \sqrt{1-\left(\frac{\nu}{k_2 a}\right)^2}} \qquad (E\text{-}16)$$

or

$$R \approx - \frac{\frac{w_2'(t)}{w_2(t)} - q}{\frac{w_1'(t)}{w_1(t)} - q} , \qquad (E\text{-}17)$$

where

$$q = - i \frac{\left(\frac{ka}{2}\right)^{\frac{1}{3}} \sqrt{\left(\frac{k_2}{k}\right)^2 - \left(\frac{\nu}{ka}\right)^2}}{\left(\frac{k_2}{k}\right)^2} , \qquad (E\text{-}18)$$

which will be considered constant (independent of ν) from now on, since $k_2 > > k$ and $\nu \approx ka$.

Expanding the denominator of (E-17) in a Taylor's series about $t = t_s$ where t_s is determined by

$$\frac{w_1'(t_s)}{w_1(t_s)} = q, \qquad (E\text{-}19)$$

gives

$$\frac{w_1'(t)}{w_1(t)} - q \approx (t_s - q^2)(t - t_s) + \frac{1 - 2q(t_s - q^2)}{2}(t-t_s)^2 , \qquad (E\text{-}20)$$

since w_1 satisfies the Stoke's differential equation

$$\frac{w_1''(t)}{w_1(t)} = t \quad .$$

(E-21)

Therefore, (E-17) becomes

$$R \approx - \frac{\dfrac{w_2'(t)}{w_2(t)} - q}{(t_s - q^3)(t - t_s)\left(1 + \left(\dfrac{1}{2(t_s - q^3)} - q\right)(t - t_s)\right)} \quad .$$

(E-22)

From (E-14),

$$d\nu = \left(\frac{ka}{2}\right)^{\frac{1}{3}} dt \quad .$$

(E-23)

For $\nu = ka$, the simpler Hankel approximation is valid:

$$H_\nu^{(1)}(ka) \approx - \frac{i}{\sqrt{\pi}} \left(\frac{2}{ka}\right)^{\frac{1}{3}} w_2(t)$$

(E-24)

$$H_\nu^{(2)}(ka) \approx \frac{i}{\sqrt{\pi}} \left(\frac{2}{ka}\right)^{\frac{1}{3}} w_1(t),$$

where t is given by (E-14). Substituting (E-22), (E-23), and (E-24) into (E-11) gives

$$E_O = \sum_s \int_{c_s} f(\nu) H_\nu^{(2)}(kb) H_\nu^{(2)}(kr) \frac{w_2(t)}{w_1(t)}$$

$$\text{(E-25)}$$

$$\frac{\left(\frac{w_2'(t)}{w_2(t)} - q\right)\left(\frac{ka}{2}\right)^{\frac{1}{3}} dt}{(t_s - q^2)(t - t_s)\left(1 + \left(\frac{1}{2(t_s - q^2)} - q\right)(t - t_s)\right)},$$

where c_s is a contour surrounding the sth pole. Evaluating by residues gives

$$E_O = 2\pi i \sum_s f(\nu_s) H_{\nu_s}^{(2)}(kb) H_{\nu_s}^{(2)}(kr) \frac{w_2(t_s)}{w_1(t_s)} \frac{\frac{w_2'(t_s)}{w_2(t_s)} - q}{(t_s - q^2)} \left(\frac{ka}{2}\right)^{\frac{1}{3}}, \quad \text{(E-26)}$$

where, from (E-14),

$$\nu_s = ka + \left(\frac{ka}{2}\right)^{\frac{1}{3}} t_s \quad . \tag{E-27}$$

Using the Wronskian (Wait, 1961) and (E-19) gives

$$\frac{w_2'(t_s)}{w_2(t_s)} - q = \frac{-2i}{w_1(t_s) w_2(t_s)} \quad . \tag{E-28}$$

Substituting (E-28) into (E-26) and dropping the subscript s, but still remembering that t is a root of (E-19) and that ν is given by (E-27), we have

$$E_O = 4\pi \left(\frac{ka}{2}\right)^{\frac{1}{3}} \sum_t \frac{f(\nu) H_\nu^{(2)}(kb) H_\nu^{(2)}(kr)}{w_1(t) w_1(t)} \frac{1}{t - q^2}, \quad \text{(E-29)}$$

or, from (E-8),

$$E_o = -\frac{iL\pi^2}{kr^{3/2}b^{3/2}} \left(\frac{ka}{2}\right)^{\frac{1}{3}} \sum_t \nu(\nu-\tfrac{1}{2})(\nu+\tfrac{1}{2})$$

$$\frac{P_{\nu-\frac{1}{2}}(-\cos\theta)\, H_\nu^{(2)}(kb)\, H_\nu^{(2)}(kr)}{\cos\nu\pi\,(t-q^2)\,w_1(t)\,w_1(t)} \,. \tag{E-30}$$

For $\nu \gg 1$, the asymptotic approximation for the Legendre function is valid (Berry, 1964b):

$$\frac{P_{\nu-\frac{1}{2}}(-\cos\theta)}{\cos\nu\pi} \approx \sqrt{\frac{2}{\pi\nu\sin\theta}}\; e^{-i\frac{\pi}{4}}\, e^{-i\nu\theta}\,. \tag{E-31}$$

Substituting into (E-30) gives

$$E_o = -\frac{iL\pi^{3/2}\sqrt{2}}{kr^{3/2}b^{3/2}} \left(\frac{ka}{2}\right)^{\frac{1}{3}} \sum_t \frac{\nu^{5/2}}{\sqrt{\sin\theta}}\; e^{-i\pi/4}\, e^{-i\nu\theta}\, \frac{H_\nu^{(2)}(kb)H_\nu^{(2)}(kr)}{w_1(t)^2(t-q^2)}\,. \tag{E-32}$$

Appendices G, H, I, and J use special cases of (E-32) to evaluate diffraction coefficients.

When the receiver is in the shadow, it is practical to calculate the mth hop as a sum of residues. From (E-12),

$$E_m = \int_c f(\nu) H_\nu^{(2)}(kb)\, H_\nu^{(2)}(kr) \frac{H_\nu^{(1)}(ka)}{H_\nu^{(2)}(ka)} (p_b{}^a + R)(p_r{}^a + R)R^{m-1}$$

$$(pT)^m d\nu\,. \tag{E-33}$$

Substituting for R from (E-22) and dν from (E-23) gives

$$E_m = \left(\frac{ka}{2}\right)^{\frac{1}{3}} \sum_s \left(\frac{1}{t_s - q^2}\right)^{m+1} \int_{c_s} \frac{f_m(t)}{(t-t_s)^{m+1}} \, dt \, , \qquad (E-34)$$

where c_s is a contour surrounding the sth pole,

$$f_m(t) = Af(\nu) H_\nu^{(2)}(kb) H_\nu^{(2)}(kr) \frac{H_\nu^{(1)}(ka)}{H_\nu^{(2)}(ka)} \, p^m T^m \, , \qquad (E-35)$$

and

$$A = \left[p_b^{\,a}(t_s - q^2)(t-t_s)\left(1 + \left(\frac{1}{2(t_s - q^3)} - q\right)(t-ts)\right) - \frac{w_2'(t)}{w_2(t)} + q \right] \cdot$$

$$\left[p_r^{\,a}(t_s - q^2)(t-t_s)\left(1 + \left(\frac{1}{2(t_s - q^2)} - q\right)(t-t_s)\right) - \frac{w_2'(t)}{w_2(t)} + q \right] \qquad (E-36)$$

$$\left[\frac{\left(q - \frac{w_2'(t)}{w_2(t)}\right)^{m-1}}{\left(1 + \left(\frac{1}{2(t_s - q^3)} - q\right)(t-t_s)\right)^{m+1}} \right] \cdot$$

Evaluating (E-34) by residues, we get

$$E_m = \left(\frac{ka}{2}\right)^{\frac{1}{3}} \sum_s \left(\frac{1}{t_s - q^3}\right)^{m+1} \left(\frac{2\pi i}{m!}\right) \left[\frac{\partial^m f_m(t)}{\partial t^m}\right]_{t=t_s} \cdot \qquad (E-37)$$

From (E-35) and (E-14),

$$f_m'(t) = f_m(t) \left[-i \frac{d\nu}{dt} \, \hat{\alpha} \right] \, , \qquad (E-38)$$

where

$$\hat{\alpha} = i \left[\frac{f''(\nu)}{f(\nu)} + \frac{\frac{\partial}{\partial \nu} H_\nu^{(2)}(kb)}{H_\nu^{(2)}(kb)} + \frac{\frac{\partial}{\partial \nu} H_\nu^{(2)}(kr)}{H_\nu^{(2)}(kr)} + \frac{\frac{\partial}{\partial \nu} H_\nu^{(1)}(ka)}{H_\nu^{(1)}(ka)} \right.$$

(E-39)

$$\left. - \frac{\frac{\partial}{\partial \nu} H_\nu^{(2)}(ka)}{H_\nu^{(2)}(ka)} + \frac{m}{p} \frac{\partial p}{\partial \nu} + \frac{1}{A} \frac{\partial A}{\partial \nu} \right] .$$

Taking the derivative of (E-38) gives

$$f''(t) = f_m'(t) \left[-i \frac{d\nu}{dt} \hat{\alpha} \right] + f_m(t) \left[-i \frac{d\nu}{dt} \frac{d\hat{\alpha}}{dt} \right] .$$

(E-40)

Using (E-38) in (E-40) gives

$$f_m''(t) = f_m(t) \left[\left(-i \frac{d\nu}{dt} \hat{\alpha} \right)^2 - i \frac{d\nu}{dt} \frac{d\hat{\alpha}}{d\nu} \frac{d\nu}{dt} \right] =$$

(E-41)

$$f_m(t) \left(-i \frac{d\nu}{dt} \right)^2 \left[\hat{\alpha}^2 + i \frac{d\hat{\alpha}}{d\nu} \right] .$$

I will now assume

$$\frac{d\hat{\alpha}}{d\nu} \ll \hat{\alpha}^2 ,$$

(E-42)

which is equivalent to assuming that $f_m(t)$ varies approximately exponentially with t (or ν), since in that case $\hat{\alpha}$ is nearly independent of ν. In practice, the approximation is good except near $\hat{\alpha} = 0$, which corresponds to the receiver's being on the shadow boundary of the earth (that is, on the horizon of the mth hop). Because this method is not practical in the lit region, but only where the field is diffracted

into the shadow, only the case $\hat{\alpha} > 0$ is of interest and the results are not valid near $\hat{\alpha} = 0$.

Therefore, from (E-41) and (E-42),

$$f_m''(t) \approx f_m(t) \left(-i \frac{d\nu}{dt} \hat{\alpha}\right)^2 . \qquad \text{(E-43)}$$

Similarly,

$$\frac{\partial^m f_m(t)}{\partial t^m} = f_m(t) \left(-i \frac{d\nu}{dt} \hat{\alpha}\right)^m . \qquad \text{(E-44)}$$

Using (E-31) in (E-8) we have

$$f(\nu) \approx \frac{-iL \sqrt{\pi} \, \nu^{5/2}}{2 \sqrt{2} \; kr^{3/2} b^{3/2} \sqrt{\sin\theta}} \; e^{-i\pi/4} \; e^{-i\nu\theta} . \qquad \text{(E-45)}$$

Neglecting all but exponentially varying terms in (E-45) gives

$$\frac{f'(\nu)}{f(\nu)} = -i\theta \qquad \text{(E-46)}$$

From (E-3) and (E-4),

$$p = \frac{H_\nu^{(2)}(kg)}{H_\nu^{(1)}(kg)} \; \frac{H_\nu^{(1)}(ka)}{H_\nu^{(2)}(ka)} , \qquad \text{(E-47)}$$

and then

$$\frac{1}{p}\frac{\partial p}{\partial \nu} = \frac{\frac{\partial}{\partial \nu} H_\nu^{(2)}(kg)}{H_\nu^{(2)}(kg)} - \frac{\frac{\partial}{\partial \nu} H_\nu^{(1)}(kg)}{H_\nu^{(1)}(kg)} + \frac{\frac{\partial}{\partial \nu} H_\nu^{(1)}(ka)}{H_\nu^{(1)}(ka)}$$

$$- \frac{\frac{\partial}{\partial \nu} H_\nu^{(2)}(ka)}{H_\nu^{(2)}(ka)} \quad .$$

(E-48)

Equation (E-44) must be evaluated at $t = t_s$ to use in (E-37); likewise $\hat{a}$ in (E-39) (therefore also (E-46), (E-48), and $\frac{1}{A}\frac{\partial A}{\partial \nu}$). It is easier to evaluate $\frac{1}{A}\frac{\partial A}{\partial \nu}$ at $t = t_s$ while calculating the derivative because so many terms are then zero. From (E-36), using (E-21) we get

$$\frac{1}{A}\frac{\partial A}{\partial \nu} = \left[\frac{p_b{}^a(t_s - q^3) - \left(t_s - \left(\frac{w_2'(t_s)}{w_2(t_s)}\right)^3\right)}{-\frac{w_2'(t_s)}{w_2(t_s)} + q} + \frac{p_r{}^a(t_s - q^3) - \left(t_s - \left(\frac{w_2'(t_s)}{w_2(t_s)}\right)^3\right)}{-\frac{w_2'(t_s)}{w_2(t_s)} + q} + \right.$$

(E-49)

$$\left. -(m-1)\frac{t_s - \left(\frac{w_2'(t_s)}{w_2(t_s)}\right)^2}{q - \frac{w_2'(t_s)}{w_2(t_s)}} - (m+1)\left(\frac{1}{2(t_s - q^3)} - q\right) \right] \frac{dt}{d\nu} \quad .$$

Using (E-28) gives

$$\frac{1}{A}\frac{\partial A}{\partial \nu} = \left[\frac{w_1(t_s) w_2(t_s)}{2i} \left((p_b{}^a + p_r{}^a)(t_s - q^3) - (m+1)\left(t_s - \left(\frac{w_2'(t_s)}{w_2(t_s)}\right)^2\right) \right) \right.$$

(E-50)

$$\left. -(m+1)\left(\frac{1}{2(t_s - q^3)} - q\right) \right] \frac{dt}{d\nu} \quad .$$

Using the Hankel approximation (app. D) gives

$$\frac{\frac{\partial}{\partial \nu} H_\nu^{(1)}(x)}{H_\nu^{(1)}(x)} \approx \frac{\cos^{-1}\frac{\nu}{x}}{\sqrt{-y}} \; \frac{w_2{}'(y)}{w_2(y)}$$

$$\text{(E-51)}$$

$$\frac{\frac{\partial}{\partial \nu} H_\nu^{(2)}(x)}{H_\nu^{(2)}(x)} \approx \frac{\cos^{-1}\frac{\nu}{x}}{\sqrt{-y}} \; \frac{w_1{}'(y)}{w_1(y)} \quad,$$

where

$$\frac{2}{3}(-y)^{3/2} = \sqrt{x^2-\nu^2} - \nu \cos^{-1}\frac{\nu}{x} \quad. \qquad \text{(E-52)}$$

Using (E-46), (E-51), (E-48), (E-50), and (E-23) in (E-39) gives

$$\hat{\alpha} = \theta + i\frac{\cos^{-1}\frac{\nu}{kb}}{\sqrt{-y_b}} \; \frac{w_1{}'(y_b)}{w_1(y_b)} + i\frac{\cos^{-1}\frac{\nu}{kr}}{\sqrt{-y_r}} \; \frac{w_1{}'(y_r)}{w_1(y_r)} + i\frac{\cos^{-1}\frac{\nu}{ka}}{\sqrt{-t_s}} \left(\frac{w_2{}'(t_s)}{w_2(t_s)} - \frac{w_1{}'(t_s)}{w_1(t_s)}\right)$$

$$+ mi\frac{\cos^{-1}\frac{\nu}{kg}}{\sqrt{-y_s}} \left(\frac{w_1{}'(y_s)}{w_1(y_s)} - \frac{w_2{}'(y_s)}{w_2(y_s)}\right) + mi\frac{\cos^{-1}\frac{\nu}{ka}}{\sqrt{-t_s}} \left(\frac{w_2{}'(t_s)}{w_2(t_s)} - \frac{w_1{}'(t_s)}{w_1(t_s)}\right) +$$

$$\left(\frac{2}{ka}\right)^{\frac{1}{3}} \left(\frac{w_1(t_s)\,w_2(t_s)}{2} \left((p_b{}^a + p_r{}^a)(t_s - q^2) - (m+1)\left(t_s - \left(\frac{w_2{}'(t_s)}{w_2(t_s)}\right)^2\right)\right)\right) +$$

$$-i(m+1)\left(\frac{1}{2(t_s-q^2)} - q\right)\right) , \qquad \text{(E-53)}$$

where

$$\frac{2}{3} (-y_b)^{3/2} = \sqrt{(kb)^2 - \nu^2} - \nu \cos^{-1}\frac{\nu}{kb}$$

$$\frac{2}{3} (-y_r)^{3/2} = \sqrt{(kr)^2 - \nu^2} - \nu \cos^{-1}\frac{\nu}{kr} \qquad (E-54)$$

$$\frac{2}{3} (-y_t)^{3/2} = \sqrt{(kg)^2 - \nu^2} - \nu \cos^{-1}\frac{\nu}{kg} \quad .$$

From (E-35) and (E-36),

$$f_m(t_s) = f(\nu_s) H\nu_s^{(2)}(kb) H\nu_s^{(2)}(kr) \frac{H\nu_s^{(1)}(ka)}{H\nu_s^{(2)}(ka)} \left(q - \frac{w_2'(t_s)}{w_2(t_s)}\right)^{m+1} (pT)^m \quad (E-55)$$

Using (E-45), (E-28), (E-47), and (E-24) in (E-55) gives

$$f_m(t_s) = \frac{-iL\sqrt{\pi}\,\nu_s^{5/2}\, e^{-i\pi/4}\, e^{-i\nu_s\theta}}{2\sqrt{2}\, kr^{3/2} b^{3/2} \sqrt{\sin\theta}} \left(\frac{-2i\, H\nu_s^{(2)}(kb) H\nu_s^{(2)}(kr)}{w_1(t_s)^2}\right)$$

$$\qquad (E-56)$$

$$\left(\frac{-2iT}{w_1(t_s)^2}\, \frac{H\nu_s^{(2)}(kg)}{H\nu_s^{(1)}(kg)}\right)^m \quad .$$

Using the Debye approximation (app. D),

$$\frac{H\nu_s^{(2)}(kg)}{H\nu_s^{(1)}(kg)} \approx i\, e^{-2i\sqrt{(kg)^2 - \nu^2}}\, e^{2i\nu \cos^{-1}\frac{\nu}{kg}} \quad , \qquad (E-57)$$

(E-44), and (E-56) in (E-37), and dropping the subscript s for convenience, we get

$$E_m = \frac{-L\,\pi^{3/2}\sqrt{2}}{kr^{3/2}\,b^{3/2}\sqrt{\sin\theta}\;m!}\;\frac{e^{i\pi/4}}{}\left(\frac{ka}{2}\right)^{\frac{1}{3}}\sum_t \nu^{3/2}\,e^{-i\nu\left(\theta-2m\cos^{-1}\frac{\nu}{kg}\right)}$$

<div align="right">(E-58)</div>

$$\frac{H\nu^{(2)}(kb)\,H\nu^{(2)}(kr)}{w_1(t)^2(t-q^2)}\left(\frac{-2iT\,\hat{\alpha}}{t-q^2}\left(\frac{ka}{2}\right)^{\frac{1}{3}}\frac{e^{-2i\sqrt{(kg)^2-\nu^2}}}{w_1(t)^2}\right)^m .$$

Notice that for m=0 (E-58) agrees with the ground wave E_0 given by (E-32). The Debye approximation gives

$$\frac{w_1{}'(y_b)}{w_1(y_b)} \approx i\sqrt{-y_b}$$

<div align="right">(E-59)</div>

$$\frac{w_2{}'(y_b)}{w_2(y_b)} \approx -i\sqrt{-y_b} .$$

Using (E-59) and (E-28) in (E-53), and for $\nu \approx ka$ (app. D) we have

$$\frac{\cos^{-1}\frac{\nu}{ka}}{\sqrt{-t}} \approx \left(\frac{2}{ka}\right)^{\frac{1}{3}},$$

<div align="right">(E-60)</div>

$$\hat{\alpha} = \theta - 2m\cos^{-1}\frac{\nu}{kg} + i\,\frac{\cos^{-1}\frac{\nu}{kb}}{\sqrt{-y_b}}\,\frac{w_1{}'(y_b)}{w_1(y_b)} + i\,\frac{\cos^{-1}\frac{\nu}{kr}}{\sqrt{-y_r}}\,\frac{w_1{}'(y_r)}{w_1(y_r)} +$$

<div align="right">(E-61)</div>

$$-\left(\frac{2}{ka}\right)^{\frac{1}{3}}\left(\left(\frac{m+1-p_b{}^a-p_r{}^a}{2}\right)w_1(t)\,w_2(t)(t-q^2)+i(m+1)\left(q+\frac{1}{2(t-q^2)}\right)\right).$$

Two special cases of (E-58) are of interest. First, for the transmitter and receiver high above the ground, $kb \gg \nu$ and $kr \gg \nu$, so that the Debye approximation is valid (app. D):

$$\sqrt{\frac{k\pi}{2}}\ H\nu^{(2)}(kr) \approx \frac{e^{i\pi/4}\ e^{-i\sqrt{(kr)^2-\nu^2}}\ e^{i\nu\cos^{-1}\frac{\nu}{kr}}}{\left(r^2-\left(\frac{\nu}{k}\right)^2\right)^{\frac{1}{4}}}$$

(E-62)

$$\sqrt{\frac{k\pi}{2}}\ H\nu^{(2)}(kb) \approx \frac{e^{i\pi/4}\ e^{-i\sqrt{(kb)^2-\nu^2}}\ e^{i\nu\cos^{-1}\frac{\nu}{kb}}}{\left(b^2-\left(\frac{\nu}{k}\right)^2\right)^{\frac{1}{4}}}\ .$$

Using (E-62) in (E-58) gives

$$E_m = -\frac{iL\sqrt{\pi}}{k^2 r^{3/2} b^{3/2}}\frac{2^{3/2}\ e^{i\pi/4}}{m!}\left(\frac{ka}{2}\right)^{\frac{1}{3}}\sum_t \nu^{5/2}\frac{e^{-i\nu\alpha}\ e^{-i\sqrt{(kb)^2-\nu^2}}\ e^{-i\sqrt{(kr)^2-\nu^2}}}{\left(r^2-\left(\frac{\nu}{k}\right)^2\right)^{\frac{1}{4}}\left(b^2-\left(\frac{\nu}{k}\right)^2\right)^{\frac{1}{4}}w_1(t)^2(t-q^2)}$$

(E-63)

$$\left(\frac{-2iT\hat{\alpha}}{t-q^2}\left(\frac{ka}{2}\right)^{\frac{1}{3}}\frac{e^{-2i\sqrt{(kg)^2-\nu^2}}}{w_1(t)^2}\right)^m,$$

where

$$\alpha = \theta - \cos^{-1}\frac{\nu}{kb} - \cos^{-1}\frac{\nu}{kr} - 2m\cos^{-1}\frac{\nu}{kg}\ ,$$

(E-64)

and, from (E-61),

$$\hat{\alpha} = \theta - 2m\cos^{-1}\frac{\nu}{kg} - \cos^{-1}\frac{\nu}{kb} - \cos^{-1}\frac{\nu}{kr} +$$

(E-65)

$$-\left(\frac{2}{ka}\right)^{\frac{1}{3}}\left(\frac{m+1-p_b^a-p_r^a}{2}\ w_1(t)\ w_2(t)(t-q^2) + (m+1)iq + \frac{i(m+1)}{2(t-q^2)}\right).$$

The second special case is for the transmitter and receiver on the ground.

$$b = r = a, \quad y_b = y_r = t, \quad p_b^a = p_r^a = 1 \; . \tag{E-66}$$

From (E-58), using the Hankel approximation (E-24), we get

$$E_m = \frac{L\sqrt{2\pi} \; e^{i\pi/4}}{ka^3 \, m! \, \sqrt{\sin\theta}} \left(\frac{2}{ka}\right)^{\frac{1}{3}} \sum_t \nu^{5/3} \; \frac{e^{-i\nu\left(\theta - 2m\cos^{-1}\frac{2}{kg}\right)}}{t-q^2} \tag{E-67}$$

$$\left(\frac{-2iT\,\hat{\alpha}}{t-q^2} \left(\frac{ka}{2}\right)^{\frac{1}{3}} \frac{e^{-2i\sqrt{(kg)^2-\nu^2}}}{w_1(t)^2}\right)^m \; ,$$

and from (E-60), (E-61), and (E-19)

$$\hat{\alpha} = \theta - 2m\cos^{-1}\frac{\nu}{kg} \; + \tag{E-68}$$

$$- \left(\frac{2}{ka}\right)^{\frac{1}{3}} \left(\frac{m-1}{2} \, w_1(t) \, w_2(t)(t-q^2) + (m-1)iq + \frac{i(m+1)}{2(t-q^2)}\right) \; .$$

Appendix K interprets (E-63) in terms of the geometrical theory of diffraction, and section 12 discusses (E-63) and (E-67).

APPENDIX F

INTERPRETATION OF THE PRODUCT OF A LEGENDRE
FUNCTION WITH A HANKEL FUNCTION FOR LARGE ORDER

As shown below, one interpretation of

$$A = \left(\frac{k\pi}{2}\right)^{-\frac{3}{2}} \frac{P_{\nu-\frac{1}{2}}(-\cos\theta)}{\cos\nu\pi} \frac{H_\nu^{(2)}(kr)\, H_\nu^{(2)}(kb)}{w_1(t)^2} \qquad \text{(F-1)}$$

in (E-30) is that the diffracted ray travels at a complex height,

$\frac{\nu}{k}$ - a, above the earth.

When ν is large (as it is for the LF band and higher frequencies

for terrestrial radio propagation), the Legendre and Hankel functions

may be approximated by the first term in their asymptotic expan-

sions (Berry, 1964b; app. D):

$$\frac{P_{\nu-\frac{1}{2}}(-\cos\theta)}{\cos\nu\pi} \approx \frac{e^{-\nu\theta}\, e^{-i\pi/4}}{\sqrt{\frac{\nu\pi}{2}\sin\theta}} \qquad \text{(F-2)}$$

and

$$\sqrt{\frac{k\pi}{2}} H_\nu^{(2)}(kr) \approx \frac{e^{-ik\sqrt{r^2-(\frac{\nu}{k})^2}\,+i\nu\cos^{-1}\frac{\nu}{kr}}\, e^{+i\pi/4}}{\left(r^2-\left(\frac{\nu}{k}\right)^2\right)^{\frac{1}{4}}} . \qquad \text{(F-3)}$$

The approximation for the Legendre function is valid except near

$\sin\theta = 0$. This occurs at $\theta = 0$, which corresponds to the observer's

being near the transmitter, and again at $\theta = \pi$, which corresponds

to azimuthal focusing at the antipode of the transmitter.

The approximation for the Hankel function (the Debye approxi-

mation) is valid except near $r = \frac{\nu}{k}$, which occurs when the ray

grazes the earth. An alternate expression of the Debye

approximation is

$$\sqrt{\frac{k\pi}{2}}\, H_\nu^{(2)}\, (\nu\, \sec\, \beta) \approx \frac{e^{-i\nu(\tan\,\beta\,-\,\beta)}\, e^{i\,\pi/4}}{\sqrt{\frac{\nu}{k}\, \tan\,\beta}} \quad , \qquad (F\text{-}4)$$

where

$$\beta = \cos^{-1}\frac{\nu}{kr} \quad . \qquad (F\text{-}5)$$

Using (F-2) and (F-4) gives

$$A \approx \frac{e^{-ik(\frac{\nu}{k}\,(\theta\,-\,\beta_1\,-\,\beta_2)+\frac{\nu}{k}\,\tan\,\beta_1\,+\,\frac{\nu}{k}\,\tan\,\beta_2)}\, e^{i\,\pi/4}}{\sqrt{\frac{\nu}{k}\,\sin\,\theta}\,\sqrt{\frac{\nu}{k}\,\tan\,\beta_1}\,\sqrt{\frac{\nu}{k}\,\tan\,\beta_2}\,(w_1(t_s))^2} \quad , \qquad (F\text{-}6)$$

where $\beta_1 = \cos^{-1}\frac{\nu}{kb}$ and $\beta_2 = \cos^{-1}\frac{\nu}{kr}$. $\qquad$ (F-7)

This expression has a clear geometrical interpretation, shown by figure 14. The complex phase is that of a wave with propagation constant k which travels in a straight line from the transmitter to tangency with a sphere of radius $\frac{\nu}{k}$ concentric with the earth, moves along the sphere an arc length $\frac{\nu}{k}$ (θ - β_1 - β_2), leaves the circle tangentially, and travels in a straight line to the receiver. The term $\sqrt{\frac{\nu}{k}}\,\sin\,\theta$ in the denominator gives the azimuthal focusing of these rays caused by their traveling along great circles. The terms $\sqrt{\nu/k}\,\tan\,\beta_1$ and $\sqrt{\nu/k}\,\tan\,\beta_2$ give the elevation focusing of the rays traveling along the straight line segment connecting the transmitter and receiver with the earth. Notice that the path satisfies Fermat's principle if we assume that the effective propagation constant traveling in an arc is $\frac{\nu}{r}$.

This interpretation can be applied to this expression for any value of ν, so that (E-25) can be interpreted as an integral over paths of the type shown in figure 14. However, transforming the integral to a sum of residues (E-26) chooses those particular paths of the type shown in figure 14 which contribute the most to the signal at the receiver. The value of ν is chosen to make the denominator of the ground reflection coefficient zero. This corresponds to choosing a value of ν such that the boundary conditions at the surface of the earth are satisfied with only a reflected wave and a transmitted wave (into the earth), but no incident wave. Thus for particular values of ν, considerable energy is diffracted around the earth into the shadow region.

If $\left|\dfrac{\nu}{k}\right| < a$, this interpretation of (F-1) has the ray traveling through the earth with the propagation constant k of free space. Another interpretation of (F-1) is possible if $\left|\dfrac{\nu}{k}\right| \ll a$. If $\left|\dfrac{\nu}{k}\right| \ll a$, then $|t|$ is large, and the Debye approximation for $w_1(t)$ for $0 < \arg t < \dfrac{4}{3}\pi$,

$$w_1(t) \approx \frac{e^{-i\,\pi/4}\, e^{-i\,\frac{2}{3}\,(-t)^{\frac{3}{2}}}}{(-t)^{\frac{1}{4}}}, \qquad (F-8)$$

is valid. Using

$$\frac{2}{3}(-t)^{\frac{3}{2}} = \sqrt{(ka)^2 - \nu^2} - \nu\cos^{-1}\frac{\nu}{ka} = \nu(\tan\beta_3 - \beta_3) \qquad (F-9)$$

and

$$(-t)^{\frac{1}{4}} = \left[\frac{3}{2}\nu(\tan\beta_3 - \beta_3)\right]^{\frac{1}{6}}, \qquad (F-10)$$

where

$$\beta_3 = \cos^{-1}\frac{\nu}{ka} , \tag{F-11}$$

gives

$$w_1(t) \approx \frac{e^{-i\pi/4}\, e^{-ik(\frac{\nu}{k}\tan\beta_3 - \frac{\nu}{k}\beta_3)}}{\left[\frac{3}{2}\nu(\tan\beta_3 - \beta_3)\right]^{\frac{1}{6}}} . \tag{F-12}$$

Substituting this into (F-6) gives

$$A = \frac{\left[\frac{3}{2}\nu(\tan\beta_3 - \beta_3)\right]^{\frac{1}{3}}}{\sqrt{\frac{\nu}{k}\tan\beta_1}\,\sqrt{\frac{\nu}{k}\tan\beta_2}\,\sqrt{\sin\theta}}\; e^{-i\frac{\nu}{a}(a(\theta - \beta_1 - \beta_2 + 2\beta_3))}$$

$$e^{-ik(\frac{\nu}{k}\tan\beta_1 - 2\frac{\nu}{k}\tan\beta_3 + \frac{\nu}{k}\tan\beta_2) + \frac{3\pi i}{4}} . \tag{F-13}$$

This expression also has clear geometrical interpretation, as seen in figure 15.

The phase is that of a wave which has traveled in a straight line with propagation constant k from the transmitter to the earth, is incident on the earth at an angle $\varphi = \sin^{-1}\frac{\nu}{ka}$, travels with propagation constant $\frac{\nu}{a}$ along the earth a distance $a(\theta - \beta_1 - \beta_2 + 2\beta_3)$, leaves the earth at an angle $\varphi = \sin^{-1}\frac{\nu}{ka}$, and travels in a straight line with propagation constant k from the earth to the receiver. Notice that this path obeys Fermat's principle, since Snell's law,

$$k\sin\varphi = \frac{\nu}{a} ,$$

is satisfied as the ray arrives at and leaves the earth if we assume the ground wave travels tangentially. Again, the other factors represent focusing.

Notice the difference between these two interpretations: in the first case the $w_1(t)^2$ was ignored in calculating the phase and in the second case the Debye approximation gives the contribution of $w_1(t)^2$ to the phase. In both cases the resulting geometrical interpretation of the ray path satisfies Fermat's principle. It might be possible to include the effects of a phase contribution from w_1 without making the Debye approximation in order to get a path which would vary continuously between the two extremes presented here. In practice, this is unnecessary because when $\nu = ka$ the two paths are identical, and since $\nu \approx ka$ as determined by the ground wave modal equation (E-37) and (E-19) there is little difference between the two paths. In fact, the path where the rays graze the earth assumed by Keller is probably just as accurate, but the paths in figures 14 and 15 allow a little more interpretation. All the calculations use the first interpretation of (F-1) shown in figure 14.

Bremmer (1949, page 77) has interpreted ground wave modes in a similar way with a ray which travels at a particular height above the ground. However, he uses a real instead of a complex height, which is easier to interpret, but not as accurate. Logan (1959) and Logan and Yee (1962) interpret ground wave modes as wave guide modes inside a leaky waveguide with the upper wall at a real height of about $|\nu/k|-a$.

Keller (1958) and Keller and Levy (1963) use the concept of rays in complex space in connection with diffraction in trying to solve the following problem: find a straight line through a given point tangent to a given surface (i.e., a surface caustic). The problem has two solutions. If the given point is on the convex side of the surface, the solutions are simple and easy to visualize. If the given point is on the concave side of the surface, then two solutions still exist, but the point of tangency with the surface is in complex space. Keller calls such rays imaginary rays.

APPENDIX G

EVALUATING THE DIFFRACTION COEFFICIENT (EXCITATION FACTOR) BY COMPARING THE GEOMETRICAL THEORY OF DIFFRACTION SOLUTION WITH THE RIGOROUS SOLUTION FOR A DISTANT SOURCE AND A RECEIVER AT $r = \nu/k$

Following the method of Levy and Keller (1959), I will calculate

the field of the ground wave excited by a source elevated from the

sphere when the observer is in the shadow of the sphere by first cal-

culating the field using the geometrical theory of diffraction with an

unknown diffraction coefficient, and then comparing this with the

known rigorous solution to calculate the diffraction coefficient. My

derivation differs from Keller's in two ways:

1) Rather than assume the incident rays graze the earth, it

assumes they graze a circle of radius $\frac{\nu}{k}$.

2) The diffraction coefficient is dimensionless and gives

the fraction of the incident field which is converted to a dif-

fracted ray. Keller's diffraction coefficient has the dimensions

of length $^{\frac{1}{4}}$.

From the viewpoint of the geometrical theory of diffraction, the

main contribution to the field at the observation point follows the ray

shown in figure 16 (a straight line of length l from the source, tan-

gent to the sphere of radius $\frac{\nu}{k}$, then a ray which follows the curvature

of the sphere for an angle $\theta - \theta_0$ to the observer). Both antennas

are short vertical dipoles. The solution using the geometrical

theory of diffraction is the product of several factors:

The incident field at the sphere

$$\text{ikL} \frac{e^{-ik\ell}}{\ell} \cos \theta_0 \; ; \qquad \text{(G-1)}$$

the diffraction coefficient, which gives the fraction of the incident

field converted to a ground wave,

$$D; \qquad \text{(G-2)}$$

the phase integral contribution in traveling along the arc from the

diffraction point to the observation point,

$$e^{-i\nu(\theta - \theta_0)} \; ; \qquad \text{(G-3)}$$

and a convergence factor due to azimuth focusing of rays traveling

around the earth,

$$\sqrt{\frac{\sin \theta_0}{\sin \theta}} \; . \qquad \text{(G-4)}$$

Taking the product of (G-1), (G-2), (G-3), and (G-4) gives

$$E_0 = \text{ikL} \frac{e^{-ik\ell}}{\ell} \cos \theta_0 \; D \; e^{-i\nu(\theta - \theta_0)} \sqrt{\frac{\sin \theta_0}{\sin \theta}} \; . \qquad \text{(G-5)}$$

From figure 16,

$$\cos \theta_0 = \frac{\nu}{kb} \qquad \text{(G-6)}$$

and

$$\sin \theta_0 = \frac{\ell}{b} \; , \qquad \text{(G-7)}$$

Substituting into (G-5) gives

$$E_0 = \text{ik}\ell \frac{e^{-ik\ell}}{\ell} \frac{\nu}{kb} D \; e^{-i\nu(\theta - \theta_0)} \sqrt{\frac{\ell}{b \sin \theta}} \; , \qquad \text{(G-8)}$$

or

$$E_0 = \frac{iL \, e^{-ik\ell} \, \nu \, D \, e^{-i\nu(\theta - \theta_0)}}{\sqrt{\ell} \; b^{\frac{3}{2}} \sqrt{\sin \theta}} \; . \qquad (G\text{-}9)$$

From figure 16,

$$\ell = \sqrt{b^2 - \left(\frac{\nu}{k}\right)^2} \qquad (G\text{-}10)$$

and

$$\theta_0 = \cos^{-1} \frac{\nu}{kb} \; . \qquad (G\text{-}11)$$

From (G-9), (G-10), and (G-11),

$$E_0 = \frac{iL\nu \, D \, e^{-i\sqrt{(kb)^2 - \nu^2}} \, e^{-i\nu(\theta - \cos^{-1} \frac{\nu}{kb})}}{b^{\frac{3}{2}} \left(b^2 - \left(\frac{\nu}{k}\right)^2\right)^{\frac{1}{4}} \sqrt{\sin \theta}} \; . \qquad (G\text{-}12)$$

The rigorous solution (for one mode) from (E-32) for $r = \frac{\nu}{k}$ is

$$E_0 = -\frac{iL\sqrt{\pi} \, e^{-i\pi/4}}{k^{\frac{3}{2}} \left(\frac{\nu}{k}\right)^{\frac{3}{2}} b^{\frac{3}{2}}} \left(\frac{ka}{2}\right)^{\frac{1}{3}} \frac{\nu^{\frac{5}{2}}}{\sqrt{\sin \theta}} \, e^{-i\nu\theta} \, \pi \sqrt{\frac{k}{2}} \; \frac{H_\nu^{(2)}(kb) \, H_\nu^{(2)}(\nu)}{w_1(t)^2}$$

$$\frac{2}{t - q^2} \; . \qquad (G\text{-}13)$$

Using the simpler Hankel approximation,

$$\sqrt{\pi} \, H_\nu^{(2)}(\nu) \approx i \left(\frac{2}{\nu}\right)^{\frac{1}{3}} w_1(0), \qquad (G\text{-}14)$$

and the Debye approximation,

$$\sqrt{\frac{k\pi}{2}} \, H_\nu^{(2)}(kb) \approx \frac{e^{i\pi/4} \, e^{-i\sqrt{(kb)^2 - \nu^2}} \, e^{i\nu \cos^{-1} \frac{\nu}{kb}}}{\left(b^2 - \left(\frac{\nu}{k}\right)^2\right)^{\frac{1}{4}}}, \qquad (G\text{-}15)$$

gives

$$E_0 = -\frac{iL\sqrt{\pi} \, \nu}{b^{\frac{3}{2}} \sqrt{\sin \theta}} \; \frac{e^{-i\nu\theta} w_1(0)}{(t - q^2)} \; \frac{e^{-i\sqrt{(kb)^2 - \nu^2}} \, e^{i\nu \cos^{-1} \frac{\nu}{kb}}}{\left(b^2 - \left(\frac{\nu}{k}\right)^2\right)^{\frac{1}{4}} w_1(t)^2} \; . \qquad (G\text{-}16)$$

Comparing with (G-12) gives

$$D = -\frac{2i\sqrt{\pi}}{t-q^2}\,\frac{w_1(0)}{w_1(t)^2}\ .$$ (G-17)

APPENDIX H

EFFECT OF THE TRANSMITTER'S BEING CLOSE TO THE GROUND— EVALUATING R_ℓ BY COMPARING THE GEOMETRICAL THEORY OF DIFFRACTION SOLUTION WITH THE RIGOROUS SOLUTION

In the previous example, the source was far from the earth, so that the incident field was only the far-zone radiation field. If the source is close to the earth, the incident field effective in exciting a ground wave will be different. Assuming that the effective incident field is equal to the far-zone radiation field times a factor R_ℓ we can determine R_ℓ by comparing the GTD solution with the rigorous solution for both the source and observation point at a height ν/k-a, separated by a central earth angle θ. The total solution is the product of several factors (see figure 17): The effective incident field a small distance ℓ from the transmitter,

$$\frac{ikL}{\ell} R_\ell ; \qquad (H-1)$$

the diffraction coefficient,

$$D = -\frac{2i\sqrt{\pi}}{t-q^2} \frac{w_1(0)}{w_1(t)^2} ; \qquad (H-2)$$

the phase integral along the arc connecting the transmitter with the receiver,

$$e^{-i\nu\theta} ; \qquad (H-3)$$

a convergence factor due to azimuthal focusing,

$$\sqrt{\frac{\sin\theta_0}{\sin\theta}} , \qquad (H-4)$$

where

$$\sin \theta_0 = \frac{\ell}{\left(\dfrac{\nu}{k}\right)} \; . \tag{H-5}$$

Taking the product of (H-1) through (H-4) and using (H-5), we get

$$E = k^{\frac{3}{2}} \; L \; \frac{R_\ell}{\sqrt{\ell}} \; \frac{2\sqrt{\pi}}{t-q^2} \; \frac{w_1(0)}{w_1(t)^2} \; e^{-i\nu\theta} \; \frac{1}{\sqrt{\nu}\,\sqrt{\sin\theta}} \; . \tag{H-6}$$

The rigorous solution for one mode from (E-32) for $b = r = \dfrac{\nu}{k}$ is

$$E = -\frac{iL}{k^{\frac{3}{2}}} \; \frac{\sqrt{\pi}}{\left(\dfrac{\nu}{k}\right)^{\frac{3}{2}}} \; \frac{\sqrt{\dfrac{k}{2}}}{\left(\dfrac{\nu}{k}\right)^{\frac{3}{2}}} \; \left(\frac{ka}{2}\right)^{\frac{1}{3}} \; \frac{\nu^{\frac{5}{3}}}{\sqrt{\sin\theta}} \; e^{-i\pi/4} \; e^{-i\nu\theta}$$

$$\pi \; \frac{H_\nu^{(2)}(\nu)\, H_\nu^{(2)}(\nu)}{w_1(t)^2} \; \frac{2}{t-q^2} \; . \tag{H-7}$$

The simpler Hankel approximation,

$$\sqrt{\pi}\; H_\nu^{(2)}(\nu) \approx i\left(\frac{2}{\nu}\right)^{\frac{1}{3}} w_1(0) \approx i\left(\frac{2}{ka}\right)^{\frac{1}{3}} w_1(0), \tag{H-8}$$

is valid for

$$\nu \approx ka . \tag{H-9}$$

Substituting into (H-7) gives

$$E = L \; \frac{\sqrt{\pi}}{\sqrt{2}} \; k^2 \left(\frac{2}{ka}\right)^{\frac{1}{3}} \; \frac{1}{\sqrt{\nu\sin\theta}} \; e^{i\pi/4} \; e^{-i\nu\theta} \; \frac{w_1(0)^2}{w_1(t)^2} \; \frac{2}{t-q^2} \; . \tag{H-10}$$

Comparing (H-6) with (H-10) we have

$$R_\ell = \left(\frac{ka}{2}\right)^{\frac{1}{6}} \sqrt{\frac{\ell}{a}} \; e^{i\pi/4} \; w_1(0). \qquad\qquad \text{(H-11)}$$

APPENDIX I

HEIGHT GAIN FUNCTIONS— THE HEIGHT PROFILE OF THE GROUNDWAVE

The diffraction coefficient calculated in appendix G allows us to calculate the strength of the ground wave at the radius $r = \dfrac{\nu}{k}$ given the incident field at the radius $\dfrac{\nu}{k}$. To find the signal strength at other heights, it is necessary to find the height variation of signal strength in the ground wave. From (E-32) the vertical electric field varies as

$$\frac{H_\nu^{(2)}(kr)}{r^{\frac{3}{2}}} .$$

(I-1)

Defining the height gain function G as the ratio of electric field at r to that at $r = \dfrac{\nu}{k}$ gives

$$G_\nu(r) = \frac{H_\nu^{(2)}(kr)}{H_\nu^{(2)}(\nu)} \left(\frac{\nu}{kr}\right)^{\frac{3}{2}} .$$

(I-2)

The Hankel approximation,

$$\sqrt{\frac{k\pi}{2}} H_\nu^{(2)}(kr) \approx \frac{i\,(-y)^{\frac{1}{4}}}{\left(r^2 - \left(\frac{\nu}{k}\right)^2\right)^{\frac{1}{4}}} w_1(y) ,$$

(I-3)

where

$$\frac{2}{3}(-y)^{\frac{3}{2}} = \sqrt{(kr)^2 - \nu^2} - \nu \cos^{-1}\frac{\nu}{kr} ,$$

(I-4)

and the simpler Hankel approximation,

$$\sqrt{\frac{k\pi}{2}} H_\nu^{(2)}(\nu) \approx i\sqrt{\frac{k}{2}}\left(\frac{2}{\nu}\right)^{\frac{1}{3}} w_1(0),$$

(I-5)

give

$$G_{\nu}(r) = \left(\frac{\nu}{kr}\right)^{\frac{3}{2}} \left(\frac{\nu}{2}\right)^{\frac{1}{3}} \frac{(-y)^{\frac{1}{4}}}{\left(r^2 - \left(\frac{\nu}{k}\right)^2\right)^{\frac{1}{4}}} \frac{w_1(y)}{\sqrt{\frac{k}{2}} \, w_1(0)} \quad . \tag{I-6}$$

If $\nu \approx kr$, then it is also valid to use the simpler Hankel approximation,

$$\sqrt{\frac{k\pi}{2}} \, H_{\nu}^{(2)}(kr) \approx i \sqrt{\frac{k}{2}} \left(\frac{2}{\nu}\right)^{\frac{1}{3}} w_1(y) \quad , \tag{I-7}$$

where

$$y = \left(\frac{2}{\nu}\right)^{\frac{1}{3}} (\nu - kr) \quad . \tag{I-8}$$

Using (I-5) and (I-7) in (I-2) gives

$$G \approx \left(\frac{\nu}{kr}\right)^{\frac{3}{2}} \frac{w_1(y)}{w_1(0)} \approx \frac{w_1\left(\left(\frac{2}{\nu}\right)^{\frac{1}{3}}(\nu - kr)\right)}{w_1(0)} \quad . \tag{I-9}$$

This height gain function can be used to calculate the effect of elevating either the transmitter or receiver. Although height gain functions are usually defined relative to the ground, I have defined the one in (I-9) relative to the sphere of radius $\frac{\nu}{k}$ because that is a more natural height in the theory.

APPENDIX J

EVALUATING THE SHEDDING COEFFICIENTS BY COMPARING THE GEOMETRICAL THEORY OF DIFFRACTION SOLUTION WITH THE RIGOROUS SOLUTION

It is possible to use the height gain function to calculate the field of the ground wave at any height. For large heights this is not the most convenient method because the product of a Legendre function and a Hankel function can then be interpreted as giving the radiation field of a ray tangent to the sphere $\frac{\nu}{k}$. Thus it is only necessary to calculate a coefficient which gives the ratio of the effective strength of the radiation field to the strength of the ground wave at the height $\frac{\nu}{k}$ - a.

The ray path connecting the source (at a distance b from the center of the earth) to the observer (at a distance r from the center of the earth) is a straight line of length ℓ_1 from the source to the point of tangency with the sphere, an arc of length $(\theta - \theta_1 - \theta_2)$ along the sphere, and a straight line of length ℓ_2 leaving the sphere $\frac{\nu}{k}$ tangentially and arriving at the observer. Both the transmitting and receiving antennas are short vertical dipoles (see fig. 18). The geometrical theory of diffraction gives the total field at the observation point as, the product of several factors: The incident field at the sphere $\frac{\nu}{k}$,

$$ iKL \; \frac{e^{-ik\ell_1}}{\ell_1} \; \cos \theta_1 \; ; \qquad (J-1) $$

the diffraction coefficient,

$$D = -\frac{2i\sqrt{\pi}}{t - q^2}\frac{w_1(0)}{w_1(t)^2} \quad ; \qquad (J-2)$$

the phase integral contribution in traveling along the arc from the diffraction point to the shedding point,

$$e^{-i\,\nu(\theta - \theta_1 - \theta_2)} \quad ; \qquad (J-3)$$

a shedding coefficient, which gives the ratio of the far zone radiation field to the near field at a small distance ℓ from the point of shedding,

$$S_\ell \quad ; \qquad (J-4)$$

the phase integral contribution in traveling from the point of shedding to the observation point,

$$e^{-ik\,\ell_2} \quad ; \qquad (J-5)$$

a divergence factor due to elevation defocusing of the ray in going from a distance ℓ from the point of shedding to the observation point,

$$\sqrt{\frac{\ell}{\ell_2}} \quad ; \qquad (J-6)$$

a convergence factor due to azimuth focusing of rays traveling around the sphere,

$$\sqrt{\frac{\frac{\nu}{k}\sin\theta_1}{r\sin\theta}} \quad ; \qquad (J-7)$$

the pattern factor of the vertical receiving antenna,

$$\cos\theta_2 \quad . \qquad (J-8)$$

Taking the product of (J-1) through (J-8) gives

$$E_0 = -iKL \frac{e^{-ik\ell_1}}{\ell_1} \cos\theta_1 \frac{2i\sqrt{\pi}}{t-q^2} \frac{w_1(0)}{w_1(t)} e^{-i\nu(\theta-\theta_1-\theta_2)} S_\ell e^{-ik\ell_2}$$

$$\times \sqrt{\frac{\ell}{\ell_2}} \sqrt{\frac{\frac{\nu}{k}\sin\theta_1}{r\sin\theta}} \cos\theta_2 \ . \tag{J-9}$$

From figure 18,

$$\cos\theta_1 = \frac{\nu}{kb} \ , \tag{J-10}$$

$$\sin\theta_1 = \frac{\ell_1}{b} \ , \tag{J-11}$$

$$\cos\theta_2 = \frac{\nu}{kr} \ . \tag{J-12}$$

Substituting into (J-9) we get

$$\overline{E}_0 = \frac{2L\nu^{\frac{5}{2}}\sqrt{\pi}}{k^{\frac{3}{2}} b^{\frac{3}{2}} r^{\frac{3}{2}} \sqrt{\ell_1}\sqrt{\ell_2}} \frac{w_1(0)}{w_1(t)^2} \frac{\sqrt{\ell}\, S_\ell}{\sqrt{\sin\theta}} \frac{e^{-ik\ell_1} e^{-ik\ell_2} e^{-i\nu(\theta-\theta_1-\theta_2)}}{(t-q^2)} \ .$$

$$\tag{J-13}$$

From figure 18,

$$\ell_1 = \sqrt{b^2 - \left(\frac{\nu}{k}\right)^2} \ , \tag{J-14}$$

$$\ell_2 = \sqrt{r^2 - \left(\frac{\nu}{k}\right)^2} \ , \tag{J-15}$$

$$\theta_1 = \cos^{-1}\frac{\nu}{kb} \ , \tag{J-16}$$

$$\theta_2 = \cos^{-1}\frac{\nu}{kr} \ . \tag{J-17}$$

Substituting into (J-13) gives

$$E_0 = \frac{2L\nu^{\frac{5}{2}} \sqrt{\pi} \, S_\ell \sqrt{\ell} \, w_1(0)}{k^{\frac{3}{2}} \, b^{\frac{3}{2}} \, r^{\frac{3}{2}} \left(b^2 - \left(\frac{\nu}{k}\right)^2\right)^{\frac{1}{4}} \left(r^2 - \left(\frac{\nu}{k}\right)^2\right)^{\frac{1}{4}} (t - q^2) \, w_1(t)^2 \, \sqrt{\sin\theta}}$$

$$e^{-i\sqrt{(kb)^2 - \nu^2}} \, e^{-i\sqrt{(kr)^2 - \nu^2}} \, e^{-i\nu\left(\theta - \cos^{-1}\frac{\nu}{kb} - \cos^{-1}\frac{\nu}{kr}\right)} .$$

$$(J-18)$$

The rigorous solution for one mode from (E-32) is

$$E_0 = \frac{-iL\sqrt{\pi}}{k^{\frac{3}{2}} \, r^{\frac{3}{2}} \, b^{\frac{3}{2}}} \left(\frac{ka}{2}\right)^{\frac{1}{3}} \left(\frac{2}{k}\right)^{\frac{1}{2}} \frac{\nu^{\frac{5}{2}}}{\sqrt{\sin\theta}} \, e^{-i\,\pi/4} \, e^{-i\nu\theta}$$

$$\left(\frac{\pi k}{2}\right) \frac{H_\nu^{(2)}(kb) \, H_\nu^{(2)}(kr)}{w_1(t)^2} \frac{2}{t - q^2} .$$

$$(J-19)$$

Using the Debye approximations,

$$\sqrt{\frac{\pi k}{2}} \, H_\nu^{(2)}(kb) \approx \frac{e^{i\pi/4} \, e^{-i\sqrt{(kb)^2 - \nu^2}} \, e^{i\nu\cos^{-1}\frac{\nu}{kb}}}{\left(b^2 - \left(\frac{\nu}{k}\right)^2\right)^{\frac{1}{4}}}$$

$$\sqrt{\frac{\pi k}{2}} \, H_\nu^{(2)}(kr) \approx \frac{e^{i\pi/4} \, e^{-i\sqrt{(kr)^2 - \nu^2}} \, e^{i\nu\cos^{-1}\frac{\nu}{kr}}}{\left(r^2 - \left(\frac{\nu}{k}\right)^2\right)^{\frac{1}{4}}} ,$$

$$(J-20)$$

gives

$$E_0 = \frac{-2iL\sqrt{\pi}}{k^{\frac{3}{2}} \, r^{\frac{3}{2}} \, b^{\frac{3}{2}}} \left(\frac{ka}{2}\right)^{\frac{1}{3}} \left(\frac{2}{ka}\right)^{\frac{1}{2}} a^{\frac{1}{2}} \frac{\nu^{\frac{5}{2}}}{\sqrt{\sin\theta}} \frac{e^{i\pi/4}}{t - q^2}$$

$$\frac{e^{-i\nu\theta} \, e^{-i\sqrt{(kb)^2 - \nu^2}} \, e^{-i\sqrt{(kr)^2 - \nu^2}} \, e^{i\nu\cos^{-1}\frac{\nu}{kb}} \, e^{i\nu\cos^{-1}\frac{\nu}{kr}}}{w_1(t)^2} .$$

$$(J-21)$$

Comparing (J-18) with (J-21) we get

$$S_\ell = \frac{e^{-i\,\pi/4}}{w_1(0)} \sqrt{\frac{a}{\ell}} \left(\frac{2}{ka}\right)^{\frac{1}{6}} .$$

$$(J-22)$$

APPENDIX K

APPLICATION OF THE GEOMETRICAL THEORY OF DIFFRACTION TO MULTI-HOP IONOSPHERIC SKY WAVE PROPAGATION

It is possible to apply the geometrical theory of diffraction to the problem of terrestrial LF radio propagation below a concentric ionosphere. If diffraction effects are important for the mth hop, the receiver must be beyond the horizon of the mth sky wave so that the rays arrive from the ionosphere tangent to a sphere of radius $\frac{\nu}{k}$, travel along that sphere, and leave the sphere tangentially to reflect off the ionosphere again, etc., for each hop. This path is indicated in figure 19.

The solution is the product of several factors: The incident field at P_1,

$$ikL \; \frac{e^{-ik\,\ell_o}}{\ell_o} \; \cos\,\theta_o ; \qquad\qquad \text{(K-1)}$$

the diffraction coefficient giving the excitation of the groundwave at P_i, $i = 1 \rightarrow m+1$,

$$D = -\; \frac{2i\,\sqrt{\pi}}{t - q^a} \; \frac{w_1(0)}{w_1(t)^2} ; \qquad\qquad \text{(K-2)}$$

the phase integral going from P_i to Q_i, $i = 1 \rightarrow m+1$,

$$e^{-i\nu\alpha_i} ; \qquad\qquad \text{(K-3)}$$

the shedding coefficient at Q_i, $i = 1 \rightarrow m+1$, giving the strength of the radiation field a small distance ℓ from Q_i,

$$S_\ell = \frac{e^{-i\,\pi/4}}{w_1(0)} \; \left(\frac{2}{ka}\right)^{1/6} \left(\frac{a}{\ell}\right)^{1/2} ; \qquad\qquad \text{(K-4)}$$

the ionospheric reflection coefficient and the phase integral going from Q_i to P_i, $i = 1 \rightarrow m$, for the ith hop,

$$Te^{-2ik\ell_i} ; \qquad\qquad (K-5)$$

a convergence factor due to elevation focusing of the ith hop by the ionosphere,

$$\left(\frac{\ell}{\ell'}\right)^{1/2} \qquad\qquad (K-6)$$

$$\left[\text{derived from (Wait, 1962b)}\right.$$

$$\left(\frac{\ell}{2\frac{\nu}{k}}\right)^{1/2} \frac{g}{\ell_i} \left[\frac{g - \frac{\nu}{k}\cos\theta_i}{g\cos\theta_i - \frac{\nu}{k}} \sin\theta_i\right]^{1/2} . \qquad (K-7)$$

Since the rays arriving at P_{i+1} from the ionosphere graze the sphere $\frac{\nu}{k}$,

$$\cos\theta_i = \frac{\nu}{kg} . \qquad\qquad (K-8)$$

Substituting (K-8) into (K-7) shows that the convergence coefficient diverges, indicating a caustic in the field incident at P_{i+1}. Because of this it is more convenient to calculate the field a small distance,

$$\ell' = 2\frac{\nu}{k}\left(\theta_i - \cos^{-1}\frac{\nu}{kg}\right), \qquad (K-9)$$

beyond the caustic. Then (K-7) gives the ratio of the field at a small distance ℓ' from P_{i+1} to that at a small distance ℓ from Q_i as $(K-6)\Big]$;

the effective excitation factor for a point source (because the caustic in the incident field at P_{i+1} is similar to a source at P_{i+1}) ,

$$R_{\ell'} = e^{i\pi/4} w_1(0)\left(\frac{ka}{2}\right)^{1/6}\left(\frac{\ell'}{a}\right)^{1/2} \qquad (K-10)$$

for $i = 1 \rightarrow m$; a divergence factor due to elevation defocusing going from Q_{m+1} to 0,

$$\left(\frac{\ell}{\ell_{m+1}}\right)^{1/2} ; \qquad\qquad (K-11)$$

the phase integral from Q_{m+1} to 0,

$$e^{-ik\ell_{m+1}}; \qquad\qquad (K-12)$$

the receiving antenna gain factor,

$$\cos \theta_{m+1} = \frac{\nu}{kr} ; \qquad\qquad (K-13)$$

a convergence factor due to azimuthal focusing,

$$\sqrt{\frac{\frac{\nu}{k} \sin \theta_0}{r \sin \theta}} . \qquad\qquad (K-14)$$

Since

$$\cos \theta_0 = \frac{\nu}{kb} \qquad\qquad (K-15)$$

and

$$\sin \theta_0 = \frac{\ell_0}{b} , \qquad\qquad (K-16)$$

the product of (K-1) through (K-6) and (K-10) through (K-14) is

$$e = ikL \frac{e^{-ik\ell_0}}{\ell_0} \frac{\nu}{kb} D^{m+1} e^{-i\nu} \sum_{i=1}^{m+1} \alpha_i$$

$$\left(\frac{e^{-\pi/4}}{w_1(0)} \left(\frac{2}{ka}\right)^{1/6} \left(\frac{a}{\ell}\right)^{1/2}\right)^{m+1} \left(Te^{-2ik\ell}\right)^m \left(\left(\frac{\ell}{\ell'}\right)^{1/2}\right)^m$$

$$\left(e^{i\pi/4} w_1(0) \left(\frac{ka}{2}\right)^{1/6} \left(\frac{\ell'}{a}\right)^{1/2}\right)^m \left(\frac{\ell}{\ell_{m+1}}\right)^{1/2} e^{-ik\ell_{m+1}}$$

$$\left(\frac{\nu}{kr}\right) \sqrt{\frac{\left(\frac{\nu}{k}\right)\left(\frac{\ell_0}{b}\right)}{r \sin \theta}} , \qquad\qquad (K-17)$$

where

$$\sum_{i=1}^{m+1} \alpha_i = \theta - \theta_0 - 2m\theta_i - \theta_{m+1} \equiv \alpha \qquad (K-18)$$

is independent of the α_i.

Using (K-2) in (K-17) gives

$$e = \frac{L\, e^{-i\pi/4}\, e^{-ik\ell_0}\, e^{-ik\ell_{m+1}}\, 2\sqrt{\pi}\, e^{-i\nu\alpha_\nu}{}^{5/2}}{k^{3/2} b^{3/2} r^{3/2} \ell_0^{1/2} \ell_{m+1}^{1/2} \sqrt{\sin\theta}\, (t-q^2) w_1(t)^2} \left(\frac{2}{ka}\right)^{1/6} a^{1/2}$$

$$\left[\frac{-2i\sqrt{\pi}}{t-q^2} \quad \frac{T e^{-2ik\ell_i} w_1(0)}{w_1(t)^2}\right]^m . \qquad (K-19)$$

Many similar paths connect the transmitter and receiver. For instance, assuming that excitation of a ground wave and shedding from a ground wave take negligible space to occur, then α_1 can vary from zero to α. (Actually, the rigorous solution from appendix E shows that this assumption is only a good approximation if the frequency is high enough. In fact, α_1 may vary from 0 to $\hat{\alpha}$, where $\hat{\alpha}$ is given by (E-65) as

$$\hat{\alpha} = \alpha - \left(\frac{2}{ka}\right)^{1/3} \left(\frac{m+1-p_b^a-p_r^a}{2} w_1(t) w_2(t)(t-q^2) + (m-1)iq + \frac{i(m+1)}{2(t-q^2)}\right).$$

I interpret the term on the right as the great circle angle needed to excite a ground wave $m+1$ times and shed a ray $m+1$ times. For a high enough frequency, it is only a small correction unless α is near zero.) If, then, α_1 can vary from 0 to $\hat{\alpha}$ then α_2 can vary from 0 to $\hat{\alpha}-\alpha_1$, and α_3 can vary from 0 to $\hat{\alpha}_2 - \alpha_1 - \alpha_2$ etc. Thus, the total field at the receiver is a multiple integration over all these paths. Assume that the observed field is equal to some constant C times the integrator, that is,

$$E_m = \int_0^{\hat{a}-\alpha_1} \cdots \int_0^{\hat{a}-\alpha_1-\alpha_2} \int_0^{\hat{a}-\alpha_1} \int_0^{\hat{a}} e C d\alpha_1 C d\alpha_2 C d\alpha_3 \cdots$$

$$C d\alpha_m . \tag{K-20}$$

Since the only dependence of e on any of the α_i is on $\sum_{i=1}^{m+1} \alpha_i = \alpha, e$

and C^m may be taken outside the integrals. It is then easy to integrate (K-20) to get

$$E_m = \frac{e C^m \hat{a}^m}{m!} . \tag{K-21}$$

Using

$$\ell_o = \sqrt{b^2 - (\frac{\nu}{k})^2} , \tag{K-22}$$

$$\ell_{m+1} = \sqrt{r^2 - (\frac{\nu}{k})^2} , \tag{K-23}$$

$$\ell_i = \sqrt{g^2 - (\frac{\nu}{k})^2} , \tag{K-24}$$

and (K-19) in (K-21) gives

$$E_m = \frac{L e^{-i\pi/4} 2\sqrt{2\pi}\, \nu^{5/2} e^{-i\sqrt{(kb)^2-\nu^2}} e^{-i\sqrt{(kr)^2-\nu^2}} e^{-i\nu\alpha}}{k^2 b^{3/2} r^{3/2} (b^2-(\frac{\nu}{k})^2)^{1/4} (r^2-(\frac{\nu}{k})^2)^{1/4} \sqrt{\sin\theta}\,(t-q^2) w_1(t)^2} (\frac{ka}{2})^{1/3}$$

$$\frac{1}{m!} \left[\frac{-2i\sqrt{\pi}\, C\, \hat{a}}{t-q^2} \frac{T e^{-2i\sqrt{(kg)^2-\nu^2}} w_1(0)}{w_1(t)^2} \right]^m . \tag{K-25}$$

The rigorous solution for one mode from (E-63) is

$$E_m = \frac{-Li2\sqrt{2\pi}\,e^{i\frac{\pi}{4}}}{k^2 r^{3/2} b^{3/2} m!\sqrt{\sin\theta}} \left(\frac{ka}{2}\right)^{1/3} \frac{\nu^{5/2}\,e^{-i\nu\alpha}}{(r^2 - (\frac{\nu}{k})^2)^{1/4}\,(b^2 - (\frac{\nu}{k})^2)^{1/4}}$$

$$\frac{e^{-i\sqrt{(kr)^2-\nu^2}}\,e^{-i\sqrt{(kb)^2-\nu^2}}}{w_1(t)^2\quad (t-q^2)} \left[\frac{-2iT\hat{a}}{t-q^2}\left(\frac{ka}{2}\right)^{1/3}\frac{e^{-2i\sqrt{(kg)^2-\nu^2}}}{w_1(t)^2}\right]^m \cdot \text{(K-26)}$$

Comparing gives

$$C = \frac{\left(\frac{ka}{2}\right)^{1/3}}{w_1(0)\sqrt{\pi}} . \qquad\qquad \text{(K-27)}$$

The agreement between (K-25) and (K-26) for C defined by (K-27) shows that my application of the geometrical theory of diffraction to the problem of terrestrial LF radio propagation below a concentric homogeneous ionosphere is valid. It also shows that the signal strength of the mth hop in the shadow varies with distance as

$$\frac{\hat{a}^m\,e^{-i\nu\alpha}}{\sqrt{\sin\theta}} \qquad\qquad \text{(K-28)}$$

where α, given by (K-18), is the distance the ray travels along the ground (the total distance between the transmitter and receiver minus that taken up by the sky-wave hops). This gives a fairly simple and accurate formula to calculate the distance variation of the mth hop in the shadow.

REFERENCES

Belrose, J. S. , and M. J. Burke (1964), "Study of the lower ionosphere using partial reflection: 1. Experimental technique and methods of analysis, J. Geophys. Res. 69, No. 13, 2799-2818.

Berry, Leslie A. (1964a), "Some remarks on the Watson transformation and mode theory, Radio Sci. J. Res. 68D, No. 1, 59-66.

Berry, Leslie A. (1964b), "Computation of Hankel functions, NBS Tech. Note 216.

Berry, Leslie A. (1964c), "Wave-hop theory of long distance propagation of low-frequency radio waves, Radio Sci. J. Res. NBS 68D, No. 12, 1275-1284.

Berry, Leslie A. , and Mary E. Chrisman (1965a), "The path integrals of LF/VLF wave hop theory, Radio Sci. J. Res. NBS 69D, No. 11, 1469-1480.

Berry, Leslie A. , and Mary E. Chrisman (1965b), "Numerical values of the path integrals for low and very low frequencies, NBS Tech. Note 319.

Booker, H. G. , and C. M. Crain (1967), "LF and VLF reflection loss in the lower ionosphere: a theorem on absorption and its application, Memorandum RM-5249-PR, Rand Corp. , Santa Monica, Calif.

Bremmer, H. (1949), "Terrestrial Radio Waves; Theory of Propagation (Elsevier, New York).

Budden, K. G. (1961), "Radio Waves in the Ionosphere; the Mathematical Theory of the Reflection of Radio Waves from Stratified Ionised Layers (University Press, Cambridge, England).

Epstein, Paul S. (1930), "Geometrical optics in absorbing media", Proc. Nat. Acad. Sci. 16, 37-45.

Handbook of Mathematical Functions with Formulas, Graphs, and Mathematical Tables (1964), ed. Milton Abramowitz and Irene A. Stegun (U.S. Gov't. Printing Office, Washington, D. C.).

Handbook of Geophysics and Space Environments (1965), ed. Shea L. Valley (McGraw Hill, New York).

Haselgrove, Jenifer (1954), "Ray theory and a new method for ray tracing", Report of the Physical Society Conference on the Physics of the Ionosphere, 355-364, (Physical Society, London).

Johler, J. Ralph (1966), "Zonal harmonics in low frequency terrestrial radio wave propagation", NBS Tech. Note 335.

Johler, J. Ralph and Leslie A. Berry (1962), "Propagation of terrestrial radio waves of long wave length; theory of zonal harmonics with improved summation techniques", J. Res. NBS 66D, No. 6, 737-773.

Johler, J. Ralph and Leslie A. Berry (1964), "A complete mode sum for LF, VLF, ELF terrestrial radio wave fields", NBS Monograph 78.

Johler, J. Ralph and John D. Harper (1962), "Reflection and transmission of radio waves at a continuously stratified plasma with arbitrary magnetic induction", J. Res. NBS 66D, No. 1, 81-99.

Jones, Richard Michael (1966), "A three-dimensional ray tracing computer program, "ESSA Tech. Rept. IER 17-ITSA 17.

Keller, Joseph B. (1958), "A geometrical theory of diffraction, calculus of variations and its applications", Proceedings of Symposia in Applied Mathematics 8, 27-52, (McGraw Hill for the American Mathematical Society, New York).

Keller, Joseph B. (1962), "Geometrical theory of diffraction",
J. Opt. Soc. Am. 52, No. 2, 116-130.

Keller, Joseph B., and Herbert B. Keller (1950), "Determination of reflected and transmitted fields by geometrical optics", J. Opt. Soc. Am. 40, No. 1, 48-52.

Keller, Joseph B., and Bertram R. Levy (1963), "Scattering of short waves", Electromagnetic Scattering, ed. M. Kerker, 3-24, (Macmillan, New York).

Knecht, Robert W. (1965), "The distribution of electrons in the lower and middle ionosphere", Progress in Radio Science 1960-1963, ed. Geoffrey M. Brown, 3, 14-15, (Elsevier, Amsterdam).

Kelso, John M. (1964), "Radio Ray Propagation in the Ionosphere", (McGraw Hill, New York).

Kouyoumjian, Robert G. (1965), "Asymptotic high-frequency methods", Proc. IEEE 53, No. 8, 864-876.

Levy, Bertram R., and Joseph B. Keller (1959), "Diffraction by a smooth object", Commun Pure Appl. Math. 12, No. 1, 159-209.

Lewis, Robert M., Norman Bleistein, and Donald Ludwig (1967), "Uniform asymptotic theory of creeping waves", Commun. Pure Appl. Math. 20, No. 2, 295-328.

Logan, Nelson A. (1959), "General research in diffraction theory", Lockheed Missiles and Space Division Rept. LMSD-288087 and -288088.

Logan, Nelson A., and K. S. Yee (1962), "A mathematical model for diffraction, Electromagnetic waves": Proceedings of a Symposium Conducted by the Mathematics Research Center, U. S. Army at the University of Wisconsin, Madison, April 10-12, 1961, ed. Rudolph E. Langer, 139-180 (University of Wisconsin Press, Madison).

Ludwig, Donald (1966), "Uniform asymptotic expansions at a caustic", Commun. Pure Appl. Math. 19, No. 2, 215-250.

Rugg, Donald E. (1967), "Theoretical investigation of the diurnal phase and amplitude variations of VLF signals", Radio Sci. 2, No. 6, 551-556.

Titheridge, J. E. (1967), "Calculation of the virtual height and absorption of radio waves in the ionosphere", Radio Sci. 2, No. 2, 133-138.

Wait, James R. (1960), "Terrestrial propagation of VLF radio waves", J. Res. NBS 64D, No. 2, 153-204.

Wait, James R. (1961), "A diffraction theory for LF sky-wave propagation", J. Geophys. Res. 66, No. 6, 1713-1723.

Wait, James R. (1962a), "Mode conversion in the earth-ionosphere waveguide", NBS Tech. Note 151.

Wait, James R. (1962b), "Introduction to the theory of VLF propagation", Proc. IRE 50, No. 7, 1624-1647.

Wait, James R. (1962c), "Electromagnetic waves in stratified media" (Macmillan, New York).

Wait, James R. (1964a), "Electromagnetic surface waves", Advances in Radio Research, ed. J. A. Saxton, 157-217, (Academic Press, London and New York).

Wait, James R. (1964b), "Two-dimensional treatment of mode theory of the propagation of VLF radio waves", Radio Sci. J. Res. 68D, No. 1, 81-93.

Wait, James R. (1964c), "On phase changes in very-low-frequency propagation induced by an ionospheric depression of finite extent", J. Geophys. Res. 69, No. 3, 441-445.

Wait, James R. (1964d), "Influence of a circular ionospheric depression on VLF propagation", Radio Sci. J. Res. 68D, No. 8, 907-914.

Wait, James R. (1967a), "Electromagnetic whispering gallery modes in a dielectric rod", Radio Sci. 2, No. 9, 1005-1017.

Wait, James R. (1967b), "Applications and of the mode theory of long wave radio propagation, M. F., L. F., and V. L. F." Radio Propagation Conference Publication No. 36, 57-62, (Institution of Electrical Engineers, London).

Wait, James R., and Alyce M. Conda (1958), "Pattern of an antenna on a curved lossy surface", IRE Trans. Ant. Prop. AP-6, No. 4, 348-359.

Wait, James R. and Alyce M. Conda (1959), "Diffraction of electromagnetic waves by smooth obstacles for grazing angles", J. Res. NBS 63D, No. 2, 181-197.

Wait, James R., and Lillie C. Walters (1963), "Reflection of VLF radio waves from an inhomogeneous ionosphere: Part 1, Exponentially varying isotropic model", J. Res. NBS 67D, No. 3, 361-367.

Watson, G. N. (1918), "The diffraction of electric waves by the earth", Proc. Royal Soc. of London 95A, No. 666, 83-99.

Watson, G. N. (1919), "The transmission of electric waves round the earth", Proc. Royal Soc. of London 95A, No. 673, 546-563.

ADDITIONAL BIBLIOGRAPHY

Altman, C. (1965), "Use of the phase-integral method to determine the reflection properties of a stratified ionosphere", Radio Sci. J. Res. 69D, No. 4, 511-519.

Bremmer, H. (1951), "The W. K. B. approximation as the first term of a geometric-optical series", Commun. Pure Appl. Math. 4, No. 1, 105(S169)-115(S179).

Budden, K. G. (1961), "The wave-guide mode theory of wave propagation" (Prentice-Hall, Englewood, Cliffs, N. J.).

Budden, K. G. (1964), "Lectures on magneto-ionic theory" (Gordon and Breach, New York).

Budden, K. G. (1965), "Effect of electron collisions on the formulas of magneto-ionic theory", Radio Sci. J. Res. 69D, No. 2, 191-211.

Clemmow, P.C. (1966), "The plane wave spectrum representation of electromagnetic fields" (Pergamon Press, Oxford).

Cooper, Elisabeth A. (1964), "Phase integral calculations of ionospheric reflections including a variable collision frequency", J. Atmosph. Terr. Phys. 26, No. 10, 995-1005.

Felsen, L. B., and N. Marcuvitz (1959), "Modal analysis and synthesis: Chap. 4, Asymptotic evaluation of integrals", Air Force Cambridge Research Center Tech. Note AFCRC-TN-59-991.

Fock, V. A. (1965), "Electromagnetic Diffraction and Propagation Problems" (Pergamon Press, Oxford).

Gould, R. N., and R. Burman (1964), "Some electromagnetic wave functions for propagation in stratified media", J. Atmosph. Terr. Phys. 26, No. 3, 335-340.

Hines, C. O. (1951), "Wave packets, the poynting vector, and energy flow: Part 1, Non-dissipative (anisotropic), homogeneous media", J. Geophys. Res. 56, No. 1, 63-72.

Hines, C. O. (1951), "Wave packets, the poynting vector, and energy flow: Part 2, Group propagation through dissipative isotropic media", J. Geophys. Res. 56, No. 2, 197-206.

Hines, C. O. (1951), "Wave packets, the poynting vector, and energy flow: Part 3, Packet propagation through dissipative anisotropic media", J. Geophys. Res. 56, No. 2, 207-220.

Hines, C. O. (1951), "Wave packets, the poynting vector, and energy flow: Part 4, Poynting and MacDonald velocities in dissipative anisotropic media (conclusion)", J. Geophys. Res. 56, No. 4, 535-544.

Johler, J. Ralph (1961), "On the analysis of LF ionospheric radio propagation phenomena", J. Res. NBS 65D, No. 5, 507-529.

Johler, J. Ralph (1962), "Propagation of the low-frequency radio signal", Proc. IRE 50, No. 4, 404-427.

Johler, J. Ralph (1964), "Concerning limitations and further corrections to geometric-optical theory for LF, VLF propagation between the ionosphere and the ground", Radio Sci. J. Res. NBS 68D, No. 1, 67-68.

Johler, J. Ralph, W. J. Kellar, and Lillie C. Walters (1956), "Phase of the low radio frequency groundwave", NBS Circular 573.

Johler, J. Ralph and Lillie C. Walters (1960), "On the theory of reflection and low- and very-low-radio frequency waves from the ionosphere", J. Res. NBS 64D, No. 3, 269-285.

Johler, J. Ralph, Lillie C. Walters, and J. D. Harper (1960),
"Low- and very-low-radio frequency model ionosphere
reflection coefficients", NBS Tech. Note 69.

Johler, J. Ralph, Lillie C. Walters, and C. M. Lilley (1960),
"Amplitude and phase of the low- and very-low-radio
frequency ground wave", NBS Tech. Note 60, PB 161 561.

Kline, Morris (1951), "An asymptotic solution of Maxwell's
equations", Commun. Pure Appl. Math. $\underline{4}$, No. 2/ 3,
225(S225)-262(S262).

Kline, Morris and Irvin W. Kay (1965), "Electromagnetic theory
and geometrical optics" (Interscience Publishers,
New York).

Levy, Bertram R. , and Joseph B. Keller (1960), "Diffraction
by a spheroid", Can. J. Phys. $\underline{38}$, No. 1, 128-144.

Ludwig, Donald (1967), "Uniform asymptotic expansion of the
field scattered by a convex object at high frequencies",
Commun. Pure Appl. Math. $\underline{20}$, No. 1, 103-138.

Morgenstern, J. C. , and J. Ralph Johler (1965), "Attenuation of
the groundwave of a low frequency electromagnetic pulse",
NBS Tech. Note 310.

Norton, Kenneth A. (1959), "Transmission loss in radio
propagation 2", NBS Tech. Note 12, PB151 371.

Proceedings of the Symposium on Quasi-Optics, New York,
June 8-10, 1964 (1964), (Polytechnic Press, New York).

Schulkunoff, S. A. (1951), "Remarks concerning wave propagation
in stratified media", Commun. Pure Appl. Math. $\underline{4}$, No. 1,
117(S181)-128(S192).

The Theory of Electromagnetic Waves; a Symposium June 6-8,
1950 (1951), (Interscience Publishers, New York).

Trotter, Hale F., and John W. Tukey (1956), "Conditional Monte Carlo for normal samples", Symposium on Monte Carlo Methods held at the University of Florida, March 16 and 17, 1954, 64-79 (John Wiley, New York).

Wait, James R. (1960), "A survey and bibliography of recent research in the propagation of VLF radio waves", NBS Tech. Note 58, PB 161 559.

Wait, James R. (1961), "A new approach to the mode theory of VLF propagation", J. Res. NBS 65D, No. 1, 37-46.

Wait, James R. (1963), "Influence of the lower ionosphere on propagation of VLF waves to great distances", J. Res. NBS 67D, No. 4, 375-381.

Wait, James R. (1965), "Concerning the mechanism of reflection of electromagnetic waves from an inhomogeneous lossy plasma", Radio Sci. J. Res. 69D, No. 6, 865-869.

Wait, James R., and Kenneth P. Spies (1960), "Influence of earth curvature and the terrestrial magnetic field on VLF propagation", J. Geophys. Res. 65, No. 8, 2325-2329.

Wait, James R. and Kenneth P. Spies (1964), "Characteristics of the earth-ionosphere waveguide for VLF radio waves", NBS Tech. Note 300.

Wait, James R., and Lillie C. Walters (1963), "Reflection of VLF radio waves from an inhomogeneous ionosphere: Part 2, Perturbed exponential model," J. Res. NBS 67D, No. 5, 519-523.

Wait, James R., and Lillie C. Walters (1963), "Reflection of VLF radio waves from an inhomogeneous ionosphere: Part 3, Exponential model with hyperbolic transition", J. Res. NBS 67D, No. 6, 747-752.

Wait, James R. , and Lillie C. Walters (1964), "Reflection of electromagnetic waves from a lossy magnetoplasma, " Radio Sci. J. Res. 68D, No. 1, 95-101.

Walters, Lillie C. , and J. Ralph Johler (1962), "On the diffraction of spherical radio waves by a finitely conducting spherical earth", J. Res. NBS 66D, No. 1 101-106.

Walters, Lillie C. , and James R. Wait (1963), "Numerical calculations for reflection of electromagnetic waves from a lossy magnetoplasma", NBS Tech. Note 205.

Yabroff, Irving (1961), "Computation of Whistler ray paths", J. Res. NBS 65D, No. 5, 485-505.

Zauderer, Erich (1967), "An integral representation approach to diffraction by a smooth object", J. Math. Anal. Appl. 18, No. 1, 17-37.

Zauderer, Erich (1964), "Wave propagation around a convex cylinder", J. Math. Mech. 13, No. 2, 171-186.